농학박사학위논문

*Fusarium graminearum*의 산화스트레스반응에 관련된 유전자들의 기능 분석

Functional analyses of the genes involved in the oxidative stress response in *Fusarium graminearum*

2017년 8월

서울대학교 대학원

농생명공학부 식물미생물전공

이 윤 지

Functional analyses of the genes involved in the oxidative stress response in *Fusarium graminearum*

A dissertation submitted in partial

fulfillment of the requirement for

the degree of

DOCTOR OF PHILOSOPHY

to the Faculty of

Department of Agricultural Biotechnology

at

SEOUL NATIONAL UNIVERSITY

By

Yoonji Lee

August, 2017

농학박사학위논문

*Fusarium graminearum*의 산화스트레스반응에 관련된 유전자들의 기능 분석

지도교수 이 인 원

이 논문을 농학박사학위논문으로 제출함
2017년 7월

서울대학교 대학원
농생명공학부 식물미생물학 전공
이 윤 지

이윤지의 박사학위논문을 인준함
2017년 6월

위 원 장 김 영 호

부 위원장 이 인 원

위 원 이 상 기

위 원 채 순 기

위 원 반 용 선

A THESIS FOR THE DEGREE OF DOCTOR OF PHILOSOPHY

Functional analyses of the genes involved in the oxidative stress response in *Fusarium graminearum*

UNDER THE DIRECTION OF DR. YIN-WON LEE

SUBMITTED TO THE FACULTY OF THE GRADUATE SCHOOL
OF SEOUL NATIONAL UNIVERSITY

BY
YOONJI LEE

MAJOR IN PLANT MICROBIOLOGY
DEPARTMENT OF AGRICULTURAL BIOTECHNOLOGY

JUNE 2017

APPROVED AS A QUALIFIED THESIS OF YOONJI LEE
FOR THE DEGREE OF DOCTOR OF PHILOSOPHY
BY THE COMMITTEE MEMBERS

CHAIRMAN Young Ho Kim

VICE CHAIRMAN Yin-Won Lee

MEMBER Sayan Rhee

MEMBER Suhn-Kee Chae

MEMBER Yong-Sun Bahn

ABSTRACT

Functional analyses of the genes involved in the oxidative stress response in *Fusarium graminearum*

Yoonji Lee

Major in Plant Microbiology

Department of Agricultural Biotechnology

The Graduate School

Seoul National University

The homothallic ascomycete fungus *Fusarium graminearum*, one of the most economically important plant pathogens, causes Fusarium head blight (FHB) in wheat, barley, and rice as well as ear rot in maize. Epidemics of FHB cause serious yield losses in major cereal crops worldwide. In addition to yield losses, this fungus is responsible for the contamination of grains with mycotoxins such as trichothecenes and zearalenone that can lead to mycotoxicoses in humans and livestock. During plant infections, phytopathogenic fungi are often exposed to oxidative stress conditions caused by the oxidative burst, a rapid and transient accumulation of reactive oxygen species (ROS). The accumulation of ROS can induce other plant defense responses and also can directly kill pathogens. To

detoxify plant-derived ROS and to successfully colonize their hosts, they have evolved effective ROS detoxifying mechanisms. ROS are also associated with various developmental processes in pathogenic fungi. Although excessive amounts of ROS that are generated as by-products of oxidative metabolism cause an internal oxidative stress, some ROS, particularly H_2O_2, act as secondary messengers in important signal transduction pathways. Therefore, studies on the genes involved in the oxidative stress response in plant pathogenic fungi are important for understanding the pathogenicity and development of fungi. In this study, I firstly identified the *F. graminearum* ortholog of yeast Elongator complex protein 3 (*ELP3*) using a forward genetics approach. Elp3 is a histone acetyl-transferase (HAT) and previous studies have reported that it is required for the activation of a group of stress-inducible genes in eukaryotes. Deletion of *ELP3* caused pleiotropic defects in various developmental processes including asexual and sexual development and virulence in *F. graminearum*. In particular, the *elp3* deletion mutant was more sensitive to oxidative stress than wild-type, and the expression of genes encoding putative antioxidant enzymes was reduced. Since the function of these enzymes in oxidative stress response was not studied in *F. graminearum*, I performed a genome-wide functional characterization of putative peroxidase genes in *F. graminearum*. Peroxidases are a group of ROS-detoxifying enzymes that are involved in the oxidative stress response and in a variety of physiological processes. I identified 31 putative peroxidase genes and generated deletion mutants for these genes. Twenty-six of the deletion mutants showed developmental phenotypes indistinguishable from that of the wild type, and five deletion mutants exhibited phenotypic changes in at least one phenotypic category. Four deletion mutants,

fca6, *fca7*, *fpx1*, and *fpx15*, showed increased sensitivity to extracellular H_2O_2. Deletion mutants of *FCA7* also exhibited reduced virulence and increased trichothecene production compared with those of the wild-type strain, suggesting that Fca7 may play important roles in the host-pathogen interaction in *F. graminearum*. To identify the transcription factors (TFs) regulating *FCA6*, *FCA7*, *FPX1*, and *FPX15* in response to oxidative stress, I screened an *F. graminearum* TF mutant library for growth in the presence of H_2O_2 and found that multiple TFs co-regulated the expression of *FCA7* under oxidative stress conditions. These results demonstrated that a complex network of transcriptional regulators of antioxidant genes is involved in the oxidative stress response in *F. graminearum*. In conclusion, studies of *ELP3* and peroxidase genes should provide insights into the roles of antioxidant genes in developmental processes and host-pathogen interactions in plant pathogenic fungi.

Keywords: *Fusarium graminearum*, Oxidative stress response, Elongator protein 3, peroxidase, Transcription factor

Student Number: 2011-21306

CONTENTS

CHAPTER 2. Genome-wide functional characterization of putative peroxidases in the head blight fungus *Fusarium graminearum*

LIST OF TABLE

CHAPTER 1

CHAPTER 2

LIST OF FIGURES

CHAPTER 1

CHAPTER 2

CHAPTER 1

Elp3 is involved in sexual and asexual development, virulence, and the oxidative stress response in *Fusarium graminearum*

ABSTRACT

Fusarium graminearum is an important fungal plant pathogen that causes serious losses in cereal crop yields and mycotoxicoses in humans and livestock. In this study, I characterized an insertion mutant, Z39R9282, with pleiotropic defects in sexual development and virulence. I determined that the insertion occurred in a gene encoding an ortholog of yeast Elongator complex protein 3 (Elp3). Deletion of *ELP3* led to significant defects in sexual and asexual development in *F. graminearum*. In the *elp3* deletion mutant, the number of perithecia formed was reduced and maturation of perithecia was delayed. This mutant also produced morphologically abnormal ascospores and conidia. Histone acetylation in the *elp3* deletion mutant was reduced compared to wild-type, which likely caused the developmental defects. Trichothecenes were not produced at detectable levels, and expression of trichothecene biosynthesis genes were significantly reduced in the *elp3* deletion mutant. Infection of wheat heads revealed that the *elp3* deletion mutant was unable to spread from inoculated florets to neighboring spikelets. Furthermore, the *elp3* deletion mutant was more sensitive to oxidative stress than wild-type, and the expression of putative catalase genes was reduced. I demonstrate that Elp3 functions in sexual and asexual development, virulence, and the oxidative stress response of *F. graminearum* by regulating the expression of genes involved in these various developmental processes

INTRODUCTION

The homothallic ascomycete fungus *Fusarium graminearum* is an important plant pathogen of major cereal crops such as wheat, maize, barley, and rice (Leslie and Summerell, 2006). Epidemics of Fusarium head blight (FHB) caused by *F. graminearum* result in serious losses in wheat and barley yields. Infected grains are commonly contaminated with mycotoxins, such as trichothecenes and zearalenone, that can lead to mycotoxicoses in humans and livestock (Desjardins and Proctor, 2007).

The random insertion mutagenesis method called restriction enzyme-mediated integration (REMI) was first described in *Saccharomyces cerevisiae* (Schiestl and Petes, 1991) and was later used to identify pathogenicity genes in several plant pathogenic fungi including *Cochliobolus heterostrophus*, *Ustilago maydis*, and *Magnaporthe grisea* (Lu et al., 1994; Bölker et al., 1995; Sweigard et al., 1998). REMI has been used to identify genes involved in *F. graminearum* sexual development and virulence (Han et al., 2004; Seong et al., 2005; Kim et al., 2009; Wang et al., 2011).

For pathogenic fungi to successfully colonize their hosts, various transcriptional regulatory mechanisms must control gene expression in response to environmental perturbations, such as osmotic and oxidative stress. Post-translational modifications of chromatin, such as histone acetylation, are closely associated with transcriptional activation (Wolffe and Pruss, 1996). Acetylation of lysine residues within the N-terminal tails of histone proteins changes chromatin structure by neutralizing positively-charged nucleosomes and, consequently,

increasing the accessibility of transcription factors to their target genes (Grunstein, 1997). Histone acetylation is mediated by histone acetyltransferases (HATs) and is reversed by histone deacetylases (HDACs). HATs transfer the acetyl groups from acetyl-coenzyme A to the lysine residues of histones, whereas HDACs remove the acetyl groups (Kuo and Allis, 1998). The general control non-derepressible 5 (Gcn5)-related acetyltransferase (GNAT) superfamily is one of the conserved HAT families (Carrozza et al., 2003), and members of the GNAT family have similar three-dimensional structures and catalytic domains (Vetting et al., 2005).

Elongator protein 3 (Elp3), a member of the GNAT family, is the catalytic subunit of the Elongator complex. Elongator complex was first identified in *S. cerevisiae* as a multisubunit complex associated with elongating RNA polymerase II (RNAPII) (Otero et al., 1999); it was later found to be comprised of six subunits, ELP1-ELP6. In yeast, purified Elp3 acetylated histones *in vitro*, and the HAT activity of Elp3 was essential for its function *in vivo* (Wittschieben et al., 1999; Wittschieben et al., 2000). Mammalian Elp3 was also purified and its ability to acetylate histones H3 and H4 was verified (Hawkes et al., 2002).

Previous studies revealed that *ELP3* was required for the activation of a group of stress-inducible genes in eukaryotes (Wittschieben et al., 2000; Han et al., 2007a; Nelissen et al., 2010; Creppe and Buschbeck, 2011). In *S. cerevisiae*, loss of *ELP3* reduced the activation of genes involved in the adaptation to stressful growth conditions (Wittschieben et al., 2000). In *Arabidopsis*, *ELP3* was required for the transcription of stress-induced and auxin-related genes (Chen et al., 2006; Nelissen et al., 2010). Using human cells, *ELP3* was found to regulate the heat shock response gene, *hsp70* (Han et al., 2007a). Although the biochemical function of

elp3 is conserved in eukaryotes, *elp3* target genes vary by species.

In this study, I identified the *F. graminearum* ortholog of *S. cerevisiae* Elp3 using a forward genetics approach. The *F. graminearum elp3* deletion mutant showed defects in sexual and asexual development, trichothecene production, virulence, and the oxidative stress response. I hypothesized that the pleiotropic defects seen in the *elp3* deletion mutant was caused by reduced histone acetylation and that *ELP3* might play a role in regulating pathogenicity genes in *F. graminearum*. The objectives of this study were to characterize the role (s) of *ELP3* in *F. graminearum* and to identify the stress-inducible genes regulated by *ELP3*. Our results demonstrated that Elp3 functioned in sexual and asexual development, virulence, and regulation of oxidative stress-induced genes in *F. graminearum.*

MATERIALS AND METHODS

I. Fungal strains and culture media

The *F. graminearum* wild-type strain Z-3639 (Bowden and Leslie, 1999) and mutants derived from this strain were used in this study (Table 1). All strains were stored as conidial suspensions in 20% glycerol at -70 °C. Culture media used in this study were prepared following the *Fusarium* laboratory manual (Leslie and Summerell, 2006). For conidia production, carboxymethyl cellulose (CMC) liquid culture media (Cappellini and Peterson, 1965) and yeast extract-malt extract agar (YMA) media (Harris, 2005) were used. Minimal media containing 5 mM agmatine (MMA) was used for trichothecene production (Gardiner et al., 2009).

II. Nucleic acid manipulations, primers, PCR conditions, and DNA sequencing

Genomic DNA was extracted from mycelia powder as previously described (Leslie and Summerell, 2006). Total RNA was extracted from mycelia in liquid nitrogen using the Easy-Spin Total RNA Extraction Kit (Intron Biotech, Seongnam, Korea). Standard techniques were used for restriction endonuclease digestion, Southern hybridization with ^{32}P-labeled probes, agarose gel electrophoresis, and plasmid rescue (Sambrook and Russell, 2001). The PCR primers used in this study (Table 2) were synthesized by an oligonucleotide synthesis facility (Bionics, Seoul, Korea). PCR was performed according to manufacturer's instructions (Takara Bio Inc., Ostu, Japan). DNA sequencing was performed at the National Instrumentation Center for Environmental Management (Seoul National University, Seoul, Korea) and sequences were compared against the *Fusarium* Comparative Database at the

Table 1 *F. graminearum* strains used in this study

Strain	Genotype	Reference
Z-3639	*F. graminearum* wild-type	(Bowden and Leslie, 1999)
Z39R9282	REMI mutant	This study
YJ17	Δ*elp3::GEN*	This study
YJ18	Δ*elp3::ELP3-HYG*	This study
hH1-GFP	*hH1::hH1-GFP-HYG*	(Hong et al., 2010)
Δ*mat1*	Δ*mat1-1::GEN*	(Lee et al., 2003)
mat1g	Δ*mat1-1::GEN hH1::hH1-GFP-HYG*	(Hong et al., 2010)
YJ19	Δ*elp3::GEN hH1::hH1-GFP-HYG*	This study
YJ20	Δ*mat1-1::GEN* Δ*elp3::GEN*	This study
YJ21	Δ*fca1::GEN*	This study
YJ22	Δ*fca2::GEN*	This study
YJ23	Δ*fca3::GEN*	This study
YJ24	Δ*fca4::GEN*	This study
YJ25	Δ*fca5::GEN*	This study
YJ26	Δ*fca6::GEN*	This study
YJ27	Δ*fca7::GEN*	This study
YJ28	*FCA7::GEN-*$P_{ef1\alpha}$*-FCA7*	This study
YJ29	Δ*elp3::GEN FCA7::GEN-*$P_{ef1\alpha}$*-FCA7*	This study

Table 2 Primers used in this study

Primer	Sequence (5' → 3')	Description
ELP3-5F	TGCTTCGGAACAGATGGTATGACT	Forward and reverse primers for amplification of 5' flanking region of *ELP3* with tail for geneticin resistance gene cassette fusion
ELP3-5R	GCACAGGTACACTTGTTTAGAGTGGGGACTGATTTTGCGATTTG	
ELP3-3F	CCTTCAATATCATCTTCTGTCGGAGCAGCCCGAGTAAATAGGAGAA	Forward and reverse primers for amplification of 3' flanking region of *ELP3* with tail for geneticin resistance gene cassette fusion
ELP3-3R	TTATGCTGGTGCGTAGGGCG	
ELP3-5N	TGAAGAAGCCAGCAAGAGACACAG	Forward and reverse nest primers for third fusion PCR for amplification of *ELP3* deletion construct
ELP3-3N	GTATGCGATGGATGAGGTGGTG	
ELP3-5R-com	GAATAGAGTAGATGCCGACCGCGTCGTAACTTTTCATTCCCATCCAA	Reverse primer for amplification of 5' flanking region and ORF of *ELP3* with tail for complementation
ELP3-3F-com	CCTTCAATATCATCTTCTGTCGGGCACCTGATTGGTCCAGTCTG	Forward primer for amplification of 3' flanking region of *ELP3* with tail for hygromycin resistance gene cassette fusion
FCA1-5F	ATATTTGCCGGCGTATTTCTCGTA	Forward and reverse primers for amplification of 5'

FCA1-5R	GCACAGGTACACTTGTTTAGAGTGTTCTGCTTGACACCATAATCGG	flanking region of *FCA1* with tail for geneticin resistance gene cassette fusion
FCA1-3F	CCTTCAATATCATCTTCTGTCGTGACTGTTGAAATTGCCGAGTTAGC	Forward and reverse primers for amplification of 3' flanking region of *FCA1* with tail for geneticin resistance gene cassette fusion
FCA1-3R	TCAATAACCCTACCACCCTGAGCA	
FCA1-5N	GGTTGGCAAGATTTCAAGCGAGTT	Forward and reverse nest primers for third fusion PCR for amplification of *FCA1* deletion construct
FCA1-3N	CTTTTGGGGGATGATGTCTGTGATACT	
FCA2-5F	AAGCTAAGGATGAGGTCGCAGTTCT	Forward and reverse primers for amplification of 5' flanking region of *FCA2* with tail for geneticin resistance gene cassette fusion
FCA2-5R	GCACAGGTACACTTGTTTAGAGTAGGGACATTGTGCAGCGGTTAG	
FCA2-3F	CCTTCAATATCATCTTCTGTCGAAGATTTAAAGGATGGGTTGGCTACT	Forward and reverse primers for amplification of 3' flanking region of *FCA2* with tail for geneticin resistance gene cassette fusion
FCA2-3R	GCCAAATGTCTCCAAAGGTCTGC	
FCA2-5N	AAAGAAGGGATGGCTGAGGAACACA	Forward and reverse nest primers for third fusion PCR for amplification of *FCA2* deletion construct
FCA2-3N	CTATGGCATCCCCGCTTGTCAG	

FCA3-5F	CACTTCCAATATTTATCTGCCTGCTAGA	Forward and reverse primers for amplification of 5' flanking region of *FCA3* with tail for geneticin resistance gene cassette fusion
FCA3-5R	GCACAGGTACACTTGTTTAGAGAGGACTGAAACTGGCTGGCTACG	
FCA3-3F	CCTTCAATATCATCTTCTGTCGTTGAACGGAACAAATGGTAAATAGGAG	Forward and reverse primers for amplification of 3' flanking region of *FCA3* with tail for geneticin resistance gene cassette fusion
FCA3-3R	ACGAGGAGATTGATGAGTTTAGCACC	
FCA3-5N	CACCGAATGGGGAGACGAAGG	Forward and reverse nest primers for third fusion PCR for amplification of *FCA3* deletion construct
FCA3-3N	GCTGCGGCGCTTGTTCCTATT	
FCA4-5F	TGGACCATGGCACCGATACG	Forward and reverse primers for amplification of 5' flanking region of *FCA4* with tail for geneticin resistance gene cassette fusion
FCA4-5R	GCACAGGTACACTTGTTTAGAGATTGTTGAAAAGCAGAGAAAACCACAT	
FCA4-3F	CCTTCAATATCATCTTCTGTCGAGCGCACTTTCCTCGTATTTCTAGC	Forward and reverse primers for amplification of 3' flanking region of *FCA4* with tail for geneticin resistance gene cassette fusion
FCA4-3R	GGTACGGTAAGAATGTAGTGCGATAAGAA	
FCA4-5N	AGTGCAGGGGGTTTGGTGTGAC	Forward and reverse nest primers for third fusion PCR for

FCA4-3N	GAGTATGCTCAATGTTGCTTCGTGTCA	amplification of *FCA4* deletion construct
FCA5-5F	GCCATGTTCCTTCTTCCGTCTCTA	Forward and reverse primers for amplification of 5' flanking region of *FCA5* with tail for geneticin resistance gene cassette fusion
FCA5-5R	GCACAGGTACACTTGTTTAGAGTCGAGAGAAGAAGAGGAATGTGGAGA	
FCA5-3F	CCTTCAATATCATCTTCTGTCGAGATCAAGTATCTCGCGCAGGTGTA	Forward and reverse primers for amplification of 3' flanking region of *FCA5* with tail for geneticin resistance gene cassette fusion
FCA5-3R	GTCCAGTTCCACCCCCTCGCTTAT	
FCA5-5N	TGTGCCAATTGAAGTGGTTGATAGTTG	Forward and reverse nest primers for third fusion PCR for amplification of *FCA5* deletion construct
FCA5-3N	TGCGGCCGCTGAGAAATAATACTT	
FCA6-5F	GGAGTTCCGCGCAAATGTGATA	Forward and reverse primers for amplification of 5' flanking region of *FCA6* with tail for geneticin resistance gene cassette fusion
FCA6-5R	GCACAGGTACACTTGTTTAGAGAGGAGAAACCGAGGCATAGAGAAAA	
FCA6-3F	CCTTCAATATCATCTTCTGTCGTGACTTATTGGCCCTTTACCTATTGTG	Forward and reverse primers for amplification of 3' flanking region of *FCA6* with tail for geneticin resistance gene cassette fusion
FCA6-3R	TTGCTTGAGTCAGTTAACCCCTACAG	

FCA6-5N	GCCTCAGCTGCCGCACTAAGAC	Forward and reverse nest primers for third fusion PCR for amplification of *FCA6* deletion construct
FCA6-3N	CCACTCATCAAATGCAAGCGTATCC	
FCA7-5F	AAGACCGGACGATTGCTGCTAC	Forward and reverse primers for amplification of 5' flanking region of *FCA7* with tail for geneticin resistance gene cassette fusion
FCA7-5R	GCACAGGTACACTTGTTTAGAGCAACAAGTTCTGCTGGGTATCACG	
FCA7-3F	CCTTCAATATCATCTTCTGTCGCACACGCGCTGATCTTGTCTTC	Forward and reverse primers for amplification of 3' flanking region of *FCA7* with tail for geneticin resistance gene cassette fusion
FCA7-3R	CTAAGCGTGATCTGAGAATAAGGTCGTA	
FCA7-5N	ACAGCATATTGCCCTTGTCACGAG	Forward and reverse nest primers for third fusion PCR for amplification of *FCA7* deletion construct
FCA7-3N	TGAGATCAGCTTCAAATGTGCCCA	
FCA7-OE-5R	GATAGTGGAAACCGACGCCCCGACGAGTAGGTCTTGTCAGATCT	Reverse primer for amplification of 5'flanking region of *FCA7* with tail for gen tagging overexpression
FCA7-OE-3F	TATCACAAAAGGAACCCAATCTTCAAAGTCGTCATGCACGCCAAAACT	Forward primer for amplification of *FCA7* ORF with tail for EF1α promoter tagging overexpression
FCA7-OE-3R	AGTAAGGAGACCAGCACGG	Reverse primer for amplification of *FCA7* ORF for overexpression

FCA7-OE-5N	CATATTGCCCTTGTCACGAGT	Forward and reverse nest primers for third fusion PCR for amplification of *FCA7* overexpression construct
FCA7-OE-3N	AGCAGTCCCGAGATCACG	
FCA1- RT-F	ACACTATTGCCGAGATGGTTGGT	For realtime-PCR of *FCA1*
FCA1-RT-R	GCGTTAAAGGCGACAGG	
FCA2-RT-F	CCTAGTATGGGACGAAGCACAGC	For realtime-PCR of *FCA2*
FCA2-RT-R	CCAGAACATCAAATCCAAACGCC	
FCA3-RT-F	GATTCATTCGCTTTCTGGGACTAC	For realtime-PCR of *FCA3*
FCA3-RT-R	CTGTATCCCCTGTTCGTTGTTAGT	
FCA4-RT-F	GCTATTGAGAAAGGCGACTATCCA	For realtime-PCR of *FCA4*
FCA4-RT-R	GCTTACATTCTTTTTCAACGTCAT	
FCA5-RT-F	CACTACTGGCATGAGGGGAAAAA	For realtime-PCR of *FCA5*
FCA5-RT-R	TACACCTGCGCGAGATACTTGAT	
FCA6-RT-F	AACGGGAACAAGGGAACCACTAA	For realtime-PCR of *FCA6*

FCA6-RT-R	ATCAGGTCAATCGGTAAGGGAAAG	
FCA7-RT-F	TCTCTTGGGCTGATCTTATGCTC	For realtime-PCR of *FCA7*
FCA7-RT-R	CGTAGATGTCAGTGCTGCCGTT	
Tri5-RT-F	GCCATTTTGGACCTTTCTGCTCATT	For realtime-PCR of *TRI5*
Tri5-RT-R	GCCATAGAGAAGCCCCAACACAAT	
Tri6-RT-F	GGCAACCATTCAAGCGCTTTTTCT	For realtime-PCR of *TRI6*
Tri6-RT-R	CACCCTGCTAAAGACCCTCAGACATT	
Cyp1-RT-F	TCAAGCTCAAGCACACCAAGAAGG	For realtime-PCR of *CYP1*
Cyp1-RT-R	GGTCCGCCGCTCCAGTCT	

Broad Institute (http://www.broadinstitute.org/annotation/genome/fusarium_group).

III. Genetic manipulations and fungal transformations

The double-joint (DJ) PCR method was used to generate fusion PCR products for the creation of targeted gene deletion, complementation, and overexpression strains (Yu et al., 2004). To create deletion strains, geneticin resistance gene (*GEN*) was amplified from pII99 (Namiki et al., 2001), and the 5′ and 3′ flanking regions of target genes were amplified from the wild-type strain. The three amplicons (5′ flanking, 3′ flanking, and *gen*) were fused by DJ PCR as previously described (Hong et al., 2010). For complementation of the *elp3* deletion mutant, a wild-type copy of *ELP3* was fused with hygromycin resistance gene (*HYG*) from pBCATPH (Gritz and Davies, 1983). The fusion construct was transformed into the deletion mutant as previously described (Han et al., 2007b). To construct the *FCA7* overexpression mutant, a fusion construct containing the 5′ flanking region of *FCA7*, the *FCA7* ORF, and the *GEN*-$P_{efl\alpha}$ region from pSKgen (Lee et al., 2011) was created and transformed into the wild-type strain.

IV. Conidia production and germination

Fungal strains were incubated in 50 ml of complete media (CM) for 72 h at 25 °C on a rotary shaker (150rpm). Mycelia were harvested and washed twice with sterile distilled water. To induce conidiation, harvested mycelia were spread onto YMA and incubated for 48 h at 25 °C under near UV light (wavelength: 365 nm, HKiv Import & Export Co., Ltd., Xiamen, China). Conidia were collected in sterile distilled water, filtered through cheesecloth, washed with sterile distilled water, and

collected by centrifugation (5000 rpm, 25 °C, 5 min). Conidia production was measured by counting the number of conidia produced after inoculating 5 ml of CMC with 10 µl of conidia suspension (10^5 conidia/ml) and incubating for 72 h at 25 °C on a rotary shaker (150 rpm). The rate of conidia germination was determined as previously described (Lee et al., 2009b). In brief, 10 ml of CM was inoculated with 1 ml of conidia suspension (10^6 conidia/ml) and incubated for 2, 4, 6, 8, and 12 h. The number of germinating conidia was counted at each timepoint.

V. Sexual crosses

For self-fertilizations, fungal strains were grown on carrot agar plates at 25 °C for 5 days. The mycelia grown on carrot agar plates were mock fertilized with 700 µl of a 2.5% Tween 60 solution (Leslie and Summerell, 2006) to induce sexual reproduction. After sexual induction, cultures were incubated under near UV light (wavelength: 365 nm, HKiv Import & Export Co., Ltd, Xiamen, China) at 25 °C. Perithecia and ascospores were observed 7 to 10 days after fertilization. For outcrosses, mycelia of heterothallic female strains grown on carrot agar plates for 5 days were fertilized with 1 ml of a male strain conidia suspension. After sexual induction, cultures were incubated under near UV light at 25 °C for 7 days. Ascospores were discharged onto 2% water agar plates. Ascospores were isolated and pure-cultured in CM.

VI. Ascospore discharge and germination

Ascospore discharge was observed using small acrylic chambers (1 by 2.5 by 5 cm) as previously described (Trail et al., 2005). A semicircular agar block (9.5

mm in diameter) covered with mature perithecia was placed on a coverslip and incubated in the chamber for 24 h.

Ascospore germination tests were performed as previously described (Lee et al., 2009b). Ascospores were harvested by placing the carrot agar upside down and allowing the mature perithecia to discharge ascospore on petri dish covers. One ml of ascospore suspension (10^6 conidia/ml) was incubated in 10 ml of CM for 2, 4, 6, 8, and 12 h. The number of germinating ascospores was counted at each timepoint. The experiments performed twice with three replicates.

VII. Virulence assays and trichothecene analysis

Virulence tests were performed using the susceptible wheat cultivar Eunpamil as previously described (Lee et al., 2009a). Ten μl of conidial suspensions (10^6 conidia/ml) harvested from CMC were injected into center spikelets of wheat heads at midanthesis. After inoculation, plants were incubated in a humidity chamber for 3 days and were then transferred to a greenhouse. Spikelets displaying symptoms of FHB were counted 21 days after inoculation.

Six days after inoculation, wheat spikes infected with green fluorescent protein (*GFP*)-tagged strains were evaluated. Freehand longitudinal sections of spikes were cut using a clean scalpel (Baldwin et al., 2010). Sectioned spikes were viewed with reflected light and fluorescent light (excitation 470 and emission 525) using a SteREO Lumar V12 microscope (Carl Zeiss).

Trichothecene production was measured as previously described (Son et al., 2011). In brief, MMA cultures were extracted with ethyl acetate and the extracts were dehydrated. Each dehydrated extract was derivatized with trimethylsilylating

reagent (BSA + TMCS + TMSI, 3:2:3, Supelco, Bellefonte, PA, USA) and analyzed on a Shimadzu QP-5000 gas chromatograph-mass spectrometer (GC-MS) (Shimadzu, Kyoto, Japan) using the selective ion-monitoring mode as previously described (Seo et al., 1996).

VIII. Stress sensitivity assays

To evaluate the effects of diverse stressors on mycelial growth, agar plugs from actively growing cultures were transferred to CM agar plates supplemented with osmotic stress agents (1.5 M D-sorbitol, 1.2 M NaCl, 1.2 M KCl), an oxidative stress agent (5 mM H_2O_2), cell wall damaging agents (5 mg/L SDS, 60 mg/L Congo red), and fungicides (0.023 mg/L fludioxonil, 8.6 mg/L iprodione, 0.65 mg/L benomyl). Plates were incubated at 25 °C for 5 days. For the temperature sensitivity test, the wild-type, *elp3* deletion mutant, and complementation strains were grown in CM at 25 °C, 30 °C, and 32 °C for 5 days in the dark. At least two independent tests were performed for each assay and each strain was tested in triplicate.

IX. Identification of catalase genes *F. graminearum*

To identify putative catalase and catalase-peroxidase genes in *F. graminearum*, a BLASTp search with *Magnaporthe oryzae* catalase and catalase-peroxidase sequences (Skamnioti et al., 2007) was performed in the *Fusarium* Comparative Database (http://www.broadinstitute.org/annotation/genome/fusarium_graminearum).

X. quantitative real-time (qRT) PCR analysis

Total RNA was extracted from wild-type and *elp3* deletion mutant strains grown for 3 h in CM only or in CM supplemented with 10 mM H_2O_2. cDNA was synthesized from the total RNA using SuperScriptⅢ reverse transcriptase (Invitrogen, Carlsbad, CA, USA). qRT-PCR was performed using SYBR Green Super mix (Bio-Rad, Hercules, CA, USA), a 7500 real-time PCR system (Applied Biosystems, Foster City, CA, USA), and primer pairs specific for catalase genes (Supplementary Table 1). The cyclophilin gene (*CYP1*; FGSG_07439.3) was used as the endogenous control for normalization (Kwon et al., 2009). qRT-PCR reactions were performed three times, and the transcript level of each target gene was calculated as previously described (Livak and Schmittgen, 2001).

To analyze transcription of the trichothecene biosynthesis genes,*TRI5* and *TRI6*, I incubated conidia from wild-type and *elp3* deletion mutant strains in MMA media for 5 days, isolated total RNA from each strain, and performed qRT-PCR as described above.

XI. Microscopic observations

Spore morphology was observed by differential interference contrast (DIC) microscopy. DIC images were obtained with a DE/Axio Imager A1 microscope (Carl Zeiss, Oberkochen, Germany) equipped with an UPlanApo 100X objective lens (1.3 numerical aperture; Carl Zeiss). AxioVision software (release 4.7; Carl Zeiss) was used to measure spore dimensions. Chitin staining was conducted by adding Calcofluor white stock solution (10 mg/ml; Sigma, 18909) to ascospore samples on slide glasses as previously described (Son et al., 2012). Ascospores

were observed using filter set 49 (excitation 356; emission 445/50). To visualize GFP expression in spores, microscopy was performed with the DE/Axio Imager A1 microscope (Carl Zeiss, Oberkochen, Germany) using the 38H (excitation 470/40; emission 525/50) filter set.

XII. Western blotting

Whole cell extracts (WCEs) were prepared as previously described (Son et al., 2011). In brief, mycelia harvested from carrot agar cultures were ground in liquid nitrogen and were extracted with 1 ml of breaking buffer (50 mM Tris at pH 8.4, 192 mM glycine, and 0.1% SDS) supplemented with 1 mM PMSF, a protease inhibitor. WCEs were separated on 15% sodium dodecyl sulfate polyacrylamide gels (SDS-PAGE) and transferred to nitrocellulose membranes (Amersham Pharmacia Biotech). Western blot analyses were performed using chemiluminescence (Amersham™ ECL Select™ Western Blotting Detection Reagent; Amersham Pharmacia Biotech) according to the manufacturer's instructions. Primary rabbit anti–histone H3 (Cell Signaling Technology, Beverly, MA) and anti-acetyl-Lys-4 H3 antibodies (07-353, Upstate Biotechnology, Inc.) were used at a 1:1,000 dilution. Anti-rabbit secondary antibody conjugated to horseradish peroxidase (Amersham Pharmacia Biotech) was used at a 1:4,000 dilution. The blocking buffer was composed of 5% dry nonfat milk in 0.1% Tween 20-TBS (pH 7.6). The detection method used was chemiluminescence and bands were visualized and quantified with Image Studio software (version 2.0; Li-Cor Biosciences, Lincoln, NE).

RESULTS

I. Identification of *ELP3*

A REMI mutant named Z39R9282 exhibited defects in sexual development and virulence relative to the wild type-strain (Fig. 1A). This mutant also had reduced aerial mycelia and excess accumulation of red pigments (Fig. 1A). Southern hybridization of Z39R9282 *Bgl*II-digested-genomic DNA using pBCATPH as a probe revealed that single insertion of the vector had occurred (Fig. 2B). Plasmid rescue was utilized to identify the insertion site, and it was found to be at the *Hind*III site located 274 bp downstream of the start codon of FGSG_02040.3, which encodes an ortholog of yeast Elp3 (Fig. 1B; Fig. 2A). *ELP3* contains a histone acetyltransferase (HAT) domain, a putative S-adenosylmethionine-binding domain, and iron-sulfur cluster domains. Elp3 is highly conserved among eukaryotes and a phylogenetic analysis of Elp3 orthologs revealed that they clustered into distinct groups according to their phyla. Fungal orthologs of Elp3 clustered into two groups corresponding to the subphyla Pezizomycotina and Saccharomycotina (Fig. 1C).

II. Targeted deletion and complementation

To elucidate the functions of *ELP3* in *F. graminearum*, targeted gene deletion and complementation strains were created by homologous recombination. The *ELP3* ORF in the *F. graminearum* wild-type strain Z-3639 was replaced with *GEN* to create the *elp3* deletion mutant strain. To generate the *ELP3* complementation strain, *GEN* was replaced on the wild-type allele of *ELP3* fused to *HYG*. Southern hybridizations were performed on *Sal*I-digested genomic DNA

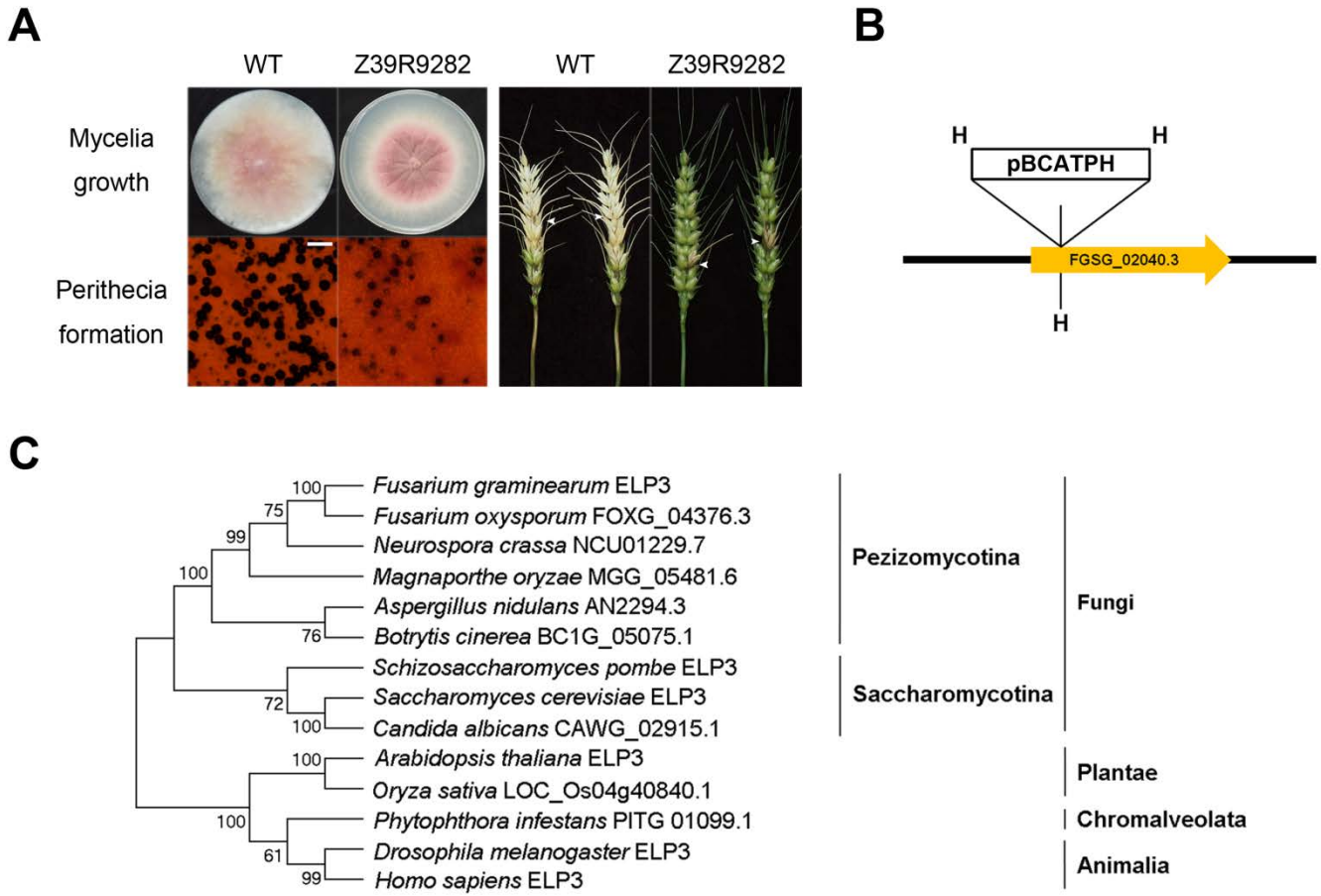
A
WT
Z39R9282
WT
Z39R9282
Mycelia growth
Perithecia formation
B
H
H
pBCATPH
FGSG_02040.3
H
C
100
75
99
100
76
72
100
100
100
61
99
Fusarium graminearum ELP3
Fusarium oxysporum FOXG_04376.3
Neurospora crassa NCU01229.7
Magnaporthe oryzae MGG_05481.6
Aspergillus nidulans AN2294.3
Botrytis cinerea BC1G_05075.1
Schizosaccharomyces pombe ELP3
Saccharomyces cerevisiae ELP3
Candida albicans CAWG_02915.1
Arabidopsis thaliana ELP3
Oryza sativa LOC_Os04g40840.1
Phytophthora infestans PITG 01099.1
Drosophila melanogaster ELP3
Homo sapiens ELP3
Pezizomycotina
Saccharomycotina
Fungi
Plantae
Chromalveolata
Animalia

Fig. 1 Identification of *ELP3*. (A) Phenotypes of the Z39R9282 mutant. Mycelial growth on complete medium (CM), perithecium formation on carrot agar, and virulence on wheat heads. Pictures were taken 5 days after inoculation on CM, 7 days after sexual induction on carrot agar, and 21 days after inoculation on wheat heads. Scale bar = 500 μm. Arrowheads mark the inoculated spikelets. (B) Schematic showing where the pBCATPH vector inserted into the Z39R9282 genome. (C) Phylogenetic tree of Elp3 orthologs in eukaryotes by ClustalW alignment. MEGA program Version 5.2 was used to perform a 1,000-bootstrap phylogenetic analysis using the neighbor joining method. WT, the *F. graminearum* wild-type strain Z-3639; H, *Hind*III.

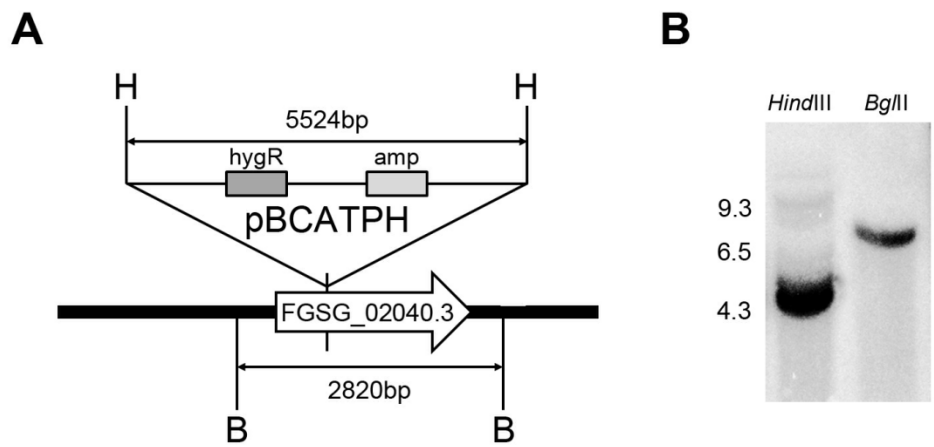

Fig. 2 Schematic and Southern blot of REMI strain Z39R9282. (A) Schematic showing the location and contents of the vector insertion in strain Z39R9282. H, *Hind*III; B, *Bgl*II; hyg, hygromycin B resistance gene. (B) Southern blot of Z39R9282 genomic DNA digested with *Hind*III (lane 1) or *Bgl*II (lane 2) and probed with pBCATPH. The DNA size standards (kb) are indicated on the left of the blot.

from these strains using the 5′ flanking region of *ELP3* as a probe, and these hybridizations confirmed successful gene deletion and complementation (Fig. 3). When cultured on CM, the *elp3* deletion mutant produced sparse aerial mycelia and more red pigments compared to the wild-type and complementation strains (Fig. 4A). However, there was no significant difference in radial growth among the strains (Table 1). The *elp3* deletion mutant showed indistinguishable phenotypes with a REMI mutant Z39R9282 in sexual and asexual development, virulence, and toxin production (data not shown).

III. Sexual and asexual development

When self-fertilized, the *elp3* deletion mutant produced fewer perithecia compared to the wild-type and complementation strains (Fig. 4B). Perithecia maturation was also delayed, but not abolished, in the *elp3* deletion mutant. Seven days after sexual induction, perithecia produced asci with mature ascospores in the wild-type strain, whereas immature perithecia with young asci were observed in the *elp3* deletion mutant. Ten days after sexual induction, several asci containing mature ascospores were observed in the *elp3* deletion mutant (Fig. 4C). The *elp3* deletion mutant produced ascospore cirrhi (Fig. 4B) and discharged ascospores (Fig. 2D) similar with the wild-type strain. Reduced number of discharged ascospores of the *elp3* deletion mutant was due to fewer perithecia (Fig. 4D).

Although both the wild-type and the *elp3* deletion mutant strains produced and discharged ascospores, their morphologies differed (Fig. 5A). To visualize the nucleus in the elp3 deletion mutant, I generated strain YJ19 (Δ*elp3::GEN hH1::hH1-GFP-HYG*) by outcrossing mat1g (Hong et al., 2010) and the *elp3*

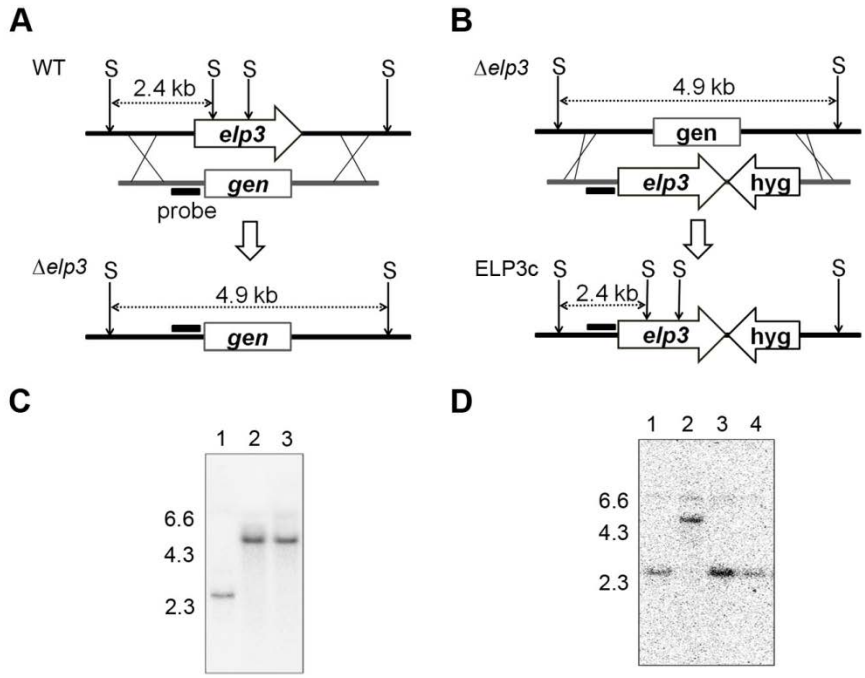

Fig. 3 Targeted deletion and complementation of *ELP3*. (A) The *elp3* deletion mutant was constructed by homologous recombination with the wild-type strain and a gene fusion containing the geneticin resistance gene. (B) The complementation strain ELP3c was constructed by homologous recombination with the *elp3* deletion strain and an *ELP3*-hygromycin B resistance gene fusion. WT, the *F. graminearum* wild-type strain Z-3639; Δ*elp3*, the *elp3* deletion mutant; ELP3c, the Δ*elp3* mutant-derived strain complemented with *ELP3*; S, SalI; *gen*, geneticin resistance gene cassette; *hyg*, hygromycin B resistance gene. (C) Southern hybridization confirmation of the *elp3* deletion mutant. Lane 1, WT; lanes 2 and 3, isolates of the *elp3* deletion mutant. (D) Southern hybridization confirmation of the *ELP3* complementation strain. Lane 1, WT; lane 2, *elp3* deletion mutant; lanes 3 and 4, isolates of the *ELP3* complementation strain. The DNA size standards (kb) are indicated on the left of the blot.

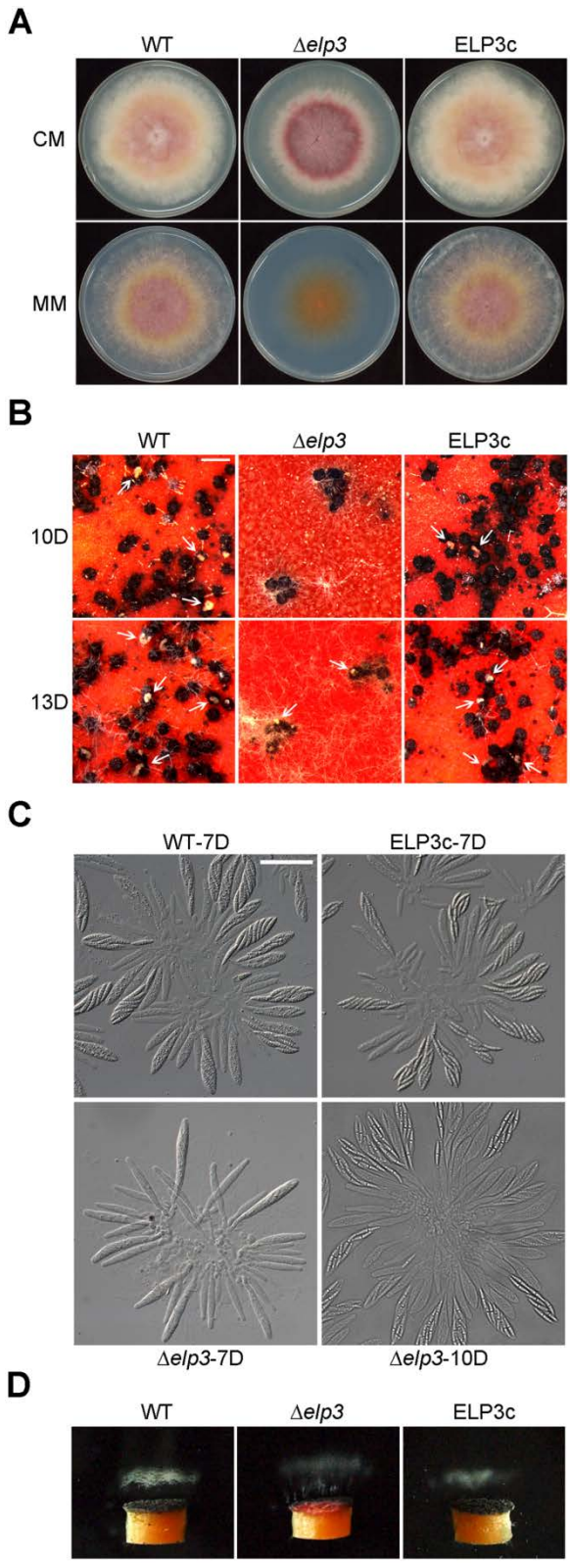
A
WT
Δelp3
ELP3c
CM
MM
B
WT
Δelp3
ELP3c
10D
13D
C
WT-7D
ELP3c-7D
Δelp3-7D
Δelp3-10D
D
WT
Δelp3
ELP3c

Fig. 4 Vegetative growth and sexual development of *F. graminearum* strains. (A) Mycelial growth of *F. graminearum* strains. Pictures were taken 5 days after inoculation on complete medium (CM). WT, the *F. graminearum* wild-type strain Z-3639; Δ*elp3*, the *elp3* deletion mutant (YJ17); ELP3c, the Δ*elp3* mutant-derived strain complemented with *ELP3* (YJ18). (B) Perithecium formation by *F. graminearum* strains. Cirrhi (indicated with white arrow) were observed in the wild-type and complementation strains 10 days (D) after sexual induction. Thirteen days after sexual induction, the *elp3* deletion mutants formed cirrhi. Pictures were taken 10 and 13 days after sexual induction on carrot agar. Scale bar = 500 μm. (C) Morphologies of asci rosettes. Microscopic observations were performed 7 and 10 days (D) after sexual induction. Scale bar = 50 μm. (D) Forcible discharge of ascospores from perithecia produced on carrot agar. A semicircular agar block covered with mature perithecia was placed on a coverslip.

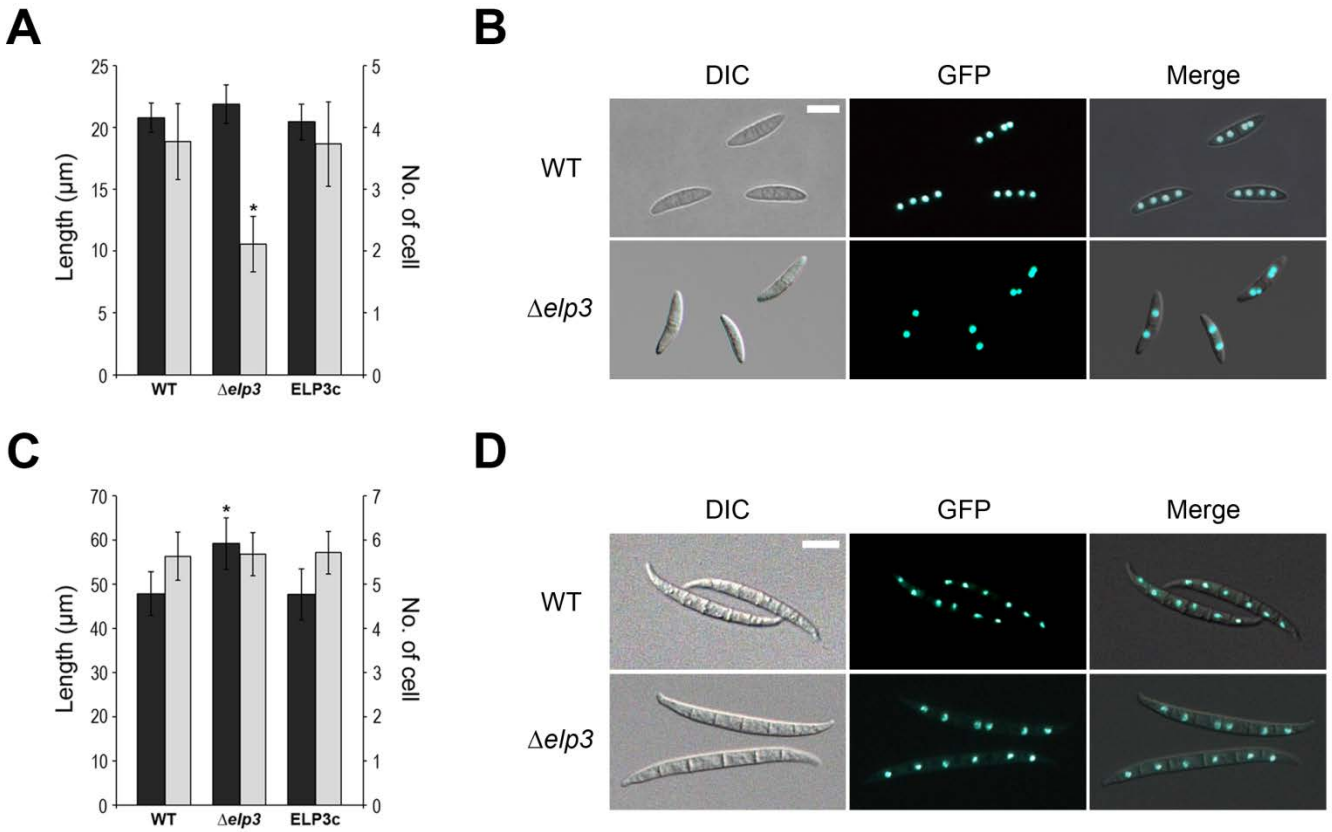
A
Length (μm)
No. of cell
WT
Δelp3
ELP3c
B
DIC
GFP
Merge
WT
Δelp3
C
Length (μm)
No. of cell
WT
Δelp3
ELP3c
D
DIC
GFP
Merge
WT
Δelp3

Fig. 5 Morphologies of ascospores and conidia. (A) Length (dark gray) and number of septa (light gray) of ascospores from *F. graminearum* strains. Error bars indicate the standard deviations. An asterisk indicates a significant difference ($P < 0.01$, Tukey's test). WT, the *F. graminearum* wild-type strain Z-3639; Δ*elp3*, the *elp3* deletion mutant (YJ17); ELP3c, the Δ*elp3* mutant-derived strain complemented with *ELP3* (YJ18). (B) Microscopic observations of ascospores. Fluorescent green dots represent hH1-GFP. DIC, differential interference contrast image; GFP, fluorescence microscopy image; Merge, overlays of the DIC and fluorescence microscopy images. Scale bar = 10 μm. (C) Length (dark gray) and number of septa (light gray) of conidia on YMA. (D) Microscopic observations of conidia. Scale bar = 10 μm.

deletion mutant. In the wild-type strain, the majority of ascospores were four-celled and the individual cells were uninucleate and of equal size. In contrast, the ascospores in the *elp3* deletion mutant were mainly two-celled and each cell tended to contain two nuclei (Fig. 5B). The mean ascospore length of the *elp3* deletion mutant (21.9 μm) was similar to that of the wild-type strain (20.8 μm) regardless of the number of cells (Fig. 5A). The germinability of ascospores was not affected by the deletion of *elp3* (Table 3). Binucleate two-celled ascospores from the *elp3* deletion mutant germinated on CM without changes in septation (Fig. 6).

Conidia production and germination of the *elp3* deletion mutant did not differ from the wild-type and complementation strains (Table 3). The average length of conidia produced from the *elp3* deletion mutant YMA was approximately 20% longer than conidia produced from the wild-type strain ($P < 0.01$). The mean length of conidia from the *elp3* deletion mutant was 59.2 μm, while that of the wild-type strain was 47.8 μm (Fig. 5C). Despite the increased length of the conidia in the *elp3* deletion mutant, the number of septa was similar to wild-type (Fig. 5C).

IX. Trichothecene production and virulence

The production of trichothecenes was analyzed in MMA by GC-MS. Deoxynivalenol and 15-acetyldeoxynivalenol, major trichothecenes produced in MMA, were not detected in the *elp3* deletion mutant (Fig. 7A), whereas trichothecene production by the complementation strain did not differ from that of the wild-type strain. The qRT-PCR results showed that transcription of the trichothecene biosynthesis genes, *TRI5* and *TRI6*, was significantly reduced in the *elp3* deletion mutant compared to the wild-type strain (Fig. 7B).

Table 3 Radial growth, ascospore germination, and conidiation in *F. graminearum* strains

Strain	Radial growth (cm)[a]	Ascospore germination (%)[b]	Conidia	
			Germination (%)[c]	Production (no. of conidia/ml)[d]
Z-3639	9.8 A[e]	69.0 A	48.3 A	2.7×10^6 A
YJ17	9.8 A	70.3 A	47.7 A	2.7×10^6 A
YJ18	10.0 A	68.3 A	50.3 A	2.6×10^6 A

[a] Radial growth was measured after 5 days incubation on complete medium (CM)

[c] Percentage of germinating ascospores was measured after 8 h of incubation

[c] Percentage of germinating conidia was measured after 8 h of incubation

[d] Number of conidia were counted after 3 days of incubation in carboxymethyl cellulose (CMC)

[e] All data were repeated twice with three replications. Values within a column that are significantly different ($p < 0.05$) based on a Tukey's test are indicated with letters.

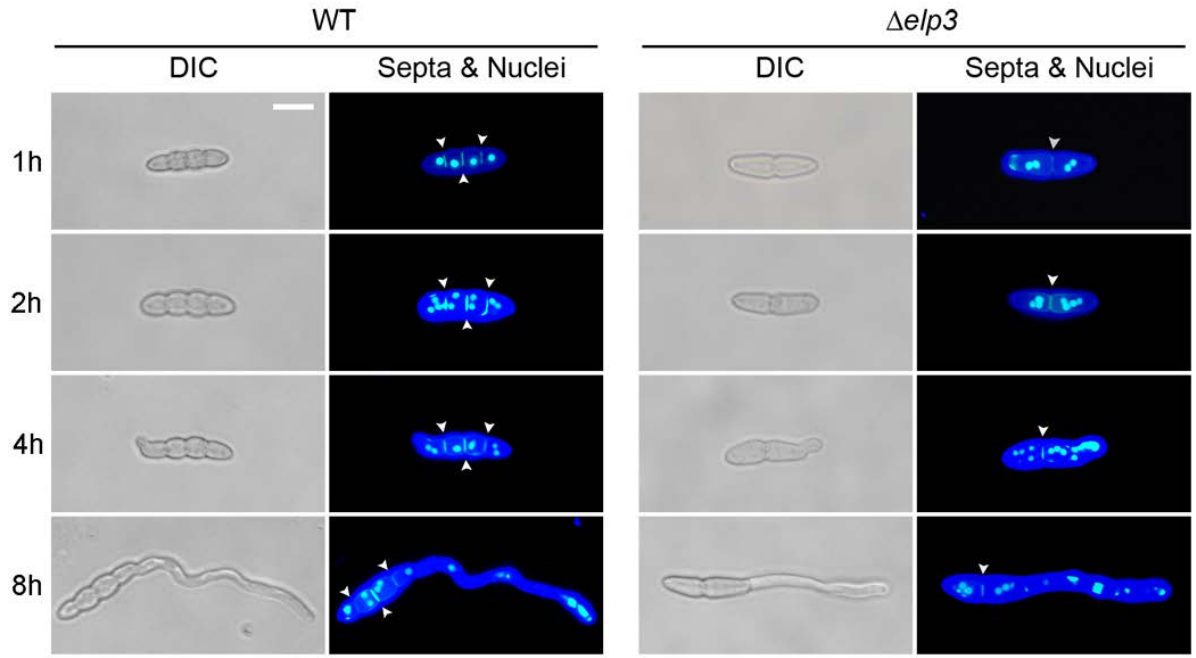

Fig. 6 Germination of *F. graminearum* strains. Histone H1 was tagged with green fluorescent protein (GFP) to visualize nuclei. Cell wall was stained with calcofluor white. Arrowheads indicate septa. Binucleate two-celled ascospores from *elp3* deletion mutant underwent mitotic nuclear division without cellular division of cytoplasm before formation of germ tubes as seen in the wild-type strain. Scale bar = 10 μm. WT, the *F. graminearum* wild-type strain Z-3639; Δ*elp3*, the *elp3* deletion mutant YJ17.

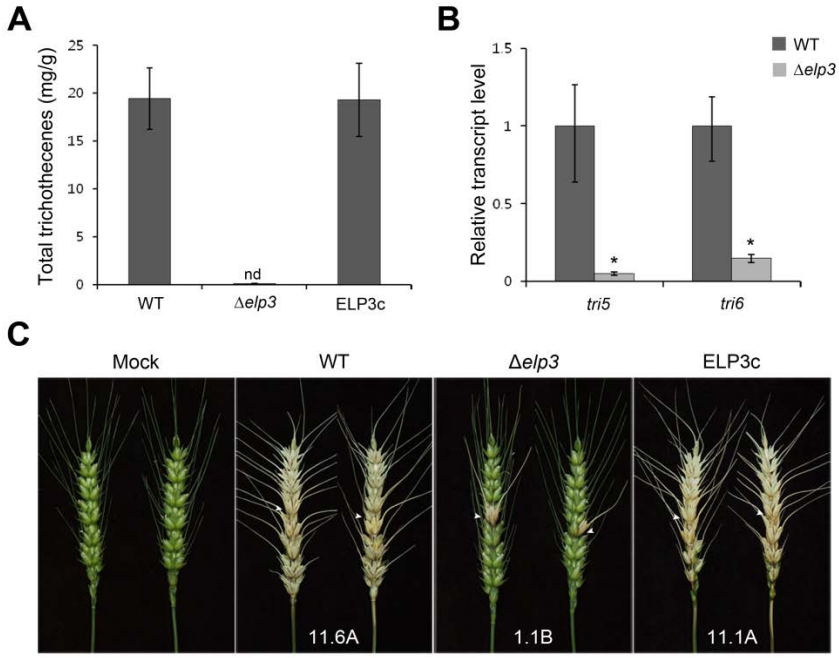

Fig. 7 Trichothecene production and virulence of *F. graminearum* strains. (A) Total trichothecene production by *F. graminearum* strains. Each strain was grown in minimal media containing MMA for 7 days. Trichothecenes were analyzed by GC-MS and were quantified based on the biomass of each strain. WT, the *F. graminearum* wild-type strain Z-3639; Δ*elp3*, the *elp3* deletion mutant; ELP3c, the Δ*elp3* mutant-derived strain complemented with *ELP3*; nd, not detected. (B) Transcript levels of *TRI5* and *TRI6* in the wild-type and *elp3* deletion mutant strains. Transcript levels were analyzed by qRT-PCR 4 days after inoculation in MMA. An asterisk indicates a significant difference ($P < 0.01$, Tukey's test). (C) Virulence on wheat heads. The center spikelet of each wheat head was injected with 10 µl of a conidial suspension, and pictures were taken 21 days after inoculation. Arrowheads indicate the inoculated spikelets. Significantly different ($P < 0.01$, Tukey's test) disease indices (diseased spikelets per wheat head) are designated with different letters. Mock, mock-inoculated with 0.01 % of Tween 20.

In a virulence test, 21 days after wheat head inoculation, the *elp3* deletion mutant caused significantly reduced disease symptoms ($P < 0.01$), whereas the wild-type and complementation strains caused typical head blight symptoms (Fig. 7C). In wheat heads inoculated with the *elp3* deletion mutant, the spread of the disease within a spike was blocked and only artificially inoculated spikelets showed necrosis. To visualize the spread of mycelia on wheat heads during infection, strains constitutively expressing GFP were injected into the center spikelets of wheat heads. Six days after inoculation with the *elp3* deletion mutant that constitutively expresses GFP (YJ19), hyphae were seen throughout the rachis but failed to spread to the adjacent spikelet (Fig. 8), whereas inoculation with the wild-type GFP-expressing strain (hH1-GFP) led to the spread of hyphae to the adjacent spikelet through rachis node.

X. Stress sensitivity assay

Previous studies on *ELP3* in other eukaryotes revealed that it regulated the expression of stress-inducible genes (Wittschieben et al., 2000; Chen et al., 2006; Han et al., 2007a). To determine whether *ELP3* is required for the stress response in *F. graminearum*, strains were inoculated onto CM supplemented with various stress agents including osmotic stress agents (NaCl, KCl, and D-sorbitol), an oxidative stress agent (H_2O_2), cell wall damaging agents (SDS and Congo red), and fungicides (fludioxonil, iprodione, and benomyl), and their sensitivities to these agents were evaluated. In addition, sensitivity to high temperature stress was tested. Hyphal growth of the *elp3* deletion mutant was severely inhibited by oxidative stress compared to the wild-type strain (Fig. 9A), but none of the other stress

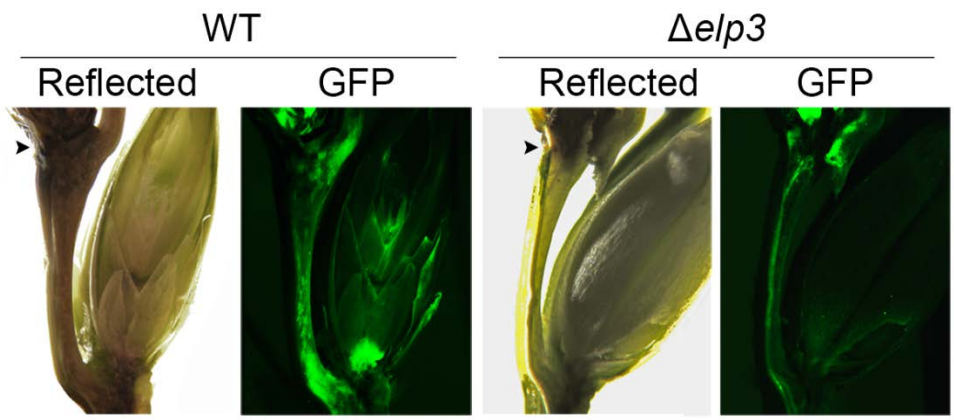

Fig. 8 Longitudinal sections of infected wheat heads. Wheat spikelets were inoculated with suspensions of conidia from GFP-expressing *F. graminearum* strains. Infected wheat heads were dissected 6 days after inoculation and examined by fluorescence microscopy. Spreading of the GFP signal represents spreading of hyphae from the points of inoculation. Arrowheads mark the inoculated spikelets. WT, the *F. graminearum* wild-type strain Z-3639; Δ*elp3*, the *elp3* deletion mutant YJ17; Reflected, reflected light.

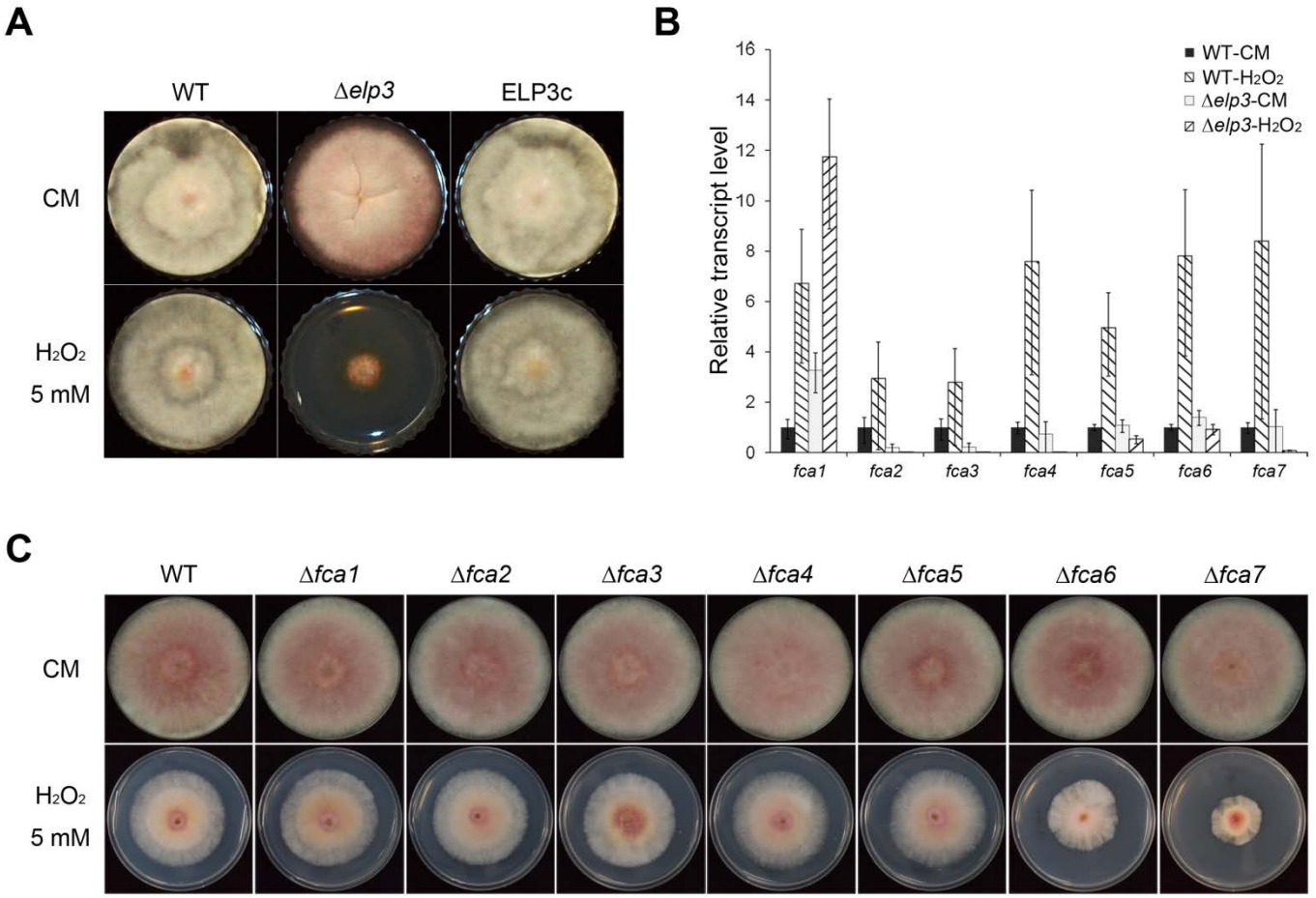
A
WT
Δelp3
ELP3c
CM
H2O2
5 mM
B
Relative transcript level
WT-CM
WT-H2O2
Δelp3-CM
Δelp3-H2O2
fca1
fca2
fca3
fca4
fca5
fca6
fca7
C
WT
Δfca1
Δfca2
Δfca3
Δfca4
Δfca5
Δfca6
Δfca7
CM
H2O2
5 mM

Fig. 9 Sensitivity of *F. graminearum* strains to oxidative stress and transcriptional analyses of catalase genes. (A) Mycelial growth of *F. graminearum* strains on CM supplemented with 5 mM H_2O_2. WT, the *F. graminearum* wild-type strain Z-3639; Δ*elp3*, the *elp3* deletion mutant (YJ17); ELP3c, the Δ*elp3* mutant-derived strain complemented with *ELP3* (YJ18). (B) Transcript levels of catalase genes in the wild-type and *elp3* deletion mutant strains. Total RNA was isolated from the wild-type and *elp3* deletion mutant strains grown for 3 h in CM only or in CM supplemented with 10 mM H_2O_2, and gene transcripts were analyzed by qRT-PCR. (C) Mycelial growth of wild-type and catalase deletion mutant strains on CM supplemented with 5 mM H_2O_2. Δ*fca1*, the *fca1* deletion mutant (YJ21); Δ*fca2*, the *fca2* deletion mutant (YJ22); Δ*fca3*, the *fca3* deletion mutant (YJ23); Δ*fca4*, the *fca4* deletion mutant (YJ24); Δ*fca5*, the *fca5* deletion mutant (YJ25); Δ*fca6*, the *fca6* deletion mutant (YJ26); Δ*fca7*, the *fca7* deletion mutant (YJ27).

conditions affected hyphal growth of the *elp3* deletion mutant (Fig. 10 and Fig. 11), indicating that *ELP3* was specifically involved in the oxidative stress response.

XI. Identification of catalase genes in *F. graminearum*

To investigate the expression of oxidative stress-induced genes in the *elp3* deletion mutant, I first identified catalase genes in *F. graminearum*. Five putative monofunctional catalase genes (FGSG_06554.3, FGSG_06733.3, FGSG_16526.3, FGSG_02881.3, and FGSG_06596.3) were previously identified by BLASTp searches using *Cryptococcus neoformans* catalase sequences (Giles et al., 2006). I identified two bifunctional catalase-peroxidase genes (FGSG_02974.3 and FGSG_12369.3) by BLASTp searches in the *Fusarium* Comparative Database (http://www.broadinstitute.org/annotation/genome/fusarium_graminearum) using *M. oryzae* catalase-peroxidase sequences (Skamnioti et al., 2007). I designated these seven *F. graminearum* catalase genes *fca1* to *fca7* (Table 1).

XII. Expression and functional analyses of catalase genes in *F. graminearum*

I performed qRT-PCR to measure transcript levels of the putative catalase genes in the wild-type and *elp3* deletion mutant strains under oxidative stress. In the wild-type strain, catalase gene transcripts were upregulated in 10 mM H_2O_2. However, in the *elp3* deletion mutant, catalase gene transcripts, except *FCA1*, were either down-regulated or unchanged in 10 mM H_2O_2 (Fig. 6B). The qRT-PCR results indicated that the *elp3* deletion mutant was unable to regulate catalase gene transcription in response to oxidative stress.

To further investigate the functions of the putative catalase genes in *F.*

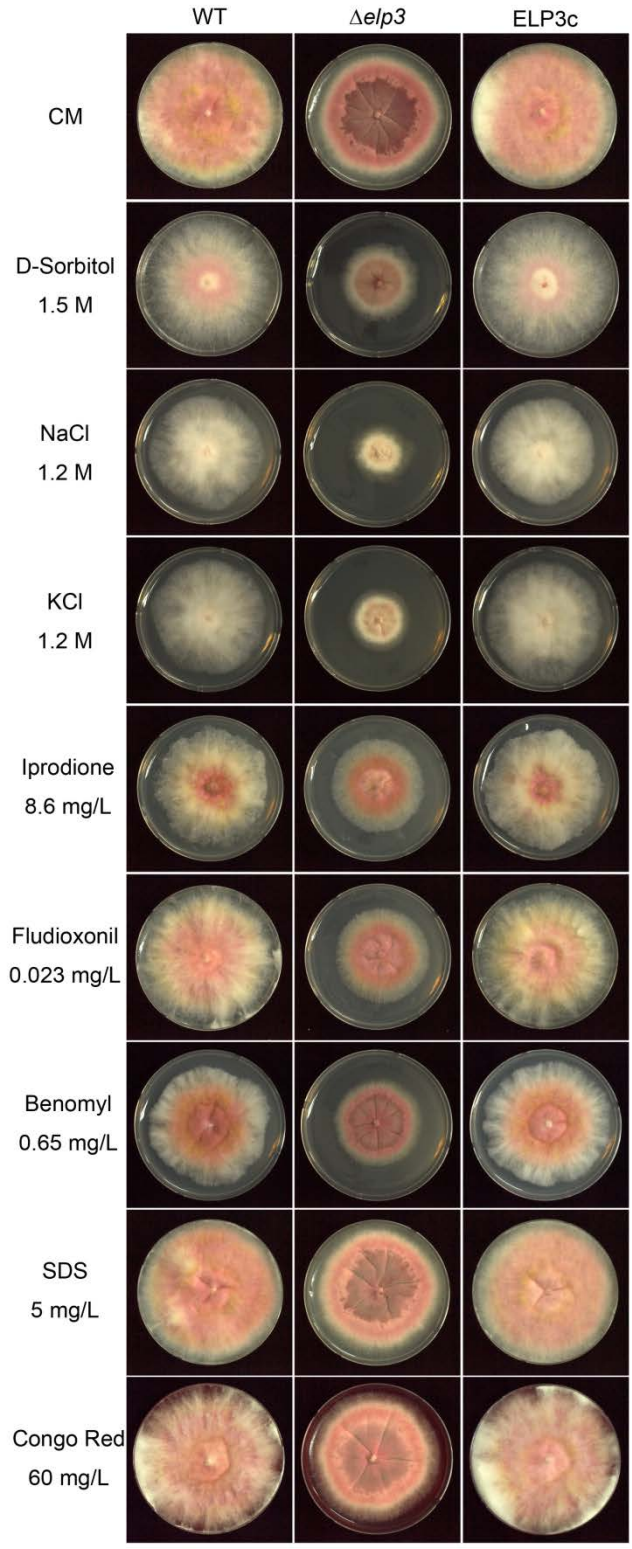
WT
Δelp3
ELP3c
CM
D-Sorbitol
1.5 M
NaCl
1.2 M
KCl
1.2 M
Iprodione
8.6 mg/L
Fludioxonil
0.023 mg/L
Benomyl
0.65 mg/L
SDS
5 mg/L
Congo Red
60 mg/L

Fig. 10 Mycelial growth of *F. graminearum* strains on CM supplemented with osmotic stress agents (1.5 M D-sorbitol, 1.2 M NaCl, and 1.2 M KCl), an oxidative stress agent (5 mM H_2O_2), cell wall damaging agents (5 mg/L SDS and 60 mg/L Congo red), and fungicides (0.023 mg/L fludioxonil, 8.6 mg/L iprodione, and 0.65 mg/L benomyl). WT, the *F. graminearum* wild-type strain Z-3639; Δ*elp3*, the *elp3* deletion mutant (YJ17); ELP3c, the Δ*elp3* mutant-derived strain complemented with *ELP3* (YJ18).

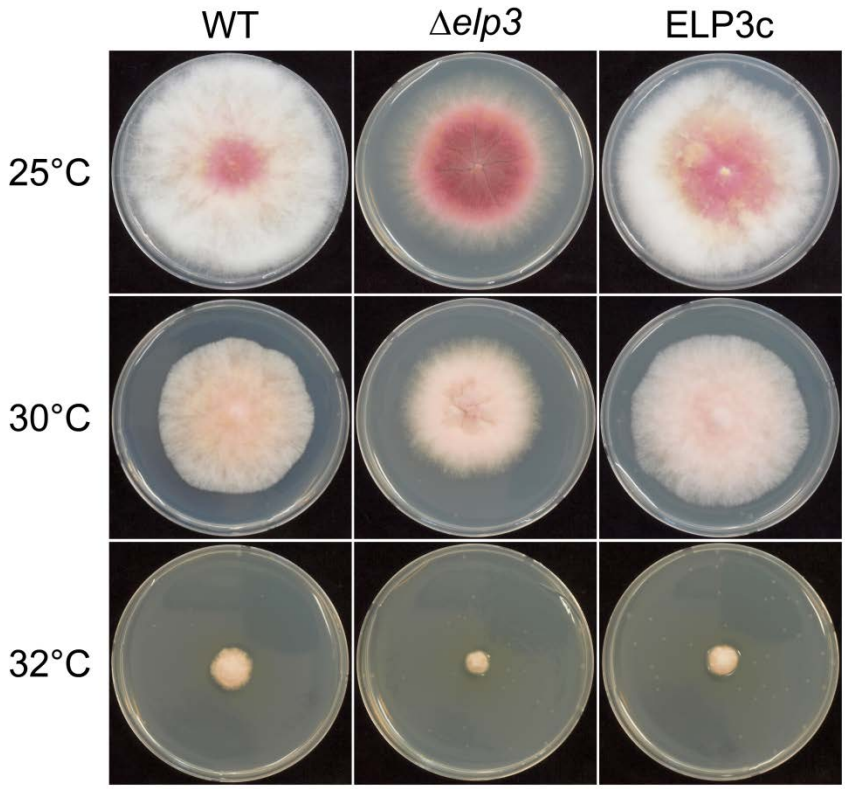

Fig. 11 Sensitivity of *F. graminearum* strains to higher temperatures. WT, the *F. graminearum* wild-type strain Z-3639; Δ*elp3*, the *elp3* deletion mutant (YJ17); ELP3c, the Δ*elp3* mutant-derived strain complemented with *ELP3* (YJ18).

graminearum, I generated deletion mutants of these genes through homologous recombination (Table 1; Fig. 12) and assayed the sensitivities of these deletion mutants to 5 mM H_2O_2. Only the *fca6* and *fca7* deletion mutant strains exhibited increased sensitivities to oxidative stress compared to the wild-type strain (Fig. 9C). Hyphal growth of the *fca7* deletion mutant was significantly reduced in the presence of H_2O_2 suggesting that Fca7 plays a major role in degrading extracellular H_2O_2 during vegetative growth.

I then created an *FCA7*-overexpression strain (*FCA7::GEN-*$P_{ef1\alpha}$*-FCA7*, YJ28) in which *FCA7* expression was controlled by the elongation factor 1 alpha (ef1α) promoter (Fig. 13A). qRT-PCR was used to quantify *FCA7* transcripts in the wild-type and *FCA7*-overexpression strains and *FCA7* overexpression was confirmed in strain YJ28 (Fig. 13B). We tested the *FCA7*-overexpression strain for sensitivity to oxidative stress and found that it was more tolerant to H_2O_2 than the wild-type strain (Fig. 13C). To determine whether the oxidative stress sensitivity of the *elp3* deletion mutant was due to the reduced expression of *FCA7*, we generated strain YJ29 (Δ*elp3::GEN FCA7::GEN-*$P_{ef1\alpha}$*-FCA7*) by outcrossing the heterothallic strain carrying the *elp3* mutation (strain YJ20; Δ*mat1-1::GEN* Δ*elp3::GEN*) with strain YJ28 (*FCA7::GEN-*$P_{ef1\alpha}$*-FCA7*) and confirmed the genotype of strain YJ29 by PCR. The oxidative stress sensitivity of the *elp3* deletion mutant strain was partially restored by overexpression of *fca7* (Fig. 13C).

XIII. Western blot analysis of histone acetylation

To investigate whether the deletion of *elp3* affected histone H3 acetylation in *F. graminearum*, we measured acetylation of lysine 14 in H3 (H3K14Ac) in the

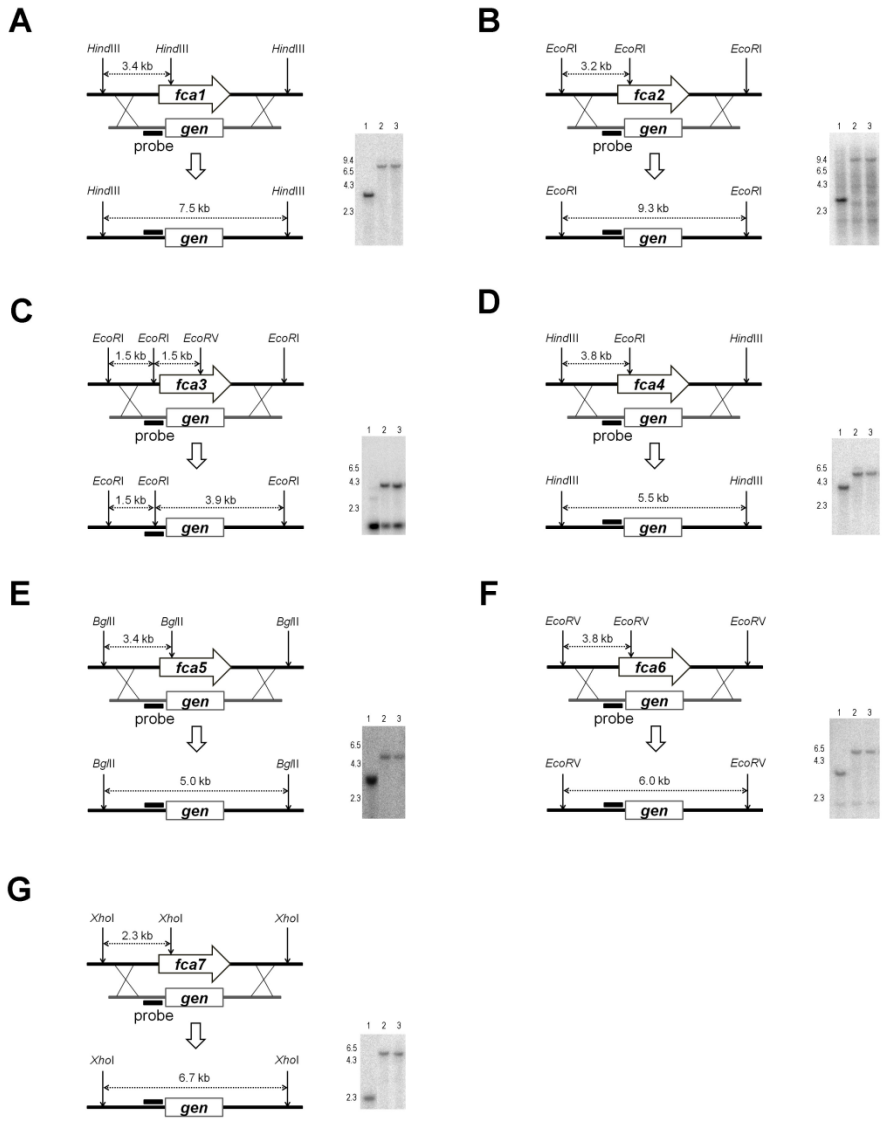

Fig. 12 Schematics and Southern blots of catalase gene deletions. WT, the *F. graminearum* wild-type strain Z-3639; Δ*fca1*, the *fca1* deletion mutant; Δ*fca2*, the *fca2* deletion mutant; Δ*fca3*, the *fca3* deletion mutant; Δ*fca4*, the *fca4* deletion mutant; Δ*fca5*, the *fca5* deletion mutant; *fca6*, the *fca6* deletion mutant; Δ*fca7*, the *fca7* deletion mutant; gen, geneticin resistance gene. Lane 1, WT; lanes 2 and 3, deletion mutants. The DNA size standards (kb) are indicated on the left of the blot.

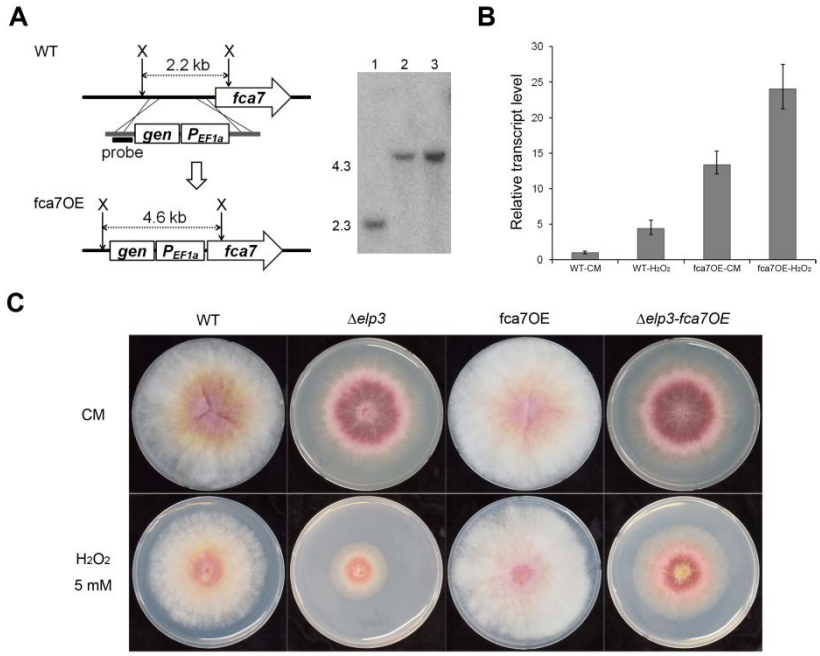

Fig. 13 Sensitivity of the *fca7* overexpression strain to oxidative stress. (A) The *ef1α* promoter was inserted into the natural promoter of *FCA7*. The left panel shows how the *FCA7* overexpression strain was constructed and the right panel confirms insertion by Southern analysis. WT, the *F. graminearum* wild-type strain Z-3639; fca7OE, overexpression strain in which the natural *FCA7* promoter was replaced with the *ef1α* promoter (YJ28); X, *Xal*I; *gen*, geneticin resistance gene ; Lane 1, Z-3639; lanes 2 and 3, isolates of the *FCA7* overexpression strain. The DNA size standards (kb) are indicated on the left of the blot. (B) Transcript levels of *FCA7* in the wild-type and *FCA7* overexpression strains. Total RNA was isolated from the wild-type and *FCA7* overexpression strains grown for 3 h in CM only or in CM supplemented with H_2O_2, and transcript levels were analyzed by qRT-PCR. (C) Mycelial growth of fungal strains on CM supplemented with 5 mM H_2O_2. Δ*elp3*, the *elp3* deletion mutant (YJ17); Δ*elp3-FCA7OE*, the *elp3* deletion mutant that overexpresses *FCA7* (YJ29).

wild-type and the *elp3* deletion mutant strains by Western blot analysis (Fig. 14A). We chose lysine 14 of H3 because, in yeast, it is one of the main acetylation sites of the Elongator complex (Winkler et al., 2002). Although relative histone acetylation level was highest three days after sexual induction for both the wild-type and the *elp3* deletion mutant, histone acetylation was markedly reduced in the *elp3* deletion mutant (Fig. 14B).

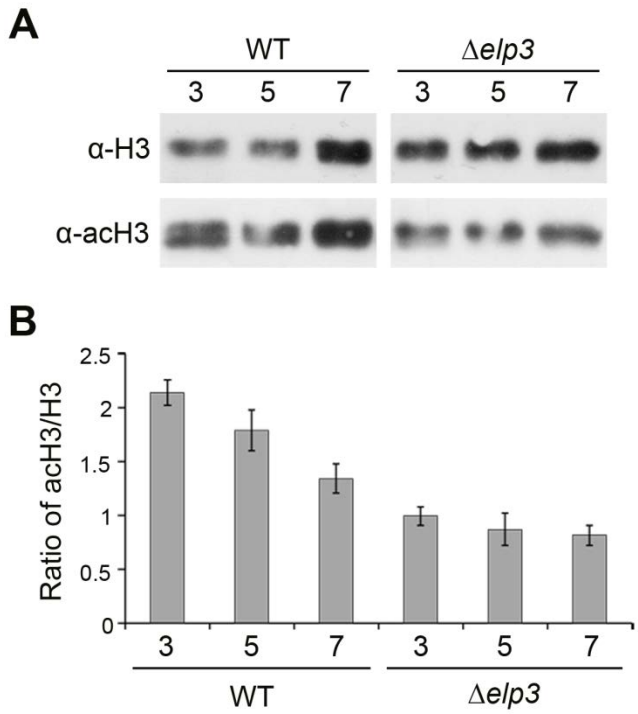

Fig. 14 Western blot of whole cell extracts of *F. graminearum* strains. (A) Whole cell extracts were prepared from carrot agar cultures. WT, the *F. graminearum* wild-type strain Z-3639; Δ*elp3*, the *elp3* deletion mutant (YJ17); α-H3, primary antibody against histone H3; α-acH3, primary antibody against histone H3 acetylated at Lys14. The numbers above the blots indicate the number of days of incubation after sexual induction. (B) The levels of α-acH3 and α-H3 binding were quantified using Image Studio software, and the data is presented as the ratio of α-acH3/α-H3 binding. The error bars represent the standard deviations of three independent experiments.

DISCUSSION

In this study, we identified a gene encoding an ortholog of yeast Elp3 in *F. graminearum* using forward genetics. To elucidate the functions of Elp3 in *F. graminearum*, we created an *elp3* deletion mutant and analyzed its phenotypes. We found that Elp3 was involved in diverse biological processes including sexual and asexual reproduction, trichothecene production, and virulence in *F. graminearum*. We also found that Elp3 played a role in the oxidative stress response by regulating catalase gene expression.

In *F. graminearum*, hundreds of genes required for sexual and asexual reproduction must be tightly regulated in time and space (Qi et al., 2006; Hallen et al., 2007; Son et al., 2013; Son et al., 2014). Histone acetylation is generally important for the regulation of gene expression and is associated with gene activation, whereas deacetylation is associated with transcriptional repression (Grunstein, 1997; Kuo and Allis, 1998; Struhl, 1998). We found that the level of histone acetylation was lower in the *elp3* deletion mutant than in the wild-type strain. We previously reported that reduced histone acetylation contributed to defects in sexual development in *F. graminearum* (Son et al., 2011). Thus, the reduced acetylation in the *elp3* deletion mutant contributed to the sexual and asexual developmental defects in the *elp3* deletion mutant.

Perithecium formation is a complex cellular differentiation process mediated by diverse signaling pathways. Inappropriate expression of genes involved in cell proliferation and differentiation resulted in defects in perithecium development in *F. graminearum* (Lin et al., 2011; Lin et al., 2012). Deletion of *ELP3* affected the production and maturation of perithecia indicating that *ELP3* was required for

proper gene expression during perithecium formation. The *elp3* deletion mutant also produced abnormal ascospores. In the wild-type strain, an ascospore develops from a single uninucleate cell. Following the first mitosis, a medial septum is formed resulting in a two-celled ascospore. The nucleus in each cell undergoes a second mitosis, and the resulting two nuclei are immediately separated by an additional septum. Thus, fully-developed ascospores contain four uninucleate cells (Headrick et al., 1988). The *elp3* deletion mutant produced ascospores containing two dinucleate cells indicating a failure to progress through the second mitotic division. When assessing asexual development, we found that the *elp3* deletion mutant produced longer conidia compared to wild-type. Defects in cell cycle progression during conidiogenesis in *F. graminearum* frequently results in elongated conidia (Min et al., 2014; Son et al., 2014). Deletion of *WETA*, a *F. graminearum* transcription factor known to be involved in conidiogenesis, resulted in longer conidia (Son et al., 2014). Taken together, these results indicate that the defects in sexual and asexual development of the *elp3* deletion mutant result from impairments in cell cycle progression.

The *elp3* deletion mutant exhibited reduced virulence on wheat heads, and several *F. graminearum* genetic studies have shown that trichothecenes are virulence factors for plant disease (Proctor and McCormick, 1995; Desjardins et al., 1996; Maier et al., 2006). Thus, we hypothesized that reduced trichothecene production might contribute to the reduced virulence of the *elp3* deletion mutant. In the *elp3* deletion mutant, the transcript levels of the trichothecene biosynthesis genes *TRI5* and *TRI6* were significantly lower than in the wild-type strain. These observations suggested that Elp3 played a role in virulence by regulating

trichothecene biosynthesis gene expression.

In many organisms, Elp3 has been found to regulate genes involved in stress responses (Wittschieben et al., 2000; Nelissen et al., 2005; Han et al., 2007a; Walker et al., 2011; DeFraia et al., 2013). In yeast, an *elp3* deletion mutant showed a delayed response to high temperature and salt stress, as well as reduced activation of several genes, including *GAL1-10* and *PHO5*, which are required for survival under stressful growth conditions (Wittschieben et al., 2000). In plants, Elp3 has been found to be required for basal plant immunity (DeFraia et al., 2013), and in human cells, Elp3 regulates *HSP70* expression by acetylating histones H3 and H4 in heat shock conditions (Han et al., 2007a). Although the role of Elp3 in the stress response is conserved in eukaryotes, the subset of stress-inducible genes has diverged during evolution (Creppe and Buschbeck, 2011).

We tested the sensitivity of the *elp3* deletion mutant to diverse stress conditions and found that *F. graminearum ELP3* was mainly involved in the oxidative stress response. Oxidative stress is a stress commonly encountered by phytopathogenic fungi. During infection, fungal pathogens encounter toxic environments generated by the hosts' defense mechanisms. The oxidative burst, a rapid production of reactive oxygen species (ROS), is one of the host's earliest responses to pathogen infection (Wojtaszek, 1997; Torres et al., 2006). Several pathogens produce ROS-scavenging enzymes to protect themselves from the plant-derived oxidative stress (Schouten et al., 2002); catalase, which metabolizes H_2O_2, is one of these antioxidant enzymes. We found that, in *F. graminearum*, *ELP3* was required for catalase gene expression under oxidative stress conditions.

Seven putative catalase genes, *FCA1* to *FCA7*, have been identified in *F.*

graminearum through BLAST searches, and we generated deletion mutants for all seven genes. Among these mutants, only the *fca6* and *fca7* deletion mutants showed increased sensitivity to extracellular H_2O_2. Deletion of the other catalase genes did not affect sensitivity to oxidative stress, which may be due to the overlapping and redundant antioxidant functions of these genes. In *C. neoformans*, single and quadruple catalase mutants did not exhibit oxidative-stress phenotypes indicating that *C. neoformans* possessed a robust and redundant antioxidant defense system (Giles et al., 2006). Because Fca7 primarily contributed to the extracellular H_2O_2 resistance phenotype, we constructed an *elp3* deletion mutant that overexpressed *FCA7*. We found that the oxidative stress sensitivity of the *elp3* deletion mutant was partially complemented by overexpression of *FCA7*. Thus, Elp3 may confer resistance to oxidative stress by regulating the expression of *FCA7*.

In this study, we observed that the *elp3* deletion mutant had reduced catalase activity under oxidative stress and exhibited reduced virulence on wheat heads. In *Claviceps purpurea*, deletion of the transcription factor *CPTF1*, a general regulator of catalase activity, resulted in reduced virulence (Nathues et al., 2004). In *M. oryzae*, it was reported that the catalase gene *CATB* was involved in its pathogenicity (Skamnioti et al., 2007). In addition, the catalase-peroxidase gene *CPXB* in *M. oryzae* played a role in fungal defense against H_2O_2 accumulated in epidermal cells during early infection (Tanabe et al., 2011).

In a previous study, *F. graminearum* HDAC genes *HDF1*, *HDF2*, and *HDF3* were characterized (Li et al., 2011). The deletion of the HDAC genes led to the opposite results for pigmentation, conidial morphology, and response to oxidative

stress than the *elp3* deletion. Unlike the *hdf1* deletion mutant, which formed whitish colonies on potato dextrose agar (Li et al., 2011), the *elp3* deletion mutant displayed more red pigmentation than the wild-type strain. The conidia produced by the *elp3* deletion mutant were longer than those produced by the wild-type strain, whereas the Δ*hdf1* Δ*hdf2* double mutant produced shorter conidia (Li et al., 2011). In the *hdf1* deletion mutant, sensitivity to H_2O_2 was reduced and the putative catalase genes were upregulated (Li et al., 2011), whereas the *elp3* deletion mutant was more sensitive to H_2O_2 and catalase gene expression was reduced. Since HATs and HDACs have opposite functions (Kuo and Allis, 1998), these observations raised the possibility that *ELP3* cooperated with HDAC genes to maintain the appropriate level of histone acetylation during these biological processes. In yeast, the phenotype of a Δ*elp3* Δ*gcn5* double mutant was partially restored by mutation of specific HDAC genes demonstrating the balance between histone acetylation and deacetylation (Wittschieben et al., 2000).

In conclusion, we show that *F. graminearum* Elp3 is involved in diverse biological processes including sexual and asexual reproduction, secondary metabolite production, virulence, and the oxidative stress response. This paper demonstrated that the defects in the *elp3* deletion mutant were associated with reduced histone acetylation and demonstrated that *elp3* was required for activation of genes involved in oxidative stress, a stress that pathogens encounter upon plant invasion.

LITERATURE CITED

Baldwin, T. K., Urban, M., Brown, N. and Hammond-Kosack, K. E. (2010) A role for topoisomerase I in *Fusarium graminearum* and *F. culmorum* pathogenesis and sporulation. *Mol. Plant-Microbe Interact.,* **23,** 566-577.

Bölker, M., Böhnert, H. U., Braun, K. H., Görl, J. and Kahmann, R. (1995) Tagging pathogenicity genes in *Ustilago maydis* by restriction enzyme-mediated integration (REMI). *Mol. Gen. Genet.,* **248,** 547-552.

Bowden, R. L. and Leslie, J. F. (1999) Sexual recombination in *Gibberella zeae*. *Phytopathology,* **89,** 182-188.

Cappellini, R. A. and Peterson, J. L. (1965) Macroconidium formation in submerged cultures by a non-sporulating strain of *Gibberella zeae*. *Mycologia,* **57,** 962-966.

Carrozza, M. J., Utley, R. T., Workman, J. L. and Côté, J. (2003) The diverse functions of histone acetyltransferase complexes. *Trends Genet.,* **19,** 321-329.

Chen, Z., Zhang, H., Jablonowski, D., Zhou, X., Ren, X., Hong, X., *et al.* (2006) Mutations in ABO1/ELO2, a subunit of holo-Elongator, increase abscisic acid sensitivity and drought tolerance in *Arabidopsis thaliana*. *Mol. Cell. Biol.,* **26,** 6902-6912.

Creppe, C. and Buschbeck, M. (2011) Elongator: an ancestral complex driving transcription and migration through protein acetylation. *J. Biomed. Biotechnol.,* **2011,** 924898.

DeFraia, C. T., Wang, Y., Yao, J. and Mou, Z. (2013) Elongator subunit 3 positively regulates plant immunity through its histone acetyltransferase and radical

S-adenosylmethionine domains. *BMC Plant Biol.,* **13,** 102.

Desjardins, A. E. and Proctor, R. H. (2007) Molecular biology of *Fusarium* mycotoxins. *Int. J. Food Microbiol.,* **119,** 47-50.

Desjardins, A. E., Proctor, R. H., Bai, G., McCormick, S. P., Shaner, G., Buechley, G., *et al.* (1996) Reduced virulence of trichothecene-nonproducing mutants of *Gibberella zeae* in wheat field tests. *Mol. Plant-Microbe Interact.,* **9,** 775-781.

Gardiner, D. M., Kazan, K. and Manners, J. M. (2009) Novel genes of *Fusarium graminearum* that negatively regulate deoxynivalenol production and virulence. *Mol. Plant-Microbe Interact.,* **22,** 1588-1600.

Giles, S. S., Stajich, J. E., Nichols, C., Gerrald, Q. D., Alspaugh, J. A., Dietrich, F., *et al.* (2006) The *Cryptococcus neoformans* catalase gene family and its role in antioxidant defense. *Eukaryot. Cell,* **5,** 1447-1459.

Gritz, L. and Davies, J. (1983) Plasmid-encoded hygromycin B resistance: the sequence of hygromycin B phosphotransferase gene and its expression in *Escherichia coli* and *Saccharomyces cerevisiae*. *Gene,* **25,** 179-188.

Grunstein, M. (1997) Histone acetylation in chromatin structure and transcription. *Nature,* **389,** 349-352.

Hallen, H. E., Huebner, M., Shiu, S.-H., Güldener, U. and Trail, F. (2007) Gene expression shifts during perithecium development in *Gibberella zeae* (anamorph *Fusarium graminearum*), with particular emphasis on ion transport proteins. *Fungal Genet. Biol.,* **44,** 1146-1156.

Han, Q., Hou, X., Su, D., Pan, L., Duan, J., Cui, L., *et al.* (2007a) HELP3 subunit of the Elongator complex regulates the transcription of *HSP70* gene in

human cells. *Acta Biochim. Biophys. Sin.*, **39,** 453-461.

Han, Y.-K., Kim, M.-D., Lee, S.-H., Yun, S.-H. and Lee, Y.-W. (2007b) A novel F-box protein involved in sexual development and pathogenesis in *Gibberella zeae*. *Mol. Microbiol.*, **63,** 768-779.

Han, Y.-K., Lee, T., Han, K.-H., Yun, S.-H. and Lee, Y.-W. (2004) Functional analysis of the homoserine O-acetyltransferase gene and its identification as a selectable marker in *Gibberella zeae*. *Curr. Genet.*, **46,** 205-212.

Harris, S. D. (2005) Morphogenesis in germinating *Fusarium graminearum* macroconidia. *Mycologia*, **97,** 880-887.

Hawkes, N. A., Otero, G., Winkler, G. S., Marshall, N., Dahmus, M. E., Krappmann, D., *et al.* (2002) Purification and characterization of the human elongator complex. *J. Biol. Chem.*, **277,** 3047-3052.

Headrick, J. M., Glawe, A. and Pataky, J. K. (1988) Ascospore polymorphism in *Gibberella zeae*. *Mycologia*, 679-684.

Hong, S.-Y., So, J., Lee, J., Min, K., Son, H., Park, C., *et al.* (2010) Functional analyses of two syntaxin-like SNARE genes, *GzSYN1* and *GzSYN2*, in the ascomycete *Gibberella zeae*. *Fungal Genet. Biol.*, **47,** 364-372.

Kim, S., Park, S.-Y., Kim, K. S., Rho, H.-S., Chi, M.-H., Choi, J., *et al.* (2009) Homeobox transcription factors are required for conidiation and appressorium development in the rice blast fungus *Magnaporthe oryzae*. *PLoS Genet.*, **5,** e1000757.

Kuo, M.-H. and Allis, C. D. (1998) Roles of histone acetyltransferases and deacetylases in gene regulation. *BioEssays*, **20,** 615-626.

Kwon, S.-J., Cho, S.-Y., Lee, K.-M., Yu, J., Son, M. and Kim, K.-H. (2009)

Proteomic analysis of fungal host factors differentially expressed by *Fusarium graminearum* infected with *Fusarium graminearum virus*-DK21. *Virus Res.,* **144,** 96-106.

Lee, J., Lee, T., Lee, Y.-W., Yun, S.-H. and Turgeon, B. G. (2003) Shifting fungal reproductive mode by manipulation of mating type genes: obligatory heterothallism of *Gibberella zeae*. *Mol. Microbiol.,* **50,** 145-152.

Lee, S.-H., Han, Y.-K., Yun, S.-H. and Lee, Y.-W. (2009a) Roles of the glyoxylate and methylcitrate cycles in sexual development and virulence in the cereal pathogen *Gibberella zeae*. *Eukaryot. Cell,* **8,** 1155-1164.

Lee, S.-H., Lee, J., Lee, S., Park, E.-H., Kim, K.-W., Kim, M.-D., *et al.* (2009b) G*z**SNF1* is required for normal sexual and asexual development in the ascomycete *Gibberella zeae*. *Eukaryot. Cell,* **8,** 116-127.

Lee, S., Son, H., Lee, J., Min, K., Choi, G. J., Kim, J.-C., *et al.* (2011) Functional analyses of two acetyl coenzyme A synthetases in the ascomycete *Gibberella zeae*. *Eukaryot. Cell,* **10,** 1043-1052.

Leslie, J. F. and Summerell, B. A. (2006) *The Fusarium laboratory manual*. Ames, IA, U.S.A.: Blackwell Publishing.

Li, Y., Wang, C., Liu, W., Wang, G., Kang, Z., Kistler, H. C., *et al.* (2011) The *HDF1* histone deacetylase gene is important for conidiation, sexual reproduction, and pathogenesis in *Fusarium graminearum*. *Mol. Plant-Microbe Interact.,* **24,** 487-496.

Lin, Y., Son, H., Lee, J., Min, K., Choi, G. J., Kim, J.-C., *et al.* (2011) A putative transcription factor MYT1 is required for female fertility in the Ascomycete *Gibberella zeae*. *PLoS ONE,* **6,** e25586.

Lin, Y., Son, H., Min, K., Lee, J., Choi, G. J., Kim, J.-C., *et al.* (2012) A Putative Transcription Factor MYT2 Regulates Perithecium Size in the Ascomycete *Gibberella zeae*. *PLoS ONE,* **7,** e37859.

Livak, K. J. and Schmittgen, T. D. (2001) Analysis of relative gene expression data using real-time quantitative PCR and the $2^{-\Delta\Delta CT}$ method. *Methods,* **25,** 402-408.

Lu, S., Lyngholm, L., Yang, G., Bronson, C., Yoder, O. and Turgeon, B. G. (1994) Tagged mutations at the *Tox1* locus of *Cochliobolus heterostrophus* by restriction enzyme-mediated integration. *Proc. Natl. Acad. Sci. U.S.A.,* **91,** 12649-12653.

Maier, F. J., Miedaner, T., Hadeler, B., Felk, A., Salomon, S., Lemmens, M., *et al.* (2006) Involvement of trichothecenes in fusarioses of wheat, barley and maize evaluated by gene disruption of the trichodiene synthase (Tri5) gene in three field isolates of different chemotype and virulence. *Mol. Plant Pathol.,* **7,** 449-461.

Min, K., Son, H., Lim, J. Y., Choi, G. J., Kim, J.-C., Harris, S. D., *et al.* (2014) Transcription factor RFX1 is crucial for maintenance of genome integrity in *Fusarium graminearum*. *Eukaryot. Cell,* **13,** 427-436.

Namiki, F., Matsunaga, M., Okuda, M., Inoue, I., Nishi, K., Fujita, Y., *et al.* (2001) Mutation of an arginine biosynthesis gene causes reduced pathogenicity in *Fusarium oxysporum* f. sp. *melonis*. *Mol. Plant-Microbe Interact.,* **14,** 580-584.

Nathues, E., Joshi, S., Tenberge, K. B., von den Driesch, M., Oeser, B., Bäumer, N., *et al.* (2004) CPTF1, a CREB-like transcription factor, is involved in the

oxidative stress response in the phytopathogen *Claviceps purpurea* and modulates ROS level in its host Secale cereale. *Mol. Plant-Microbe Interact.,* **17,** 383-393.

Nelissen, H., De Groeve, S., Fleury, D., Neyt, P., Bruno, L., Bitonti, M. B., *et al.* (2010) Plant Elongator regulates auxin-related genes during RNA polymerase II transcription elongation. *Proc. Natl. Acad. Sci. U.S.A.,* **107,** 1678-1683.

Nelissen, H., Fleury, D., Bruno, L., Robles, P., De Veylder, L., Traas, J., *et al.* (2005) The elongata mutants identify a functional Elongator complex in plants with a role in cell proliferation during organ growth. *Proc. Natl. Acad. Sci. U.S.A.,* **102,** 7754-7759.

Otero, G., Fellows, J., Li, Y., de Bizemont, T., Dirac, A. M., Gustafsson, C. M., *et al.* (1999) Elongator, a multisubunit component of a novel RNA polymerase II holoenzyme for transcriptional elongation. *Mol. Cell,* **3,** 109-118.

Proctor, R. H., Hohn, T. M. and McCormick, S. P. (1995) Reduced virulence of *Gibberella zeae* caused by disruption of a trichothecene toxin biosynthetic gene. *Mol. Plant-Microbe Interact.,* **8,** 593-601.

Qi, W., Kwon, C. and Trail, F. (2006) Microarray analysis of transcript accumulation during perithecium development in the filamentous fungus *Gibberella zeae* (anamorph *Fusarium graminearum*). *Mol. Genet. Genomics,* **276,** 87-100.

Sambrook, J. and Russell, D. W. (2001) *Molecular cloning : a laboratory manual*. Cold Spring Harbor, NY, U.S.A.: Cold Spring Harbor Laboratory Press.

Schiestl, R. H. and Petes, T. D. (1991) Integration of DNA fragments by illegitimate recombination in *Saccharomyces cerevisiae*. *Proc. Natl. Acad. Sci. USA,* **88,** 7585-7589.

Schouten, A., Tenberge, K. B., Vermeer, J., Stewart, J., Wagemakers, L., Williamson, B., *et al.* (2002) Functional analysis of an extracellular catalase of *Botrytis cinerea*. *Mol. Plant Pathol.,* **3,** 227-238.

Seo, J.-A., Kim, J.-C., Lee, D.-H. and Lee, Y.-W. (1996) Variation in 8-ketotrichothecenes and zearalenone production by *Fusarium graminearum* isolates from corn and barley in Korea. *Mycopathologia,* **134,** 31-37.

Seong, K.-Y., Hou, Z., Tracy, M., Kistler, H. C. and Xu, J.-R. (2005) Random insertional mutagenesis identifies genes associated with virulence in the wheat scab fungus *Fusarium graminearum*. *Phytopathology,* **95,** 744-750.

Skamnioti, P., Henderson, C., Zhang, Z., Robinson, Z. and Gurr, S. J. (2007) A novel role for catalase B in the maintenance of fungal cell-wall integrity during host invasion in the rice blast fungus *Magnaporthe grisea*. *Mol. Plant-Microbe Interact.,* **20,** 568-580.

Son, H., Kim, M.-G., Min, K., Lim, J. Y., Choi, G. J., Kim, J.-C., *et al.* (2014) WetA is required for conidiogenesis and conidium maturation in the ascomycete fungus *Fusarium graminearum*. *Eukaryot. Cell,* **13,** 87-98.

Son, H., Kim, M.-G., Min, K., Seo, Y.-S., Lim, J. Y., Choi, G. J., *et al.* (2013) AbaA regulates conidiogenesis in the ascomycete fungus *Fusarium graminearum*. *PLoS One,* **8,** e72915.

Son, H., Lee, J. and Lee, Y.-W. (2012) Mannitol induces the conversion of conidia to chlamydospore-like structures that confer enhanced tolerance to heat,

drought, and UV in *Gibberella zeae*. *Microbiol. Res. ,* **167,** 608-615.

Son, H., Lee, J., Park, A. R. and Lee, Y.-W. (2011) ATP citrate lyase is required for normal sexual and asexual development in *Gibberella zeae*. *Fungal Genet. Biol.,* **48,** 408-417.

Struhl, K. (1998) Histone acetylation and transcriptional regulatory mechanisms. *Genes Dev.,* **12,** 599-606.

Sweigard, J. A., Carroll, A. M., Farrall, L., Chumley, F. G. and Valent, B. (1998) *Magnaporthe grisea* pathogenicity genes obtained through insertional mutagenesis. *Mol. Plant-Microbe Interact.,* **11,** 404-412.

Tanabe, S., Ishii-Minami, N., Saitoh, K.-I., Otake, Y., Kaku, H., Shibuya, N., *et al.* (2011) The role of catalase-peroxidase secreted by *Magnaporthe oryzae* during early infection of rice cells. *Mol. Plant-Microbe Interact.,* **24,** 163-171.

Torres, M. A., Jones, J. D. and Dangl, J. L. (2006) Reactive oxygen species signaling in response to pathogens. *Plant Physiol.,* **141,** 373-378.

Trail, F., Gaffoor, I. and Vogel, S. (2005) Ejection mechanics and trajectory of the ascospores of *Gibberella zeae* (anamorph *Fuarium graminearum*). *Fungal Genet. Biol.,* **42,** 528-533.

Vetting, M. W., S de Carvalho, L. P., Yu, M., Hegde, S. S., Magnet, S., Roderick, S. L., *et al.* (2005) Structure and functions of the GNAT superfamily of acetyltransferases. *Arch. Biochem. Biophys.,* **433,** 212-226.

Walker, J., Kwon, S. Y., Badenhorst, P., East, P., McNeill, H. and Svejstrup, J. Q. (2011) Role of elongator subunit Elp3 in *Drosophila melanogaster* larval development and immunity. *Genetics,* **187,** 1067-1075.

Wang, Y., Liu, W., Hou, Z., Wang, C., Zhou, X., Jonkers, W., *et al.* (2011) A novel transcriptional factor important for pathogenesis and ascosporogenesis in *Fusarium graminearum*. *Mol. Plant-Microbe Interact.*, **24,** 118-128.

Winkler, G. S., Kristjuhan, A., Erdjument-Bromage, H., Tempst, P. and Svejstrup, J. Q. (2002) Elongator is a histone H3 and H4 acetyltransferase important for normal histone acetylation levels in vivo. *Proc. Natl. Acad. Sci. U.S.A.*, **99,** 3517-3522.

Wittschieben, B. Ø., Fellows, J., Du, W., Stillman, D. J. and Svejstrup, J. Q. (2000) Overlapping roles for the histone acetyltransferase activities of SAGA and elongator in vivo. *EMBO J.*, **19,** 3060-3068.

Wittschieben, B. Ø., Otero, G., de Bizemont, T., Fellows, J., Erdjument-Bromage, H., Ohba, R., *et al.* (1999) A novel histone acetyltransferase is an integral subunit of elongating RNA polymerase II holoenzyme. *Mol. Cell*, **4,** 123-128.

Wojtaszek, P. a. (1997) Oxidative burst: an early plant response to pathogen infection. *Biochem. J.*, **322,** 681-692.

Wolffe, A. P. and Pruss, D. (1996) Targeting chromatin disruption: transcription regulators that acetylate histones. *Cell*, **84,** 817-819.

Yu, J.-H., Hamari, Z., Han, K.-H., Seo, J.-A., Reyes-Dominguez, Y. and Scazzocchio, C. (2004) Double-joint PCR: a PCR-based molecular tool for gene manipulations in filamentous fungi. *Fungal Genet. Biol.*, **41,** 973-981.

CHAPTER 2

Genome-wide functional characterization of putative peroxidases in the head blight fungus *Fusarium graminearum*

ABSTRACT

Reactive oxygen species (ROS) are associated with various developmental processes and host-pathogen interactions in pathogenic fungi. Peroxidases are a group of ROS-detoxifying enzymes that are involved in the oxidative stress response and in a variety of physiological processes. In this study, we performed a genome-wide functional characterization of putative peroxidase genes in *Fusarium graminearum*, a head blight pathogen of cereal crops. We identified 31 putative peroxidase genes and generated deletion mutants for these genes. Twenty-six of the deletion mutants showed developmental phenotypes indistinguishable from that of the wild type, and five deletion mutants exhibited phenotypic changes in at least one phenotypic category. Four deletion mutants, *fca6*, *fca7*, *fpx1*, and *fpx15*, showed increased sensitivity to extracellular H_2O_2. Deletion mutants of *FCA7* also exhibited reduced virulence and increased trichothecene production compared with those of the wild-type strain, suggesting that Fca7 may play important roles in the host-pathogen interaction in *F. graminearum*. To identify the transcription factors (TFs) regulating *FCA6*, *FCA7*, *FPX1*, and *FPX15* in response to oxidative stress, we screened an *F. graminearum* TF mutant library for growth in the presence of H_2O_2 and found that multiple TFs co-regulated the expression of *FCA7* under oxidative stress conditions. These results demonstrate that a complex network of transcriptional regulators of antioxidant genes is involved in oxidative stress responses in this fungus. Moreover, our study provides insights into the roles of peroxidases in developmental processes and host-pathogen interactions in plant pathogenic fungi.

INTRODUCTION

Fusarium graminearum, one of the most economically important plant pathogens, causes Fusarium head blight (FHB) in wheat, barley, and rice as well as ear rot in maize (Leslie & Summerell, 2006). Epidemics of FHB cause serious yield losses in major cereal crops worldwide (Windels, 2000, Goswami & Kistler, 2004). In addition to yield losses, this fungus is responsible for the contamination of grains with mycotoxins such as trichothecenes and zearalenone, which are harmful to humans and to livestock (Desjardins & Proctor, 2007). In particular, trichothecenes are potent inhibitors of protein synthesis (Arunachalam & Doohan, 2013) and are well-studied virulence factors in *F. graminearum* (Proctor *et al.*, 1995).

Reactive oxygen species (ROS), such as superoxides ($O_2^{\cdot -}$), hydroxyl radicals ($OH\cdot$), and hydrogen peroxides (H_2O_2), are generated as byproducts of aerobic respiration and metabolic pathways that primarily occur in mitochondria, peroxisomes, and chloroplasts (Heller & Tudzynski, 2011). On one hand, because excessive amounts of ROS can damage cellular components by oxidizing membrane lipids, cellular proteins, and nucleic acids, living organisms possess efficient ROS-degrading mechanisms (Camhi *et al.*, 1995). On the other hand, some ROS, particularly H_2O_2, act as secondary messengers in important signal transduction pathways (Apel & Hirt, 2004). Therefore, the delicate balance between ROS generation and scavenging is expected to be tightly regulated by a complex antioxidant defense mechanism comprising both enzymatic and non-enzymatic components.

ROS also play an important role in plant-pathogen interactions. During plant infections, phytopathogenic fungi are often exposed to oxidative stress conditions caused by the oxidative burst, a rapid and transient accumulation of ROS (Wojtaszek, 1997, Mehdy, 1994). The oxidative burst is an immediate and nonspecific plant defense response that is triggered by pathogen attack. The excessive accumulation of ROS induces other plant defense responses such as the cross-linking of cell walls and programmed cell death of plant cells at infection sites and can also directly kill microbial pathogens (Levine *et al.*, 1994, Lamb & Dixon, 1997, Torres *et al.*, 2006). Therefore, plant pathogenic fungi have evolved effective ROS scavenging mechanisms to detoxify plant-derived ROS and successfully colonize host plants.

Peroxidases are major H_2O_2-decomposing enzymes that catalyze the oxidation of various organic and inorganic compounds using H_2O_2 or organic hydroperoxides as electron acceptors (Heller & Tudzynski, 2011). Peroxidases are involved in the oxidative stress response as antioxidant enzymes, and many studies have attempted to define their roles in ROS detoxification during the initial plant infection process (Garre *et al.*, 1998, Robbertse *et al.*, 2003, Skamnioti *et al.*, 2007, Mir *et al.*, 2015). Moreover, peroxidases such as catalase, catalase-peroxidase, and peroxiredoxin are required as redox controllers in various physiological processes (Fourquet *et al.*, 2008, König *et al.*, 2012), demonstrating that they are also closely involved in a variety of biological processes.

Several important signal mediators, such as transcription factors (TFs), that orchestrate oxidative stress responses have been identified in fungi. Yap1 and Skn7 are the best characterized TFs; they play crucial roles in the oxidative stress

response by regulating the expression of genes encoding antioxidant enzymes in *Saccharomyces cerevisiae* (Lee *et al.*, 1999). Several studies have revealed that Yap1 and Skn7 have a conserved function in the oxidative stress response in various plant pathogenic fungi, including *Ustilago maydis*, *Magnaporthe oryzae*, *Alternaria alternata*, *Cochliobolus heterostrophus*, and *Botrytis cinerea* (Lev *et al.*, 2005, Molina & Kahmann, 2007, Lin *et al.*, 2009, Temme & Tudzynski, 2009, Guo *et al.*, 2011, Chen *et al.*, 2012, Shalaby *et al.*, 2014). In *F. graminearum*, several known and novel TFs involved in the oxidative stress response have been characterized (Lysøe *et al.*, 2011, Wang *et al.*, 2011, Montibus *et al.*, 2013, Jiang *et al.*, 2015). These TFs have been reported to mediate the oxidative stress response by regulating the expression of genes encoding putative antioxidant enzymes (peroxidases). However, whether or not these putative antioxidant genes are indeed important for the oxidative stress response in *F. graminearum* remains unknown.

Recent studies have revealed that oxidative stress is also related to secondary metabolite biosynthesis in fungi (Hong *et al.*, 2013a, Montibus *et al.*, 2015). In *Aspergillus* species, aflatoxin biosynthesis is triggered in response to oxidative stress (Hong et al., 2013a, Reverberi *et al.*, 2012). Accordingly, exogenous treatment with H_2O_2 led to enhanced trichothecene production and induced the expression of trichothecene biosynthetic genes in *F. graminearum* (Ponts *et al.*, 2006, Ponts *et al.*, 2007). Several studies have suggested that secondary metabolites may act in concert with antioxidant enzymes to protect cells against oxidative stress (Hong et al., 2013a, Hong *et al.*, 2013b).

In this study, we functionally characterized 31 putative peroxidase genes through an extensive phenome analysis of *F. graminearum*. The aims of this study

were 1) to characterize the function of putative peroxidases in various developmental processes including vegetative growth, conidiation, sexual development, virulence, mycotoxin production, and the oxidative stress response and 2) to identify TFs that regulate the expression of the genes encoding these putative peroxidases in response to oxidative stress. To our knowledge, this study is the first to investigate the function of genome-wide putative peroxidase genes in the development and infection processes of phytopathogenic fungi. Our results provide insights into the roles of peroxidases in intracellular processes and host-pathogen interactions.

MATERIALS AND METHODS

I. Fungal strains and culture media

The *F. graminearum* wild-type strain Z-3639 (Bowden & Leslie, 1999) and transgenic strains derived from this strain were used in this study (Table 1). The catalase deletion mutants (*fca1-fca7*) and TF deletion mutants used in this study were derived previously (Lee *et al*., 2014, Son *et al*., 2011b). Putative peroxidase genes were identified from the Fungal Peroxidase Database (fPoxDB; http://peroxidase.riceblast.snu.ac.kr) (Choi *et al*., 2014). The protein sequences of these genes were obtained from the MIPS *Fusarium* graminearum database (FGDB; http://mips.helmholtz-muenchen.de/genre/proj/FGDB/) (Wong *et al.*, 2011). All strains were stored as mycelial suspensions in 20% glycerol solution at -80 °C. The culture media used in this study were prepared following the *Fusarium* laboratory manual (Leslie & Summerell, 2006). To induce conidial production, carboxymethyl cellulose (CMC) and yeast malt agar (YMA) were used as previously described (Harris, 2005, Cappellini & Peterson, 1965). Minimal medium containing 5 mM agmatine (MMA) was used for trichothecene production (Gardiner *et al*., 2009).

II. Nucleic acid manipulations, Southern blotting, and PCR

Genomic DNA was extracted from mycelia powder according to the *Fusarium* laboratory manual (Leslie & Summerell, 2006). Total RNA was extracted from mycelia ground in liquid nitrogen using the Easy-Spin Total RNA Extraction Kit (iNtRON Biotech, Seongnam, Korea). Standard protocols were used for restriction endonuclease digestion, agarose gel electrophoresis, Southern blot,

Table 1 *Fusarium graminearum* strains used in this study.

Strain	Genotype	Reference
Z-3639	*F. graminearum* wild-type	(Bowden and Leslie, 1999)
YJ21	Δ*fca1::GEN*	(Lee et al., 2014)
YJ22	Δ*fca2::GEN*	(Lee et al., 2014)
YJ23	Δ*fca3::GEN*	(Lee et al., 2014)
YJ24	Δ*fca4::GEN*	(Lee et al., 2014)
YJ25	Δ*fca5::GEN*	(Lee et al., 2014)
YJ26	Δ*fca6::GEN*	(Lee et al., 2014)
YJ27	Δ*fca7::GEN*	(Lee et al., 2014)
YJ28	*FCA7::GEN-*$P_{EF1\alpha}$*-FCA7*	(Lee et al., 2014)
YJ30	Δ*fpx1::GEN*	This study
YJ31	Δ*fpx2::GEN*	This study

YJ32	Δ*fpx3::GEN*	This study
YJ33	Δ*fpx4::GEN*	This study
YJ34	Δ*fpx5::GEN*	This study
YJ35	Δ*fpx6::GEN*	This study
YJ36	Δ*fpx7::GEN*	This study
YJ37	Δ*fpx8::GEN*	This study
YJ38	Δ*fpx9::GEN*	This study
YJ39	Δ*fpx10::GEN*	This study
YJ40	Δ*fpx11::GEN*	This study
YJ41	Δ*fpx12::GEN*	This study
YJ42	Δ*fpx13::GEN*	This study
YJ43	Δ*fpx14::GEN*	This study
YJ44	Δ*fpx15::GEN*	This study

YJ45	Δ*fpx16::GEN*	This study
YJ46	Δ*fpx17::GEN*	This study
YJ47	Δ*fpx18::GEN*	This study
YJ48	Δ*fpx19::GEN*	This study
YJ49	Δ*fpx20::GEN*	This study
YJ50	Δ*fpx21::GEN*	This study
YJ51	Δ*noxA::GEN*	This study
YJ52	Δ*noxB::GEN*	This study
YJ53	Δ*noxC::GEN*	This study
Δ*mat2*	Δ*mat1-2::GFP-HYG*	(Lee et al., 2003)
YJ54	Δ*mat1-2::GFP-HYG* Δ*fca7::GEN*	This study
zif1	Δ*zif1::GEN*	(Wang et al., 2011)
Fgap1	Δ*Fgap1::GEN*	(Montibus et al., 2013)

Fgskn7	Δ*Fgskn7::GEN*	(Jiang et al., 2015)
gzbzip007	Δ*gzbzip007::GEN*	(Son et al., 2011)
gzzc086	Δ*gzzc086::GEN*	(Son et al., 2011)
gzzc236	Δ*gzzc236::GEN*	(Son et al., 2011)
gzhome001	Δ*gzhome001::GEN*	(Son et al., 2011)
gzc2h010	Δ*gzc2h010::GEN*	(Son et al., 2011)
YJ55	Δ*zif1::GEN FCA7::GEN-*$P_{EF1\alpha}$*-FCA7*	This study
YJ56	Δ*Fgap1::GEN FCA7::GEN-*$P_{EF1\alpha}$*-FCA7*	This study
YJ57	Δ*Fgskn7::GEN FCA7::GEN-*$P_{EF1\alpha}$*-FCA7*	This study
YJ58	Δ*gzbzip007::GEN FCA7::GEN-*$P_{EF1\alpha}$*-FCA7*	This study
YJ59	Δ*gzzc086::GEN FCA7::GEN-*$P_{EF1\alpha}$*-FCA7*	This study
YJ60	Δ*gzzc236::GEN FCA7::GEN-*$P_{EF1\alpha}$*-FCA7*	This study
YJ61	Δ*gzhome001::GEN FCA7::GEN-*$P_{EF1\alpha}$*-FCA7*	This study

YJ62	Δ*gzc2h010::GEN FCA7::GEN-P*$_{EF1\alpha}$*-FCA7*	This study
YJ63	Δ*zif1::GEN* Δ*fca7::GEN*	This study
YJ64	Δ*Fgap1::GEN* Δ*fca7::GEN*	This study
YJ65	Δ*Fgskn7::GEN* Δ*fca7::GEN*	This study
YJ66	Δ*gzbzip007::GEN* Δ*fca7::GEN*	This study
YJ67	Δ*gzzc086::GEN* Δ*fca7::GEN*	This study
YJ68	Δ*gzzc236::GEN* Δ*fca7::GEN*	This study
YJ69	Δ*gzhome001::GEN* Δ*fca7::GEN*	This study
YJ70	Δ*gzc2h010::GEN* Δ*fca7::GEN*	This study

and hybridization with ^{32}P-labeled probes (Sambrook & Russell, 2001). The primers for PCR and quantitative real-time (qRT)-PCR used in this study (Table 2) were synthesized by an oligonucleotide synthesis facility (Bionics, Seoul, Korea). PCR procedures were performed according to the manufacturer's instructions (TaKaRa Bio, Inc., Ostu, Japan).

III. Targeted gene deletion

The double-joint (DJ) PCR strategy was used to construct fusion PCR products for targeted gene deletion (Yu *et al.*, 2004). To create deletion strains, the 5′ and 3′ flanking regions of the target genes were amplified from the genomic DNA of the wild-type strain, and the geneticin resistance gene (*GEN*) was amplified from pII99 using the primer pair Gen-for/Gen-Rev. Three amplicons (5′ flanking region, 3′ flanking region, and *GEN*) were fused in a second round of DJ PCR. Finally, fusion constructs were amplified using nested primers to generate split markers. The resulting constructs were transformed into the wild-type strain as previously described (Son *et al.*, 2011a). Southern hybridization was performed to confirm single-copy integration.

IV. Vegetative growth, conidiation, and sexual development

Radial growth rates on complete media (CM) and minimal media (MM) were measured five days after inoculation with freshly grown culture plugs from MM. Conidia production was measured by counting the number of conidia after incubating culture plugs from CM in 5 ml of CMC for three days at 25 °C on a rotary shaker (200 rpm).

Table 2 Primers used in this study

Primer	Sequence (5' → 3')	Description
FPX1-5F	GTATTGGATGACACCGGAAGATTA	Forward and reverse primers for amplification of 5' flanking region of *FPX1* with tail for geneticin resistance gene cassette fusion
FPX1-5R	gcacaggtacacttgtttagagAATGGGAAAGAAGGAAAGAAAG	
FPX1-3F	cctccactagctccagccaagccAATTTCCTTTAACCTTCGCTT	Forward and reverse primers for amplification of 3' flanking region of *FPX1* with tail for geneticin resistance gene cassette fusion
FPX1-3R	AGAAACTGGTGGACAAGGTAAC	
FPX1-5N	TAGAAAGTGGTGTGAAGCCGAGTG	Forward and reverse nest primers for third fusion PCR for amplification of *FPX1* deletion construct
FPX1-3N	CGTGTTCTGACTGTGGATGA	
FPX2-5F	GGGTTACCGACAGTGCCTCTA	Forward and reverse primers for amplification of 5' flanking region of *FPX2* with tail for geneticin resistance gene cassette fusion
FPX2-5R	gcacaggtacacttgtttagagTTGCCTAGAATGAGTCGGTGAAAT	

FPX2-3F	cctccactagctccagccaagccTACTTCAGGTCAACCAGGAGCAT	Forward and reverse primers for amplification of 3' flanking region of *FPX2* with tail for geneticin resistance gene cassette fusion
FPX2-3R	TTCCTGAGCCTAAACCTAAA	
FPX2-5N	ATCAAGTCTCCGAGTAAAATGTGC	Forward and reverse nest primers for third fusion PCR for amplification of *FPX2* deletion construct
FPX2-3N	ATTGCCAGCTTTCGTTACCTATGC	
FPX3-5F	GTTGAAGGAGGGAGAGGCGTTAGA	Forward and reverse primers for amplification of 5' flanking region of *FPX3* with tail for geneticin resistance gene cassette fusion
FPX3-5R	gcacaggtacacttgtttagagTTCATGATGGGCTAAAGTG	
FPX3-3F	cctccactagctccagccaagccTTGCTGTTCCCCATGGCTCTTG	Forward and reverse primers for amplification of 3' flanking region of *FPX3* with tail for geneticin resistance gene cassette fusion
FPX3-3R	ACCAAGAGAAACAAAAGTCAGC	
FPX3-5N	TATTGTCCCACCTATCACTCCAG	Forward and reverse nest primers for third fusion PCR for amplification of *FPX3* deletion construct
FPX3-3N	TTTCTTTGCTCTTCTTTTGTGGTC	
FPX4-5F	GTCGGTTTATGGGGTTTATTAGCA	Forward and reverse primers for amplification of 5' flanking

FPX4-5R	gcacaggtacacttgtttagagTAAGTTATAAGGGAATGTAGT	region of *FPX4* with tail for geneticin resistance gene cassette fusion
FPX4-3F	cctccactagctccagccaagccGGGTGTCTGGGATATTCTGTTCTA	Forward and reverse primers for amplification of 3' flanking region of *FPX4* with tail for geneticin resistance gene cassette fusion
FPX4-3R	CCTCATCCCCGGCCAGTCATA	
FPX4-5N	TGCTTCTCCCGCTCAATCC	Forward and reverse nest primers for third fusion PCR for amplification of *FPX4* deletion construct
FPX4-3N	CACATCCTCAAACCTTCTACACCA	
FPX5-5F	AGCAAAGGTCTTATCTGTG	Forward and reverse primers for amplification of 5' flanking region of *FPX5* with tail for geneticin resistance gene cassette fusion
FPX5-5R	gcacaggtacacttgtttagagTTAAGGAATGAATGCGAATGAGA	
FPX5-3F	cctccactagctccagccaagccCTGAGTTCCTGAATACCGCATACG	Forward and reverse primers for amplification of 3' flanking region of *FPX5* with tail for geneticin resistance gene cassette fusion
FPX5-3R	TTTTCGAACCTCCAACTCAATAAG	
FPX5-5N	AGAGCCAGCTGGGATTTCAC	Forward and reverse nest primers for third fusion PCR for

FPX5-3N	CCAACACCAAAAGCCAAAGAAGGA	amplification of *FPX5* deletion construct
FPX6-5F	CTGATGAAGGCGAAAGGTGAGC	Forward and reverse primers for amplification of 5' flanking region of *FPX6* with tail for geneticin resistance gene cassette fusion
FPX6-5R	gcacaggtacacttgtttagagGGATTGCCATTGATTACG	
FPX6-3F	cctccactagctccagccaagccCCAAGGGTTCACTCAAGGGTATTA	Forward and reverse primers for amplification of 3' flanking region of *FPX6* with tail for geneticin resistance gene cassette fusion
FPX6-3R	TTCGCAAGCGCAAATGTGA	
FPX6-5N	AGTATTCAGCACCCGAGTCCTT	Forward and reverse nest primers for third fusion PCR for amplification of *FPX6* deletion construct
FPX6-3N	TCGTTTGGTGAGGGAAGCGATGTA	
FPX7-5F	CCACAACCCCATCTTTCACATTTT	Forward and reverse primers for amplification of 5' flanking region of *FPX7* with tail for geneticin resistance gene cassette fusion
FPX7-5R	gcacaggtacacttgtttagagGGTAGAAGAAAAGAAGGACTGTTA	
FPX7-3F	cctccactagctccagccaagccAGACGAGACGGATCACAATAAGTA	Forward and reverse primers for amplification of 3' flanking region of *FPX7* with tail for geneticin resistance gene

FPX7-3R	AGCCACGCACTCTTTTTATCAG	cassette fusion
FPX7-5N	GTCTTTATAACATGGCACACGA	Forward and reverse nest primers for third fusion PCR for amplification of *FPX7* deletion construct
FPX7-3N	CCACCACAAGTAAACAAATGAGAG	
FPX8-5F	GATTCACGCGCTCCTCTAAG	Forward and reverse primers for amplification of 5' flanking region of *FPX8* with tail for geneticin resistance gene cassette fusion
FPX8-5R	gcacaggtacacttgtttagagTTTTGCCAATAGTCTCGGGTCGTA	
FPX8-3F	cctccactagctccagccaagccAGTACGGCCTTTTCTGTTCTA	Forward and reverse primers for amplification of 3' flanking region of *FPX8* with tail for geneticin resistance gene cassette fusion
FPX8-3R	CAGGCAGTGTGGTTTGTGGATGGT	
FPX8-5N	CCCGCGCAGTACCAAAGTCCTAAT	Forward and reverse nest primers for third fusion PCR for amplification of *FPX8* deletion construct
FPX8-3N	GGCTATCAGGTGCAGAGGTAACAA	
FPX9-5F	GCGGCAGGTTTTGGCTCAT	Forward and reverse primers for amplification of 5' flanking region of *FPX9* with tail for geneticin resistance gene cassette fusion
FPX9-5R	gcacaggtacacttgtttagagAGCGGAGCAAAGAAAAAG	

	TAGGTT	
FPX9-3F	cctccactagctccagccaagccGCCCAAGCCAGTGCCTAAA	Forward and reverse primers for amplification of 3' flanking region of *FPX9* with tail for geneticin resistance gene cassette fusion
FPX9-3R	AGCGCTTCTTAGTCTTTTCTCGT	
FPX9-5N	GCCGACGAGGATAACGCTTTTGA	Forward and reverse nest primers for third fusion PCR for amplification of *FPX9* deletion construct
FPX9-3N	GTGGGAAACGACGCATGTAATCTG	
FPX10-5F	CTTGAAAGTACCCCATAGC	Forward and reverse primers for amplification of 5' flanking region of *FPX10* with tail for geneticin resistance gene cassette fusion
FPX10-5R	gcacaggtacacttgtttagagCAAGGAGATTAAAGACAGCGAACC	
FPX10-3F	cctccactagctccagccaagccGGCAAAGTCTTGAAATGGGCA	Forward and reverse primers for amplification of 3' flanking region of *FPX10* with tail for geneticin resistance gene cassette fusion
FPX10-3R	CTCGATCTTACAACACTTTACCTC	
FPX10-5N	CAGCGGGGCAGCGTCCTAAA	Forward and reverse nest primers for third fusion PCR for

FPX10-3N	AGCTACTAAGGACTGGGGTTCT	amplification of *FPX10* deletion construct
FPX11-5F	TCGCGATTGATTCTGGTTAGT	Forward and reverse primers for amplification of 5' flanking region of *FPX11* with tail for geneticin resistance gene cassette fusion
FPX11-5R	gcacaggtacacttgtttagagCGACATGATGAATATCCAAACCC	
FPX11-3F	cctccactagctccagccaagccCGTTACTTGCAATGATGTCCG	Forward and reverse primers for amplification of 3' flanking region of *FPX11* with tail for geneticin resistance gene cassette fusion
FPX11-3R	AGCTGCACCAAGCCTATCG	
FPX11-5N	CTTGGTACATACGCGGCAGAAT	Forward and reverse nest primers for third fusion PCR for amplification of *FPX11* deletion construct
FPX11-3N	GAACAAGGCGGCAATCTGG	
FPX12-5F	GTATGGGATCTTTCGCCTAACC	Forward and reverse primers for amplification of 5' flanking region of *FPX12* with tail for geneticin resistance gene cassette fusion
FPX12-5R	gcacaggtacacttgtttagagAAGAAGCTGAAGAAGGGGATTTTT	
FPX12-3F	cctccactagctccagccaagccTCATGGATTTGTTTAGTCGT	Forward and reverse primers for amplification of 3' flanking region of *FPX12* with tail for geneticin resistance gene

FPX12-3R	TGGCGTTATGCAAGATTCAGT	cassette fusion
FPX12-5N	TAGCTCAGGACCAGGGGGCAC	Forward and reverse nest primers for third fusion PCR for amplification of *FPX12* deletion construct
FPX12-3N	ATCGACAAGAGTGCTATTTACG	
FPX13-5F	TACTGTCGTTTGCACCACCTATGT	Forward and reverse primers for amplification of 5' flanking region of *FPX13* with tail for geneticin resistance gene cassette fusion
FPX13-5R	gcacaggtacacttgtttagagACTCAGGCCCAGATGTGC	
FPX13-3F	cctccactagctccagccaagccCTATGCCTGCTACATCGGGA	Forward and reverse primers for amplification of 3' flanking region of *FPX13* with tail for geneticin resistance gene cassette fusion
FPX13-3R	AGGGAATGGATGTCGGTCTC	
FPX13-5N	CAGAAGAGATGTGGAAAAACTA	Forward and reverse nest primers for third fusion PCR for amplification of *FPX13* deletion construct
FPX13-3N	ACGGTCTGCAGTGGATGTGGATTC	
FPX14-5F	TTCTCGCGCTAAAGTCAATCTCT	Forward and reverse primers for amplification of 5' flanking region of *FPX14* with tail for geneticin resistance gene cassette fusion
FPX14-5R	gcacaggtacacttgtttagagGGGGTCGGGGGAGAGGGATTAT	

FPX14-3F	cctccactagctccagccaagccTGAAGAACAAATGAAGAAATGAT	Forward and reverse primers for amplification of 3' flanking region of *FPX14* with tail for geneticin resistance gene cassette fusion
FPX14-3R	CTCAAACCTCAACTAACAATCTGG	
FPX14-5N	TGATCAACTCTCTGTCAATACG	Forward and reverse nest primers for third fusion PCR for amplification of *FPX14* deletion construct
FPX14-3N	ATATCCAGCCATGTTGTGCGAGTA	
FPX15-5F	TGCAGACGGCTCCTTTAGATTTGA	Forward and reverse primers for amplification of 5' flanking region of *FPX15* with tail for geneticin resistance gene cassette fusion
FPX15-5R	gcacaggtacacttgtttagagATGATGGTGTTTGTTTGGGTTGTT	
FPX15-3F	cctccactagctccagccaagccAGACTATAGACATTTGTTGACGAC	Forward and reverse primers for amplification of 3' flanking region of *FPX15* with tail for geneticin resistance gene cassette fusion
FPX15-3R	CACGAGGCGCTGGTTGAGATTA	
FPX15-5N	AGACCTACAGCTGCGGATTACTTT	Forward and reverse nest primers for third fusion PCR for amplification of *FPX15* deletion construct
FPX15-3N	GTCAAAAAGGTCGGCGATGTAGCA	

FPX16-5F	GCGACGTACCCTCATGAAGTTATC	Forward and reverse primers for amplification of 5' flanking region of *FPX16* with tail for geneticin resistance gene cassette fusion
FPX16-5R	gcacaggtacacttgtttagagATAAAAACTACCGTGTGAAGACTA	
FPX16-3F	cctccactagctccagccaagccCTTTTCGAGTGACCATTTCTG	Forward and reverse primers for amplification of 3' flanking region of *FPX16* with tail for geneticin resistance gene cassette fusion
FPX16-3R	CAAATTCTGCCAAACTCA	
FPX16-5N	CGGTAAAAAGCGAGAAATAACTGG	Forward and reverse nest primers for third fusion PCR for amplification of *FPX16* deletion construct
FPX16-3N	TGGAACCGGAGACACTTT	
FPX17-5F	GACTGACTCGGGGCTAACATT	Forward and reverse primers for amplification of 5' flanking region of *FPX17* with tail for geneticin resistance gene cassette fusion
FPX17-5R	gcacaggtacacttgtttagagGGTAGTCCTCCGTGTCTGAA	
FPX17-3F	cctccactagctccagccaagccGTCAAGAGAAGCACCAACGATAC	Forward and reverse primers for amplification of 3' flanking region of *FPX17* with tail for geneticin resistance gene cassette fusion
FPX17-3R	CGATTCTTCACGGCTATTT	

FPX17-5N	AGTTCATCATGCACAGGGCGTCTT	Forward and reverse nest primers for third fusion PCR for amplification of *FPX17* deletion construct
FPX17-3N	TCGCCCTAGTAGAGAAGTGTC	
FPX18-5F	ATCTGCATACATCACCGTTCTAA	Forward and reverse primers for amplification of 5' flanking region of *FPX18* with tail for geneticin resistance gene cassette fusion
FPX18-5R	gcacaggtacacttgtttagagCGTGAGGTAGATTGTTTGGTTTGA	
FPX18-3F	cctccactagctccagccaagccGGCCAAGAACCTAATCC	Forward and reverse primers for amplification of 3' flanking region of *FPX18* with tail for geneticin resistance gene cassette fusion
FPX18-3R	TAGTCTCTGTTTCGTCCCTGCCT	
FPX18-5N	CATGTCTCCTTTATCTCTTTCGTA	Forward and reverse nest primers for third fusion PCR for amplification of *FPX18* deletion construct
FPX18-3N	AATACTCACTTAGCTGGGACTGCC	
FPX19-5F	GTAGGCCAAGATCAGCAGACA	Forward and reverse primers for amplification of 5' flanking region of *FPX19* with tail for geneticin resistance gene cassette fusion
FPX19-5R	gcacaggtacacttgtttagagCGTAGGGGACTCTCATGGTG	
FPX19-3F	cctccactagctccagccaagccTGCGCTACCCGAGACCGT	Forward and reverse primers for amplification of 3' flanking

	GT	region of *FPX19* with tail for geneticin resistance gene cassette fusion
FPX19-3R	CGTCTTGCTACATTTCTGA	
FPX19-5N	TCCCTAGCTCGTGATACCAGATAA	Forward and reverse nest primers for third fusion PCR for amplification of *FPX19* deletion construct
FPX19-3N	GAACAGGGGCATGAACTCAATCTT	
FPX20-5F	GAGCAGGATCGAGGTCAGAAG	Forward and reverse primers for amplification of 5' flanking region of *FPX20* with tail for geneticin resistance gene cassette fusion
FPX20-5R	gcacaggtacacttgtttagagCGGGCAGTCGGCTTGGTGTA	
FPX20-3F	cctccactagctccagccaagccGACTGCAGCATCCATACTTG	Forward and reverse primers for amplification of 3' flanking region of *FPX20* with tail for geneticin resistance gene cassette fusion
FPX20-3R	CGACTCGTGATGGCTACC	
FPX20-5N	AGCAGCGAACGACTTACT	Forward and reverse nest primers for third fusion PCR for amplification of *FPX20* deletion construct
FPX20-3N	GCCGTCAAATCGTGCGTCTC	
FPX21-5F	TCGGCGATGGATGTTGTGAAG	Forward and reverse primers for amplification of 5' flanking

FPX21-5R	gcacaggtacacttgtttagagGTTGCGCAAGAGTATTTATTA	region of *FPX21* with tail for geneticin resistance gene cassette fusion
FPX21-3F	cctccactagctccagccaagccTAATCTGGTCAATATTTGGTGGCA	Forward and reverse primers for amplification of 3' flanking region of *FPX21* with tail for geneticin resistance gene cassette fusion
FPX21-3R	ATAACACAACTGAGGACATCTAC	
FPX21-5N	ACTTGACTTTATCGCTTGAGACTA	Forward and reverse nest primers for third fusion PCR for amplification of *FPX21* deletion construct
FPX21-3N	CTCTCGAAAGCCCATCTCTATCCT	
NOXA-5F	GTCTGCAACGATGAAACCACAC	Forward and reverse primers for amplification of 5' flanking region of *NOXA* with tail for geneticin resistance gene cassette fusion
NOXA-5R	gcacaggtacacttgtttagagGGTTTTGCGTCGTGTGTATG	
NOXA-3F	cctccactagctccagccaagccTCGTTTTGATTACTTTCTTTTTA	Forward and reverse primers for amplification of 3' flanking region of *NOXA* with tail for geneticin resistance gene cassette fusion
NOXA-3R	CAGGTCCAAGGTTAGTCCAATGTC	
NOXA-5N	TCAATTGAGGAGATGGTAAAACA	Forward and reverse nest primers for third fusion PCR for

NOXA-3N	GTTTACACTCAATACTCTGGACGA	amplification of *NOXA* deletion construct
NOXB-5F	TAGGGGATGGAGGGTTACA	Forward and reverse primers for amplification of 5' flanking region of *NOXB* with tail for geneticin resistance gene cassette fusion
NOXB-5R	gcacaggtacacttgtttagagCGATCGTTCCGACGGTTTCTC	
NOXB-3F	cctccactagctccagccaagccTAGGTGGATGGATAGTTGGGTTTG	Forward and reverse primers for amplification of 3' flanking region of *NOXB* with tail for geneticin resistance gene cassette fusion
NOXB-3R	TCGGCCCCTTTGAGATTACTA	
NOXB-5N	TTGGATTTTGTTTGGATGTGATAC	Forward and reverse nest primers for third fusion PCR for amplification of *NOXB* deletion construct
NOXB-3N	GGCCGACCTAGAACCACCATA	
NOXC-5F	TATTTCTTGAGTGGTCGTGCTTAC	Forward and reverse primers for amplification of 5' flanking region of *NOXC* with tail for geneticin resistance gene cassette fusion
NOXC-5R	gcacaggtacacttgtttagagTTGCAGGACAGACTACGGTTGAA	
NOXC-3F	cctccactagctccagccaagccGTTTTTGGATGAGGAAAGACTG	Forward and reverse primers for amplification of 3' flanking region of *NOXC* with tail for geneticin resistance gene

NOXC-3R	TCAATGATTTGATGCTACAGG	cassette fusion
NOXC-5N	ATGGATATCTTGCTCGCTCAC	Forward and reverse nest primers for third fusion PCR for amplification of *NOXC* deletion construct
NOXC-3N	CGAATATTCGCACCTTACG	
FCA6-RT-F	TGGTCCAACAGCTACAAGAG	For realtime-PCR of *FCA6*
FCA6-RT-R	CAACATGCTAGGTCGCTGCTTCTT	
FCA7-RT-F	TCTCTTGGGCTGATCTTATGCTC	For realtime-PCR of *FCA7*
FCA7-RT-R	CGTAGATGTCAGTGCTGCCGTT	
FPX1-RT-F	GGTCCCGCTATCCCTTAC	For realtime-PCR of *FPX1*
FPX1-RT-R	GAGAGGGCAACGATTTC	
FPX15-RT-F	GGGTGTCCTCCGCCAGAT	For realtime-PCR of *FPX15*
FPX15-RT-R	GGGTCGGCCTTCATGGTCTTTC	
Tri5-RT-F	GCCATTTTGGACCTTTCTGCTCATT	For realtime-PCR of *TRI5*

Tri5-RT-R	GCCATAGAGAAGCCCCAACACAAT	
Tri6-RT-F	GGCAACCATTCAAGCGCTTTTTCT	For realtime-PCR of *TRI6*
Tri6-RT-R	CACCCTGCTAAAGACCCTCAGACATT	
Cyp1-RT-F	TCAAGCTCAAGCACACCAAGAAGG	For realtime-PCR of *CYP1*
Cyp1-RT-R	GGTCCGCCGCTCCAGTCT	
ZIF1-RT-F	GGTTGATGGCCTTCCTTCGC	For realtime-PCR of *ZIF1*
ZIF1-RT-R	GCCTGTTGCTGCTGCTGAAT	
FgAP1-RT-F	GTGCTGGTTGTTCGCCTGAG	For realtime-PCR of *FgAP1*
FgAP1-RT-R	TGGCTTTCGCAACAGAACGG	
Fg SKN7-RT-F	AGCGATGATTCGGCACCTGA	For realtime-PCR of *FgSKN7*
FgSKN7-RT-R	GGCTTGCGGAATGACCACTG	
GzbZIP007-RT-F	TGTCCTCCTCAGCAGCATGG	For realtime-PCR of *GzbZIP007*

GzbZIP007-RT-R	TTGCTCCTCTGCAGCCCAAT	
GzZC086-RT-F	TGGGATTGCTGTCCCTGTCG	For realtime-PCR of *GzZC086*
GzZC086-RT-R	ACATACCAAGGCGCGAGACA	
GzZC236-RT-F	GCCGTACCTCAGCAGGACAT	For realtime-PCR of *GzZC236*
GzZC236-RT-R	TTAGGGCCGCTCTTCCTTCG	
GzHOME001-RT-F	CGCGGATGCAGAGAATCGTG	For realtime-PCR of *GzHOME001*
GzHOME001-RT-R	CATGGGAGCGTTGCGCTTAG	
GzC2H010-RT-F	TAGAGTTGCGGCGAGCATCA	For realtime-PCR of *GzC2H010*
GzC2H010-RT-R	GGCTGTTCAGTGCACCTTCG	

For self-fertilization, fungal strains were grown on carrot agar plates for 5 days. To induce sexual reproduction, aerial mycelia were removed with sterile 2.5% Tween 60 solution (Leslie & Summerell, 2006). For outcrosses, mycelia of heterothallic female strains grown on carrot agar plates for 5 days were fertilized with 1 ml of a conidial suspension from male strains. After sexual induction, all cultures were incubated under near-UV light (wavelength: 365 nm, HKiv Import & Export Co., Ltd, Xiamen, China) at 25 °C.

V. Virulence assays and trichothecene analysis

For the virulence test, the point inoculation method was performed using the susceptible wheat cultivar Eunpamil as previously described (Son *et al*., 2011a). Ten microliters of conidial suspension (10^6 conidia/ml) harvested from the CMC was injected into the middle of the spikelet. After inoculation, the plants were incubated in a high-humidity chamber for 3 days and transferred to a greenhouse. The number of spikelets displaying symptoms of FHB was determined 21 days after inoculation. More than five replicated inoculations per strain and two independent mutant strains were used in the experiment.

Total trichothecene production (deoxynivalenol and 15-acetyl-deoxynivalenol) was measured as previously described (Son *et al*., 2011a). Cultures grown in MMA were filtered through cheesecloth, and filtrates were extracted with an ethyl acetate/methanol solution. The dehydrated extracts were derivatized with Sylon BTZ (BSA + TMCS + TMSI, 3:2:3, Supelco, Bellefonte, PA, USA), and the derivatized products were analyzed using a Shimadzu QP-5000 gas chromatograph-mass spectrometer (GC-MS) (Shimadzu, Kyoto, Japan). The total

trichothecene concentration was quantified based on the biomass produced by each strain in MMA. The experiment was repeated five times.

VI. Oxidative stress sensitivity assays

To evaluate the effects of oxidative stress on the mycelial growth of the peroxidase deletion mutants, 10 mM H_2O_2 was used. Agar plugs from actively growing cultures were transferred to CM with or without supplementation with H_2O_2, and the plates were incubated at 25 ℃ for 5 days. To screen 657 TF deletion mutants (Son *et al*., 2011b), CM supplemented with 10 mM H_2O_2 was used. At least two independent tests were performed for each assay, and each strain was tested in triplicate.

VII. qRT-PCR analysis

Conidial suspensions (10^6 conidia/ml) harvested from YMA were inoculated into 50 ml of liquid CM and incubated for 24 h at 25 ℃ on a rotary shaker (200 rpm). Total RNA was extracted from strains grown for an additional 30 min in CM only or in CM supplemented with 5 mM H_2O_2. cDNA was synthesized from the total RNA using SuperScript III reverse transcriptase (Invitrogen, Carlsbad, CA, USA). qRT-PCR was performed using SYBR Green Super Mix (Bio-Rad, Hercules, CA, USA) and a 7500 real-time PCR system (Applied Biosystems, Foster City, CA, USA), using primer pairs specific for peroxidase genes (Table 2). The cyclophilin gene (*CYP1*; FGSG_07439) was used as a reference gene. qRT-PCR was performed three times with two replicates per run, and the transcript level of each target gene was calculated as previously described (Livak & Schmittgen, 2001).

To measure the transcript levels of the trichothecene biosynthetic genes *TRI5* and *TRI6*, we incubated conidia from the wild-type and peroxidase deletion mutant strains in MMA media for 4 days, isolated total RNA from each strain, and performed qRT-PCR as described above.

VIII. Peroxidase enzyme activity assay and hydrogen peroxide assay

Fungal strains grown for 24 h in 50 ml liquid CM were incubated for an additional 30 min in CM supplemented with 5 mM H_2O_2. Crude proteins were extracted from harvested mycelia (ground in liquid nitrogen) of wild-type and peroxidase deletion mutant strains using 1 ml of potassium phosphate buffer (250 mM, pH 7.0) supplemented with 1 mM phenylmethylsulfonyl fluoride, a protease inhibitor. The protein concentration was determined colorimetrically by the Bradford assay (Bio-Rad). Total peroxidase enzyme activities were measured using the Quantichrom Peroxidase Assay (BioAssay Systems, Hayward, CA, USA) according to the manufacturer's instructions. Quantification of H_2O_2 in the semi-dried mycelia was determined using an Amplex Red hydrogen peroxide/peroxidase assay kit (Invitrogen).

RESULTS

I. Identification of putative peroxidase genes in *F. graminearum*

We used the previously constructed fungal peroxidase database (http://peroxidase.riceblast.snu.ac.kr) to identify all of the putative peroxidase genes in *F. graminearum* (Choi *et al.*, 2014). The *F. graminearum* genome contains 23 heme peroxidases and 8 non-heme peroxidases, including five previously reported putative monofunctional catalase genes (*FCA1*, *FCA2*, *FCA3*, *FCA4*, and *FCA5*), two putative bifunctional catalase-peroxidase genes (*FCA6* and *FCA7*) (Lee *et al.*, 2014) and three NADPH oxidase genes (*NOXA*, *NOXB*, and *NOXC*) (Wang *et al.*, 2014, Takemoto *et al.*, 2007) (Table 3). We designated the remaining 21 peroxidase genes as *FPX1* to *FPX21* (*F. graminearum* peroxidase) for convenience. To investigate the phylogenetic relationships between the peroxidases of *F. graminearum*, we constructed a phylogenetic tree based on the predicted amino acid sequences of these peroxidases (Fig. 1A and B). Because there was no evolutionary relationship between heme (Fig. 1A) and non-heme peroxidases (Fig. 1B), a separate phylogenetic tree was constructed for each group. Peroxidases belonging to the same family generally clustered together, indicating genetic similarity of their protein sequences. The relationships between peroxidase families were relatively weak, as indicated by low bootstrap values.

To assess the genetic requirements for peroxidases in fungal developmental processes, we analyzed transcript level profiles during sexual and asexual development of the fungus (Fig. 1C) and during plant infection (Fig. 1D). RNA-seq and microarray results were obtained from previous studies (Son *et al.*, 2016, Son

Table 3 Putative peroxidases in *F. graminearum*.

Types of peroxidases			Locus ID	Gene name	Reference
Heme peroxidase	Catalase superfamily	Catalase	FGSG_06554	*FCA1*	(Lee et al., 2014)
			FGSG_06733	*FCA2*	(Lee et al., 2014)
			FGSG_16526	*FCA3*	(Lee et al., 2014)
			FGSG_02881	*FCA4*	(Lee et al., 2014)
			FGSG_06596	*FCA5*	(Lee et al., 2014)
	Class I peroxidase	Catalase-peroxidase	FGSG_02974	*FCA6*	(Lee et al., 2014)
			FGSG_12369	*FCA7*	(Lee et al., 2014)
		Cytochrome C peroxidase	FGSG_01245	*FPX1*	This study
			FGSG_10606	*FPX2*	This study
		Hybrid ascorbate-cytochrome C peroxidase	FGSG_04434	*FPX3*	This study
	Class II peroxidase	Other class II peroxidase	FGSG_16013	*FPX4*	This study
	Haloperoxidase	Haloperoxidase	FGSG_03708	*FPX5*	This study

	superfamily		FGSG_17448	*FPX6*	This study
			FGSG_02341	*FPX7*	This study
			FGSG_08911	*FPX8*	This study
			FGSG_03436	*FPX9*	This study
	Peroxidase-cyclooxygenase superfamily	Prostaglandin H synthase (cyclooxygenase)	FGSG_17094	*FPX10*	This study
		Linoleate diol synthase (PGHS-like)	FGSG_02668	*FPX11*	This study
			FGSG_10960	*FPX12*	This study
			FGSG_11146	*FPX13*	This study
	NADPH oxidase superfamily	NoxA	FGSG_00739	*NOXA*	(Wang et al., 2014)
		NoxB	FGSG_10807	*NOXB*	(Wang et al., 2014)
		NoxC	FGSG_11195	*NOXC*	This study
Non-heme peroxidase	Peroxiredoxin superfamily	1-cysteine peroxiredoxin	FGSG_07536	*FPX14*	This study
		Typical 2-cysteine peroxiredoxin	FGSG_03180	*FPX15*	This study
		Atypical 2-cysteine peroxiredoxin (type Q, BCP)	FGSG_10296	*FPX16*	This study

	Atypical 2-cysteine peroxiredoxin (type II, type V)	FGSG_08677	*FPX17*	This study
		FGSG_00353	*FPX18*	This study
Alkylhydroperoxidase superfamily	Carboxymuconolactone decarboxylase (no peroxidase activity)	FGSG_01796	*FPX19*	This study
		FGSG_10039	*FPX20*	This study
Glutathione peroxidase	Fungal-bacterial glutathione peroxidase	FGSG_06150	*FPX21*	This study

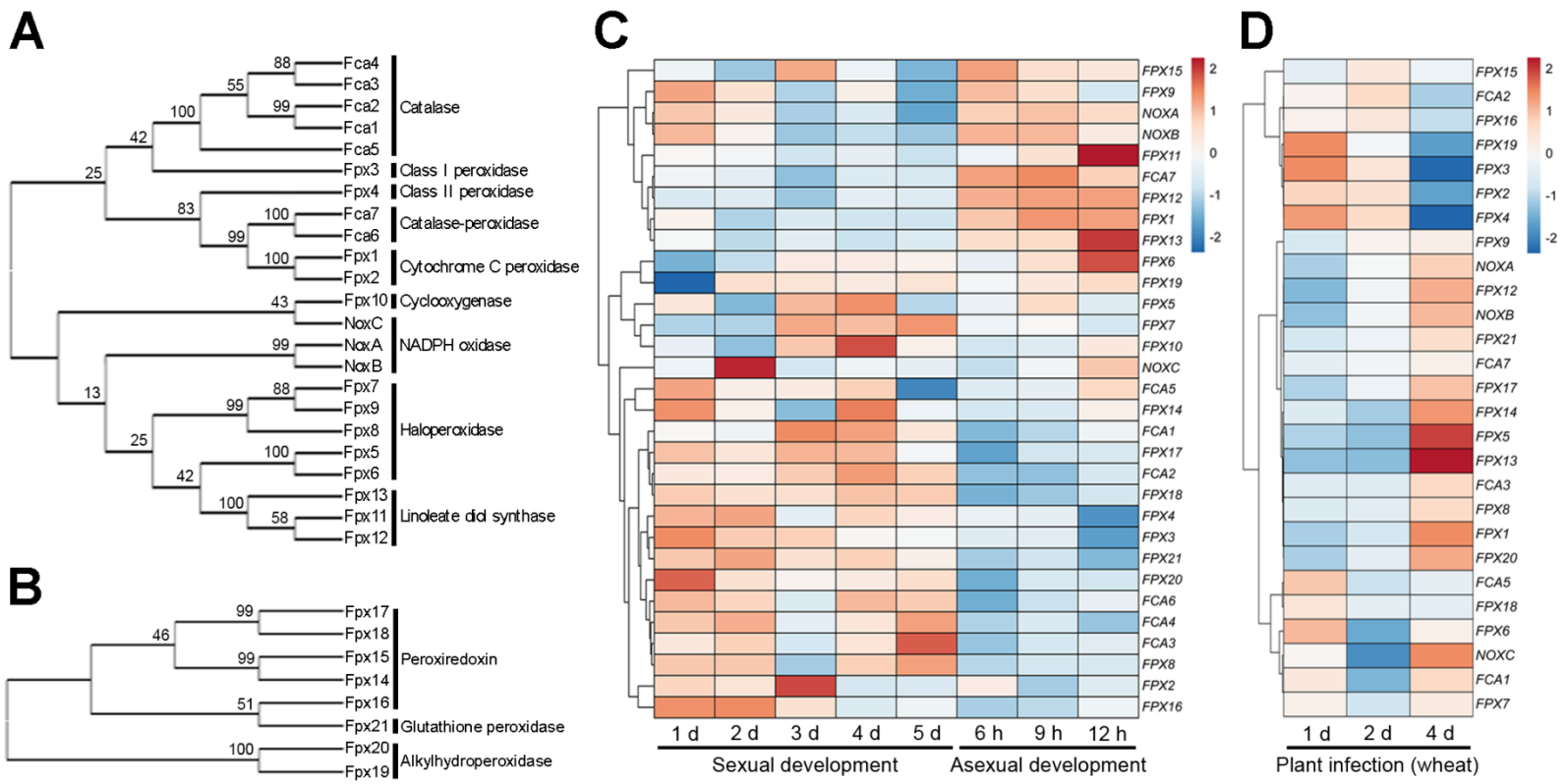
A
Fca4
Fca3
Fca2
Fca1
Fca5
Catalase
Fpx3
Class I peroxidase
Fpx4
Class II peroxidase
Fca7
Fca6
Catalase-peroxidase
Fpx1
Fpx2
Cytochrome C peroxidase
Fpx10
Cyclooxygenase
NoxC
NoxA
NoxB
NADPH oxidase
Fpx7
Fpx9
Fpx8
Fpx5
Fpx6
Haloperoxidase
Fpx13
Fpx11
Fpx12
Linoleate diol synthase
B
Fpx17
Fpx18
Fpx15
Fpx14
Fpx16
Peroxiredoxin
Fpx21
Glutathione peroxidase
Fpx20
Fpx19
Alkylhydroperoxidase
C
FPX15
FPX9
NOXA
NOXB
FPX11
FCA7
FPX12
FPX1
FPX13
FPX6
FPX19
FPX5
FPX7
FPX10
NOXC
FCA5
FPX14
FCA1
FPX17
FCA2
FPX18
FPX4
FPX3
FPX21
FPX20
FCA6
FCA4
FCA3
FPX8
FPX2
FPX16
1 d
2 d
3 d
4 d
5 d
6 h
9 h
12 h
Sexual development
Asexual development
D
FPX15
FCA2
FPX16
FPX19
FPX3
FPX2
FPX4
FPX9
NOXA
FPX12
NOXB
FPX21
FCA7
FPX17
FPX14
FPX5
FPX13
FCA3
FPX8
FPX1
FPX20
FCA5
FPX18
FPX6
NOXC
FCA1
FPX7
1 d
2 d
4 d
Plant infection (wheat)

Fig. 1 Phylogenetic and transcriptional analysis of peroxidase genes. (A) Phylogenetic tree based on the amino acid sequences of 23 putative heme peroxidases and (B) 8 putative non-heme peroxidases in *F. graminearum*. The phylogenetic tree was constructed using the MEGA program (version 6.06) by the neighbor-joining method with 2000 bootstrap replicates (Tamura *et al.*, 2013). The numbers at the nodes represent the bootstrap percentages. (C and D) Heatmap visualization of the peroxidase gene transcriptional profiles during asexual and sexual development (C) and plant infection (D). The heatmap depicts peroxidase gene transcript abundances during various asexual and sexual developmental stages based on Log2-based relative transcript abundances compared with the 0-day (sexual development), 3-h (asexual development), and mock-inoculated samples (plant infection). Red and blue represent higher and lower expression, respectively. The rows represent transcriptional units. The expression data were obtained from previous studies (Sikhakolli *et al*., 2012, Son *et al*., 2013, Son *et al*., 2016, Harris *et al*., 2016) and visualized using ClustVis (Metsalu & Vilo, 2015).

et al., 2013, Sikhakolli *et al.*, 2012, Harris *et al.*, 2016), reanalyzed, and visualized using ClustVis (Metsalu & Vilo, 2015). Expression profiles during plant infection were additionally normalized to that of *β-tubulin* (FGSG_09530). Approximately two-thirds of the studied genes (*FPX5* - *FPX16* in Fig. 1C) were upregulated during the initial or/and late stages of sexual reproduction, but most of these genes were downregulated during conidiation. The other ten genes (*FPX15* - *FPX19* in Fig. 1C) were upregulated during asexual reproduction but showed maintained or reduced expression after sexual induction, with the exception of *FPX9*, *NOXA*, and *NOXB*. During early infection of wheat, approximately half of the studied genes (*FPX15* - *FPX4* and *FCA5* - *FPX7* in Fig. 1D) were upregulated at the initial stage of infection (1 and 2 days after inoculation), whereas the other half of the genes were upregulated during the later days of infection (4 days after inoculation). These results suggest that peroxidase-mediated molecular processes are closely related to fungal development and infection in *F. graminearum*.

II. Targeted deletion of putative peroxidase genes in *F. graminearum*

To investigate the functions of the putative peroxidase genes, we performed targeted gene deletion by homologous recombination. Each peroxidase gene of the *F. graminearum* wild-type strain Z-3639 was replaced with *GEN* to create individual gene deletion mutants (Table 1). Successful disruption of 24 peroxidase genes was confirmed by Southern blot hybridization using oligonucleotides complementary to a 5′ or 3′ flanking region as a probe (Fig. 2). The seven deletion mutants of the catalase and catalase-peroxidase genes *fca1* through *fca7* were derived in a previous study (Lee *et al.*, 2014).

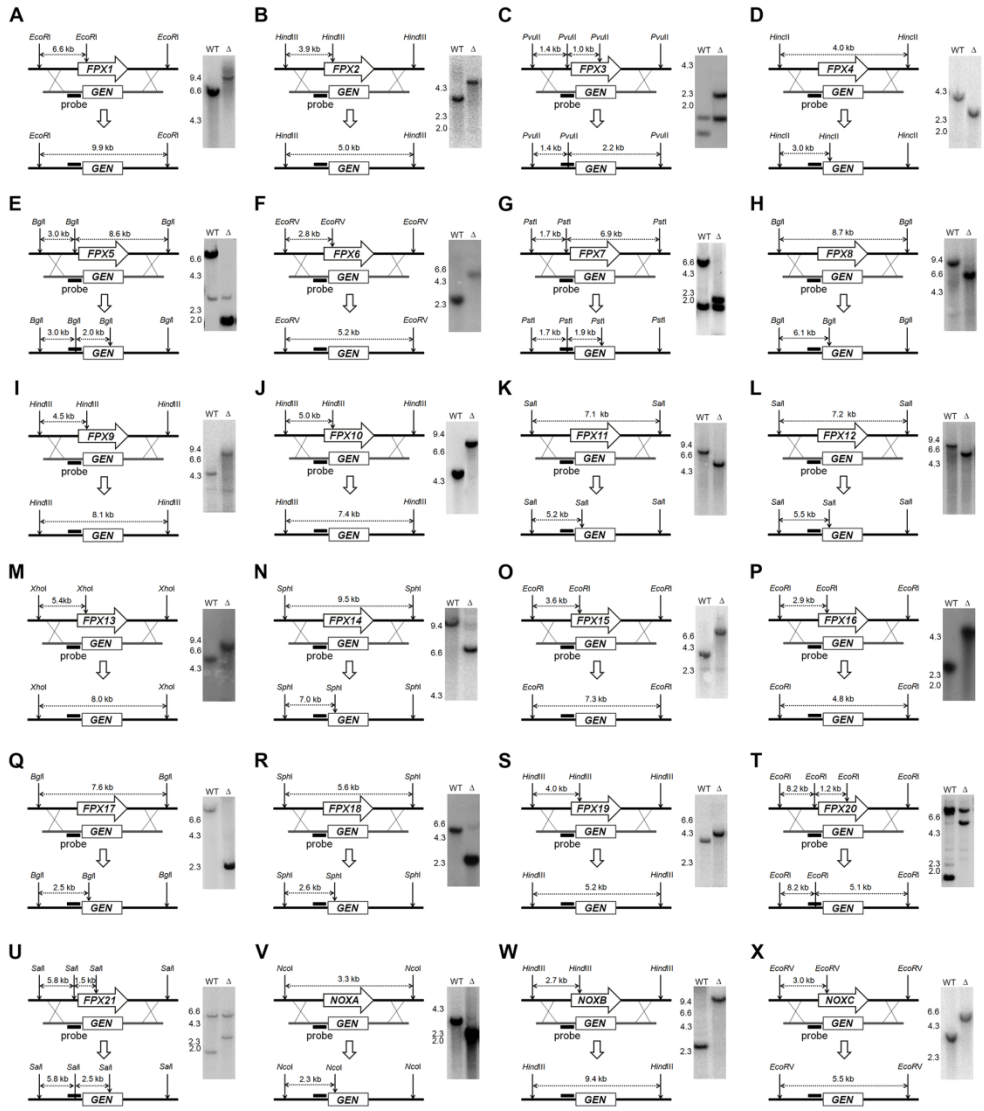

Fig. 2 Targeted gene deletion. Each peroxidase-encoding gene (A-X) was deleted individually from the genome of the *F. graminearum* wild-type strain Z-3639. *GEN*, geneticin resistance gene cassette. The sizes of the DNA standards (in kilobases) are indicated to the left of the blot.

We analyzed 31 peroxidase deletion mutants for defects in various developmental processes, including vegetative growth, sexual and asexual development, trichothecene production, virulence, and the oxidative stress response. Overall, we found that five peroxidase mutants were defective in at least one phenotypic category compared with the wild type (Table 4). None of the peroxidase deletion mutants exhibited defects in vegetative growth or conidiation (Table 5). When cultured on CM and MM, there was no significant difference in radial growth or colony morphology between the wild-type and the peroxidase deletion mutant strains. Moreover, all of the 31 peroxidase deletion mutants were normal with respect to conidia production (Table 5). With respect to sexual development, only the *noxA* deletion mutants showed defects in perithecium production (Fig. 3A). The wild-type and other peroxidase deletion mutants produced normal perithecia 7 days after sexual induction.

III. NADPH oxidase genes in *F. graminearum*

The functions of two NADPH oxidase genes, *NOXA* and *NOXB*, in sexual development and pathogenicity were characterized in previous studies (Wang et al., 2014, Zhang *et al*., 2016). Here, we identified and characterized a novel NADPH oxidase gene, *NOXC*. Disruption of *NOXA* caused significant defects in sexual development, whereas deletion mutants of *NOXB* and *NOXC* showed no defects in perithecium production or maturation (Fig. 3A). Perithecia with cirrhi were observed in *noxB* and *noxC* mutants 10 days after sexual induction. In assays of fungal infection of wheat heads, the *noxA* deletion mutant showed significantly reduced virulence ($p < 0.01$, *t* test), whereas the deletion mutants of *noxB* and *noxC*

Table 4 Summary of the phenotypes of the *F. graminearum* peroxidase mutants.

Developmental processes	Mutants showing defects
Vegetative growth[a]	None (same as wild type)
Conidiation[b]	None (same as wild type)
Sexual development[c]	*noxA*
Oxidative stress response[d]	*fca6*, *fca7*, *fpx1*, *fpx15*
Pathogenicity[e]	*noxA*, *fca7*
Trichothecene production[f]	*fca7*

[a] Radial growth was measured after 5 days of incubation on complete medium (CM) and minimal medium (MM).

[b] The conidia were counted after 3 days of incubation in carboxymethyl cellulose (CMC) medium.

[c] The formation of perithecia was observed 10 days after sexual induction on carrot agar.

[d] The sensitivity to oxidants (H_2O_2) was tested.

[e] The disease index was measured 21 days after inoculation.

[f] Trichothecene production in minimal medium containing 5 mM agmatine (MMA) was analyzed.

Table 5 Phenotypes of the peroxidase mutants.

Strain	Mycelia growth[a]		Conidiation[b]	DON production[c]	Virulence[d]	Sexual development[e]
	CM	MM				
Z-3639	7.9A	7.6A	6.8×10^5A	12.4A	13.0A	Normal
fca1	7.5A	7.9A	6.3×10^5A	12.2A	11.3A	Normal
fca2	7.5A	7.6A	6.8×10^5A	11.6A	11.9A	Normal
fca3	7.9A	7.7A	6.6×10^5A	11.1A	10.1A	Normal
fca4	7.7A	7.8A	6.3×10^5A	13.0A	10.8A	Normal
fca5	7.3A	7.7A	5.8×10^5A	12.0A	11.5A	Normal
fca6	7.5A	7.5A	6.4×10^5A	12.1A	12.1A	Normal
fca7	7.9A	7.4A	6.3×10^5A	24.9B	7.5B	Normal
fpx1	7.8A	7.5A	6.4×10^5A	12.2A	11.6A	Normal
fpx2	7.5A	7.3A	6.6×10^5A	13.8A	12.4A	Normal
fpx3	7.2A	7.3A	6.5×10^5A	12.4A	11.6A	Normal
fpx4	7.9A	7.4A	6.5×10^5A	11.3A	12.4A	Normal
fpx5	7.7A	7.5A	6.1×10^5A	13.8A	12.0A	Normal
fpx6	7.6A	7.5A	6.4×10^5A	11.2A	12.6A	Normal
fpx7	7.5A	7.4A	6.9×10^5A	11.0A	11.8A	Normal
fpx8	7.3A	7.4A	6.5×10^5A	12.5A	12.6A	Normal
fpx9	7.5A	7.3A	5.9×10^5A	13.7A	12.0A	Normal
fpx10	7.5A	7.3A	6.5×10^5A	11.4A	11.6A	Normal
fpx11	7.7A	7.5A	5.9×10^5A	13.2A	12.0A	Normal
fpx12	7.6A	7.5A	6.1×10^5A	13.1A	11.8A	Normal
fpx13	7.8A	7.3A	6.5×10^5A	13.5A	12.6A	Normal
noxA	7.7A	7.5A	6.1×10^5A	12.5A	1.1C	No perithecia
noxB	7.7A	7.3A	6.0×10^5A	11.8A	11.6A	Normal

noxC	7.3A	7.4A	6.6×10^5A	13.3A	13.0A	Normal
fpx14	7.7A	7.0A	6.5×10^5A	12.7A	13.0A	Normal
fpx15	7.5A	7.3A	5.9×10^5A	11.5A	11.4A	Normal
fpx16	7.9A	7.3A	6.8×10^5A	11.1A	13.0A	Normal
fpx17	7.5A	7.3A	6.3×10^5A	13.1A	12.0A	Normal
fpx18	7.6A	7.2A	6.9×10^5A	11.5A	12.6A	Normal
fpx19	7.6A	7.7A	6.3×10^5A	13.3A	11.8A	Normal
fpx20	7.8A	7.3A	6.1×10^5A	13.5A	12.8A	Normal
fpx21	7.6A	7.2A	6.1×10^5A	12.7A	12.6A	Normal

[a] Radial growth was measured after 5 days incubation on complete media (CM) and minimal media (MM).

[b] Number of conidia were counted after 3 days of incubation in carboxymethyl cellulose (CMC) media.

[c] Trichothecenes production in minimal media containing 5 mM agmatine (MMA) was analyzed.

[d] The disease index was measured 21 days after inoculation.

[e] The formation of perithecia was observed 10 days after sexual induction on carrot agar.

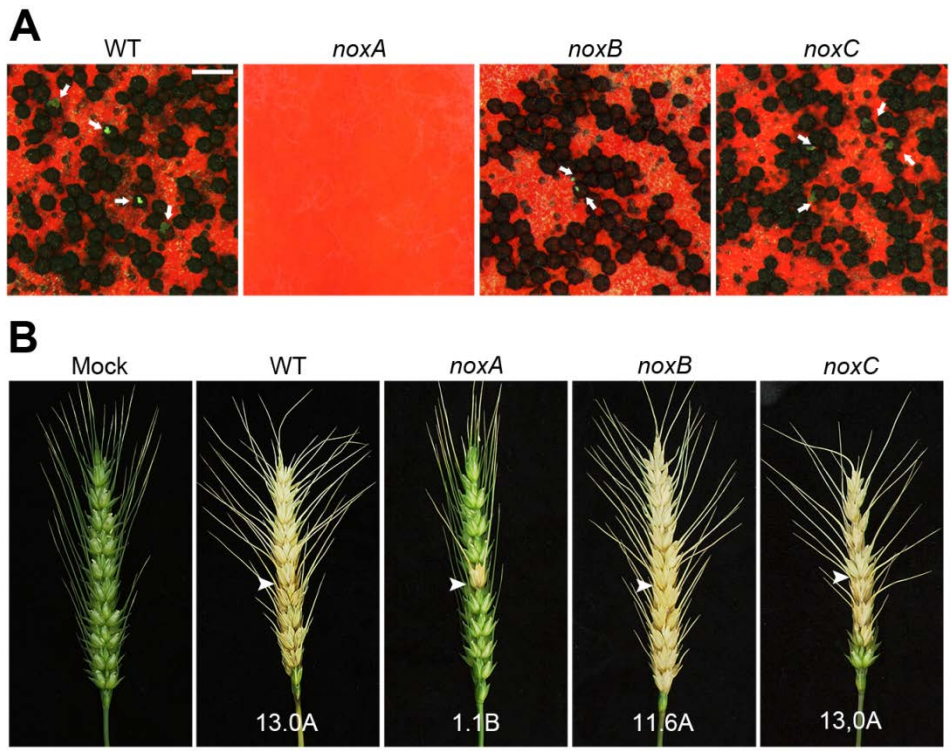

Fig. 3 Sexual development and virulence of NADPH oxidase deletion mutants. (A) Perithecium formation by the NADPH oxidase deletion mutants. Cirrhi (indicated by the white arrow) were observed in the wild-type and in the *noxB* and *noxC* deletion mutants 10 days after sexual induction. Scale bar = 500 µm. (B) Virulence on wheat heads. The center spikelet of each wheat head was injected with 10 µl of a conidial suspension, and photographs were taken 21 days after inoculation. Arrowheads indicate the inoculated spikelets. “Mock” indicates wheat heads that were mock-inoculated with 0.01% Tween 20.

caused typical head blight symptoms (Fig. 3B).

IV. Peroxidases involved in the oxidative stress response

To investigate the sensitivity of the 31 peroxidase deletion mutants to oxidative stress, all of the knockout mutants were cultured in CM supplemented with 10 mM H_2O_2. Only four deletion mutants (*fca6*, *fca7*, *fpx1*, and *fpx15*) exhibited significantly altered sensitivity to oxidative stress mediated by H_2O_2 compared with that of the wild-type strain (Fig. 4A). Of these four deletion mutants, *fca7* and *fpx15* were much more susceptible to H_2O_2 than were the other mutants.

To determine whether the deletion of these four peroxidase genes leads to decreased peroxidase enzyme activity, we measured the peroxidase activity of the deletion mutants under oxidative conditions (Fig. 4B). The total peroxidase activities of the *fca6*, *fca7*, and *fpx1* deletion mutants were significantly reduced compared with that of the wild-type strain. Under our experimental conditions, the peroxidase activity of the *fpx15* deletion mutants was similar to that of the wild-type strain. These results suggest that the oxidative stress sensitivities of the *fca6*, *fca7* and *fpx1* deletion mutants were mainly caused by decreased peroxidase enzyme activity.

To investigate the H_2O_2 degradation capabilities of Fca6, Fca7, Fpx1, and Fpx15, we measured the concentration of H_2O_2 in mycelia after short-term treatment of the cultures with H_2O_2 (Fig. 4C). We found that the H_2O_2 concentration in mycelia of the *fca7* strain was significantly increased compared with that of the wild type. The concentration of H_2O_2 in the mycelia of the other deletion mutants was slightly higher than or similar to that of the wild type.

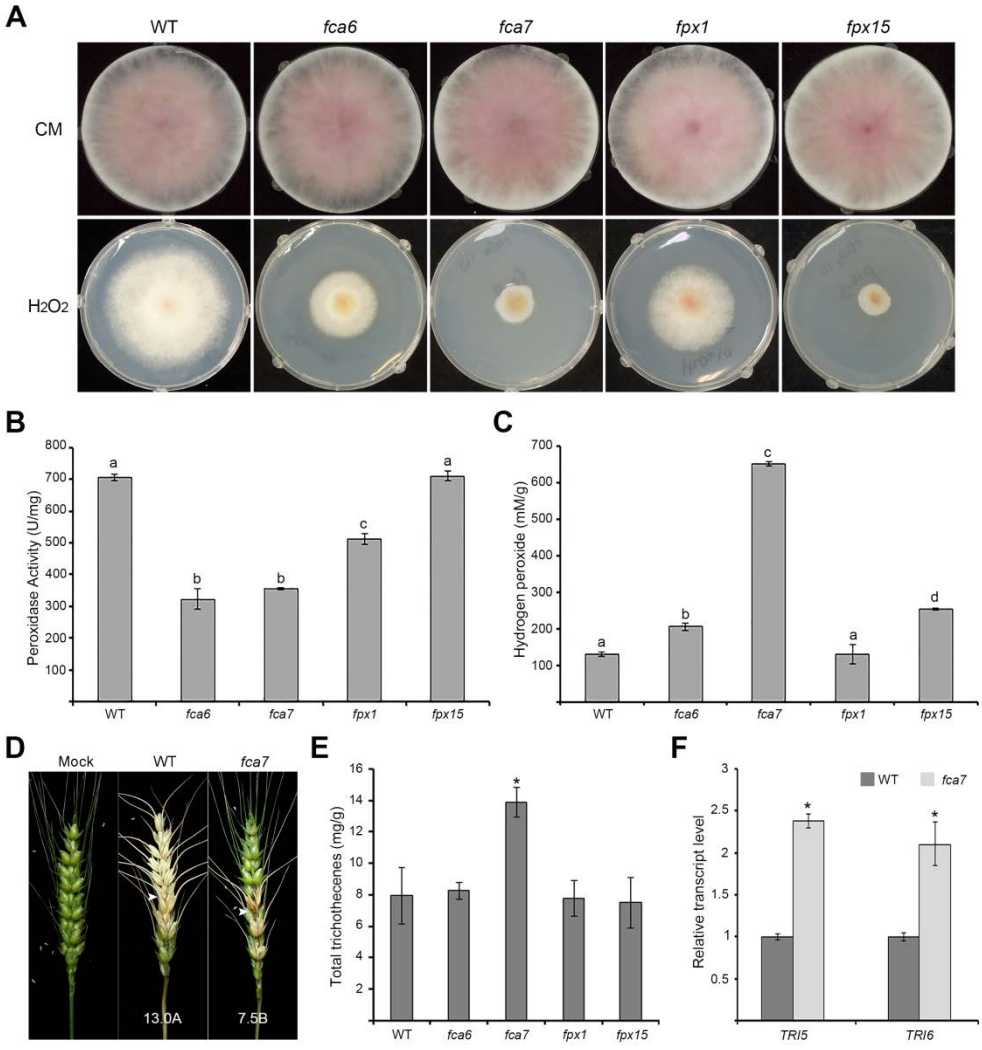
A
WT
fca6
fca7
fpx1
fpx15
CM
H2O2
B
Peroxidase Activity (U/mg)
C
Hydrogen peroxide (mM/g)
D
Mock
WT
fca7
13.0A
7.5B
E
Total trichothecenes (mg/g)
F
WT
fca7
Relative transcript level
TRI5
TRI6

Fig. 4 Peroxidases involved in oxidative stress responses in *F. graminearum*. (A) Oxidative stress sensitivity of *F. graminearum* strains. The mycelial growth of four peroxidase deletion mutants was evaluated on CM with and without supplementation with 10 mM H_2O_2. Photographs were taken 5 days after inoculation. (B) Peroxidase enzyme activities of the *F. graminearum* strains. (C) Hydrogen peroxide detection in mycelia of the *F. graminearum* strains. (D) Virulence on wheat heads. The center spikelet of each wheat head was injected with 10 µl of a conidial suspension, and photographs were taken 21 days after inoculation. Arrowheads indicate the inoculated spikelets. “Mock” indicates wheat heads that were mock-inoculated with 0.01% Tween 20. (E) Total trichothecene production by the *F. graminearum* strains. Each strain was grown in minimal medium containing 5 mM agmatine (MMA) for 7 days. Trichothecenes were analyzed by GC-MS and were quantified based on the biomass of each strain. (F) Transcript levels of *TRI5* and *TRI6* in the wild-type and *fca7* deletion mutant strains. The transcript levels were analyzed by qRT-PCR 4 days after inoculation in MMA. An asterisk indicates a significant difference ($p < 0.01$, Tukey’s test).

V. Peroxidases required for virulence and mycotoxin production

To determine whether the deletion of peroxidase genes affects the virulence of *F. graminearum*, we tested the pathogenicity of the peroxidase deletion mutants in flowering wheat. We found that the *fca6*, *fpx1*, and *fpx15* deletion mutants exhibited normal virulence, despite being highly susceptible to H_2O_2. However, the *fca7* deletion mutant showed reduced (but not abolished) virulence compared with that of the wild-type strain (Fig. 4D).

We also analyzed total trichothecene production (deoxynivalenol and 15-acetyl-deoxynivalenol) by the peroxidase deletion mutants. Interestingly, the accumulation of trichothecenes by the *fca7* deletion mutant was significantly enhanced compared with that of the wild type. The other peroxidase deletion mutants, including *fca6*, *fpx1*, and *fpx15*, produced amounts of trichothecenes similar to those of the wild-type strain (Fig. 4E). The qRT-PCR results demonstrated that the expression of the trichothecene biosynthetic genes *TRI5* and *TRI6* was highly induced in the *fca7* deletion mutant compared with the wild-type strain (Fig. 4F). These results indicate that Fca7 has non-redundant and crucial functions in virulence and trichothecene biosynthesis in *F. graminearum*. However, both the wild-type and the FCA7oe strains produced similar levels of trichothecenes, perhaps because the basal expression of *FCA7* is sufficient to negatively regulate the production of trichothecenes under our experimental conditions (Fig. 5).

VI. Identification of TFs involved in the oxidative stress response

To dissect the regulatory mechanisms of the major peroxidases, we first attempted

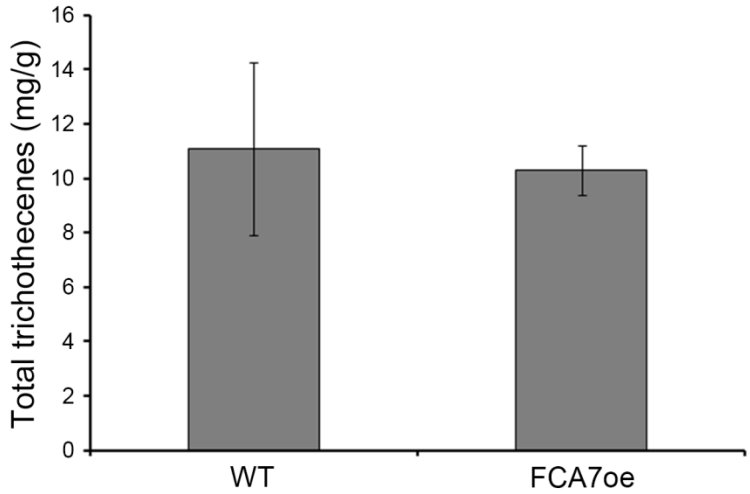

Fig. 5 Total trichothecene production of wild-type and *FCA7* overexpression strains. Each strain was grown in minimal medium containing 5 mM agmatine (MMA) for 7 days. Trichothecenes were analyzed by GC-MS and were quantified based on the biomass of each strain

to identify TFs involved in the oxidative stress response in *F. graminearum* among 657 TF mutants (Son *et al.*, 2011b). We first screened the TF mutants using various oxidative stress-inducing agents (10 mM H_2O_2, 0.1 mM menadione, and 1 mM diamide). From the TF mutants showing altered sensitivity to oxidative stress-inducing agents, we preferentially selected 8 TF mutants that were specifically sensitive to H_2O_2 for further study (Fig. 6A and Table 6). Of these, three TFs (FgAp1, FgSkn7, and Zif1) have previously been functionally characterized in *F. graminearum* (Montibus *et al*., 2013, Jiang *et al*., 2015, Wang *et al*., 2011). FGSG_05171 encodes a homolog of *Neurospora crassa* Cys-3 and *Aspergillus nidulans* MetR that is involved in regulation of the sulfur regulatory circuit (Fu *et al.*, 1989, Natorff *et al.*, 2003), and FGSG_01100 encodes a homolog of FoxO1 that is required for the oxidative stress response in mammalian cell systems (Furukawa-Hibi *et al.*, 2005). The three putative TFs containing a Zn(II)2Cys6 DNA-binding domain (FGSG_08924 and FGSG_01293) and a C2H2 zinc finger domain (FGSG_01298) have not been functionally characterized in other fungi (Table 6).

VII. Expression of four peroxidase genes in TF deletion mutants

We hypothesized that TFs involved in the oxidative stress response regulate the expression of the four peroxidase genes that are required for the oxidative stress response. We performed qRT-PCR to measure the transcript levels of *FCA6*, *FCA7*, *FPX1*, and *FPX15* in the wild-type strain and in the eight selected TF deletion mutants under normal and oxidative stress conditions (Fig. 6B). The transcript levels of *FCA6*, *FCA7*, *FPX1*, and *FPX15* were markedly upregulated in response

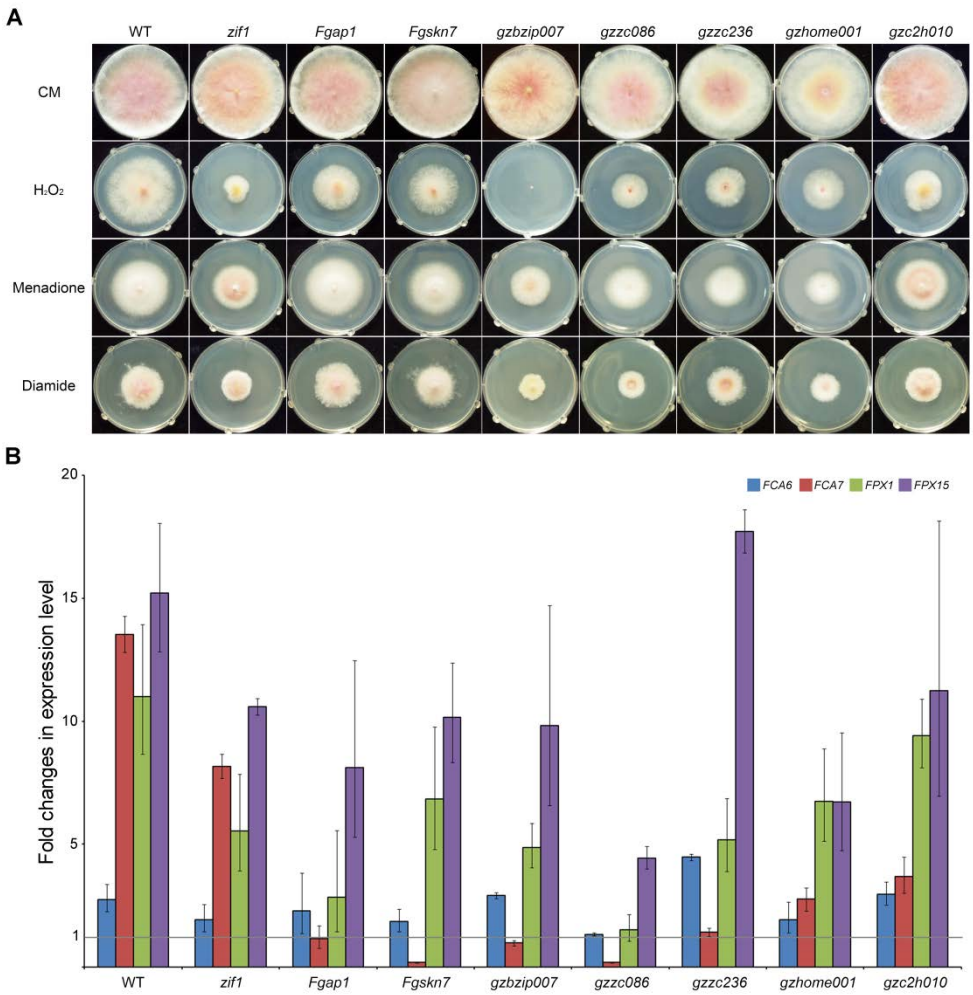

Fig. 6 Characterization of TFs involved in the oxidative stress response. (A) Oxidative stress sensitivity of eight TF mutants. The mycelial growth of the TF deletion mutants was evaluated on CM and on CM supplemented with 10 mM H_2O_2, 0.1 mM menadione, and 1 mM diamide. Photographs were taken 5 days after inoculation. (B) Transcript abundances of peroxidase genes in the TF mutants. The transcript levels of *FCA6*, *FCA7*, *FPX1*, and *FPX15* were analyzed by qRT-PCR. Total RNA was isolated from wild-type and TF deletion mutant strains grown for 30 min in CM only or in CM supplemented with 5 mM H_2O_2.

Table 6 Putative transcription factors involved in the oxidative stress response.

Locus ID	Gene name	Description of the gene product	Species	Homolog	Reference
FGSG_01555	*ZIF1*	Related to bZIP transcription factor	*F. graminearum*	*ZIF1*	(Wang *et al*., 2011)
FGSG_08800	*FgAP1*	Related to AP1-like transcription factor	*F. graminearum*	*FgAP1*	(Montibus *et al*., 2013)
FGSG_06359	*FgSKN7*	Related to SKN7	*F. graminearum*	*FgSKN7*	(Jiang *et al*., 2015)
FGSG_05171	*GzbZIP007*	Related to regulatory protein cys-3	*N. crassa*	*CYS-3*	(Fu *et al*., 1989)
FGSG_08924	*GzZC086*	Conserved hypothetical protein	N/A	N/A	(Son *et al*., 2011b)
FGSG_01293	*GzZC236*	Related to Zn(II)2Cys6 transcriptional activator	N/A	N/A	(Son *et al*., 2011b)
FGSG_01100	*GzHOME001*	Related to LIM homeobox protein	Human	*FoxO1*	(Furukawa-Hibi *et al*., 2005)
FGSG_01298	*GzC2H010*	Conserved hypothetical protein	N/A	N/A	(Son *et al*., 2011b)

to H_2O_2 in the wild-type strain. In the TF deletion mutants, the expression levels of *FCA6*, *FPX1*, and *FPX15* were increased by H_2O_2 treatment (similar to the wild type), whereas the transcript levels of *FCA7* showed a different pattern. In seven TF deletion mutants (*Fgap1*, *Fgskn7*, *gzbzip007*, *gzzc086*, *gzzc236*, *gzhome001*, and *gzc2h010*), the expression of *FCA7* was not highly induced or was even reduced by H_2O_2 treatment (Fig. 6B). In the *zif1* mutant, the expression of *FCA7* was relatively highly expressed following H_2O_2 treatment compared with the expression in other deletion mutants, indicating that *FCA7* expression is a key factor in the oxidative stress response in TF mutants.

VIII. Genetic relationship among TFs and *FCA7*

To investigate the genetic relationships between *FCA7* and eight TFs, we generated TF mutants with *FCA7* overexpression by outcrosses (Table 1). Of seven TF deletion mutants (*Fgap1*, *Fgskn7*, *gzbzip007*, *gzzc086*, *gzzc236*, *gzhome001*, and *gzc2h010*) that showed unchanged or reduced expression of *FCA7* (Fig. 6B), the oxidative stress sensitivity of six (*Fgap1*, *Fgskn7*, *gzzc086*, *gzzc236*, *gzhome001*, and *gzc2h010*) was restored to some degree by overexpression of *FCA7* (Fig. 7). Of these, the *gzzc236* mutant was reported in a previous study to show reduced virulence (Son et al., 2011b). Although the oxidative stress sensitivity of these mutants was restored by overexpression of *FCA7*, virulence was not recovered (Fig. 8). Because the *gzbzip007* deletion mutants did not grow at all on CM supplemented with 10 mM H_2O_2, we assayed the sensitivities of the *gzbzip007* mutants to relatively low oxidative stress conditions (medium containing 3 mM H_2O_2). The vegetative growth of *gzbzip007* under mild oxidative stress

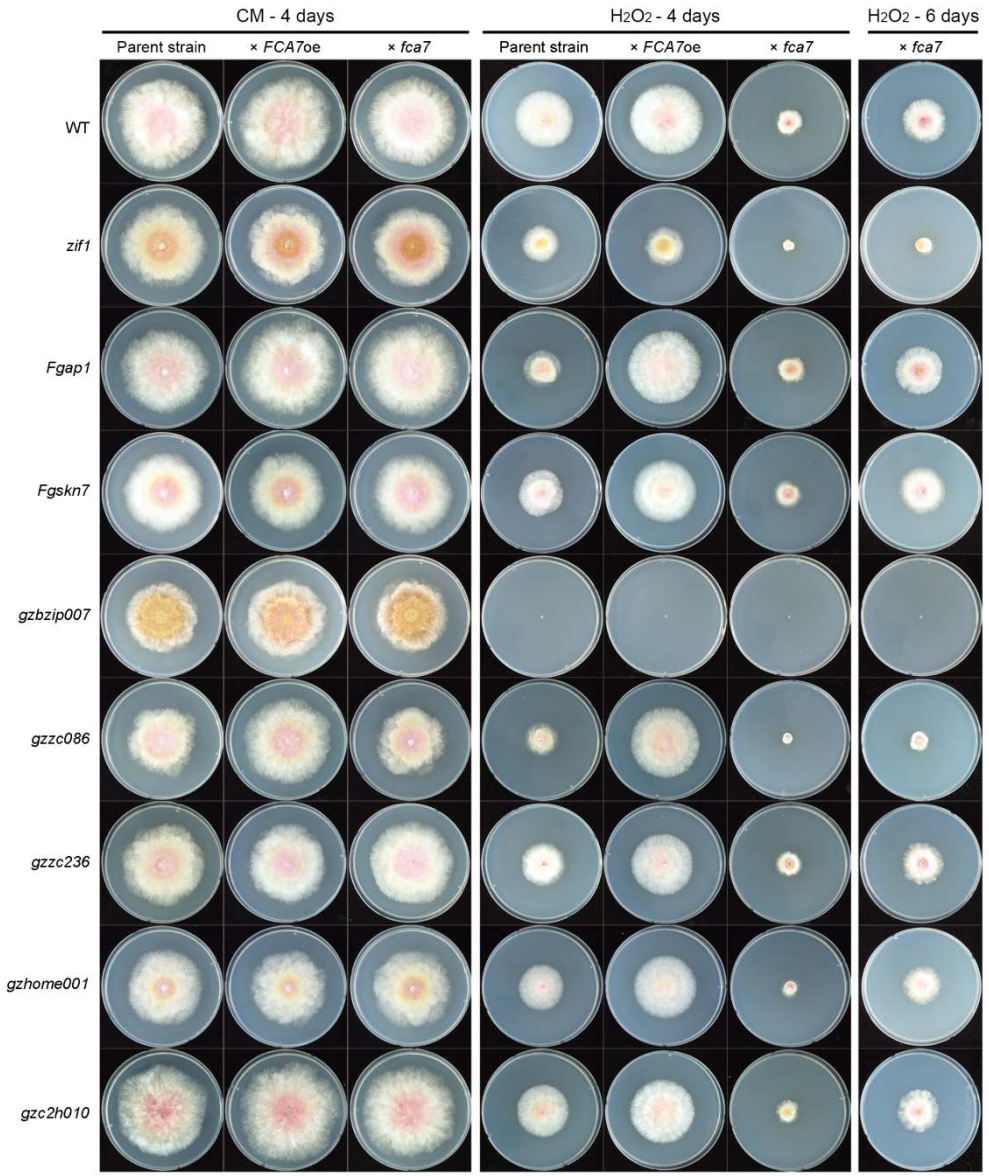

Fig. 7 Oxidative stress sensitivity of eight TF mutants carrying an *FCA7* deletion or *FCA7* overexpression. The mycelial growth of TF mutant strains on CM supplemented with 10 mM H_2O_2 is shown. Photographs were taken 4 and 6 days after inoculation.

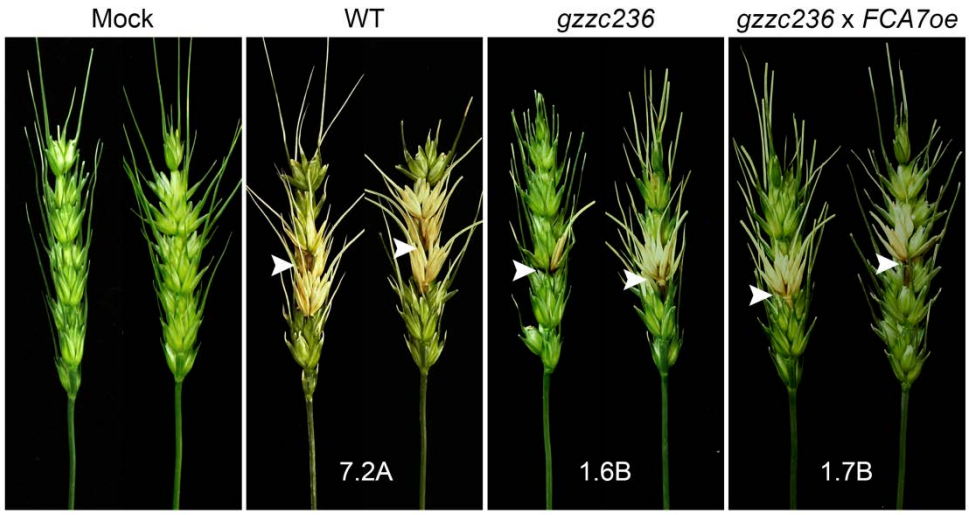

Fig. 8 Virulence on wheat heads. The center spikelet of each wheat head was injected with a conidial suspension of one of the fungal strains. The photographs were taken 21 days after inoculation. The arrowheads indicate the inoculated spikelets. “Mock” indicates wheat heads that were mock-inoculated with 0.01% Tween 20.

conditions was not restored by the overexpression of *FCA7* (Fig. 9). The oxidative stress sensitivity of the *zif1* mutant was slightly restored by *FCA7* overexpression, consistent with the qRT-PCR results. Taken together, these results demonstrate that the altered sensitivities of the TF mutants to oxidative stress were primarily caused by the repression of *FCA7*.

We also outcrossed the TF deletion mutants to a heterothallic *fca7* deletion strain, *mat2 fca7*. If these TFs are involved in a different antioxidant system, the double mutation would be expected to produce synergistic defects in the oxidative stress response. We found that two TF deletion mutants (*zif1* and *gzzc086*) showed markedly increased sensitivity to oxidative stress when combined with the deletion of *FCA7* (Fig. 7). Based on the phenotypes of the *gzzc086* mutants carrying *FCA7* deletion or overexpression, we suspected that *GzZC086* has a regulatory function for *FCA7* expression and that it is involved in multiple antioxidant pathways. Double deletion mutants of *fca7* and TFs (*Fgap1*, *Fgskn7*, *gzzc236*, *gzhome001*, and *gzc2h010*) did not show synergistic effects on oxidative stress sensitivity compared with the corresponding single-gene deletion mutants.

IX. Genetic regulatory network of the TFs involved in oxidative stress responses

We further examined the transcript levels of the TF genes in the wild-type strain under normal and oxidative stress conditions using qRT-PCR (Fig. 10A). The expression of five TF genes (*ZIF1*, *FgAP1*, *FgSKN7*, *GzbZIP007*, and *GzZC086*) was significantly upregulated in response to H_2O_2, whereas the expression of the other three TF genes (*GzZC236*, *GzHOME001*, and *GzC2H010*) was not induced

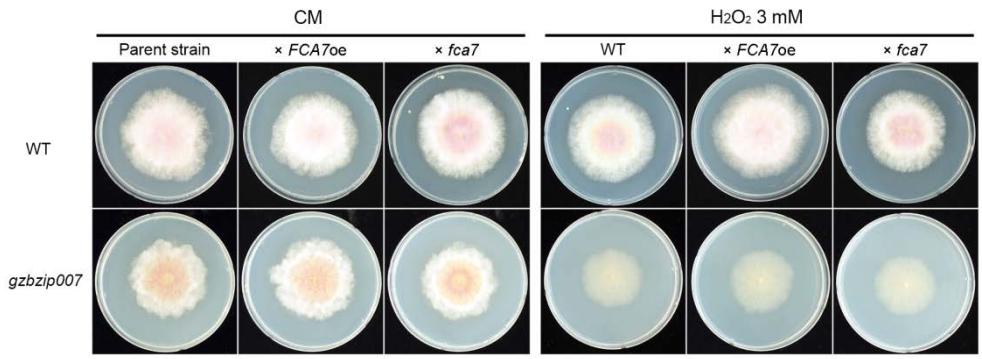

Fig. 9 Mycelial growth on CM supplemented with 4 mM H_2O_2 of *gzbzip007* mutant strains carrying an *FCA7* deletion or with *FCA7* overexpression. The photographs were taken 4 days after inoculation.

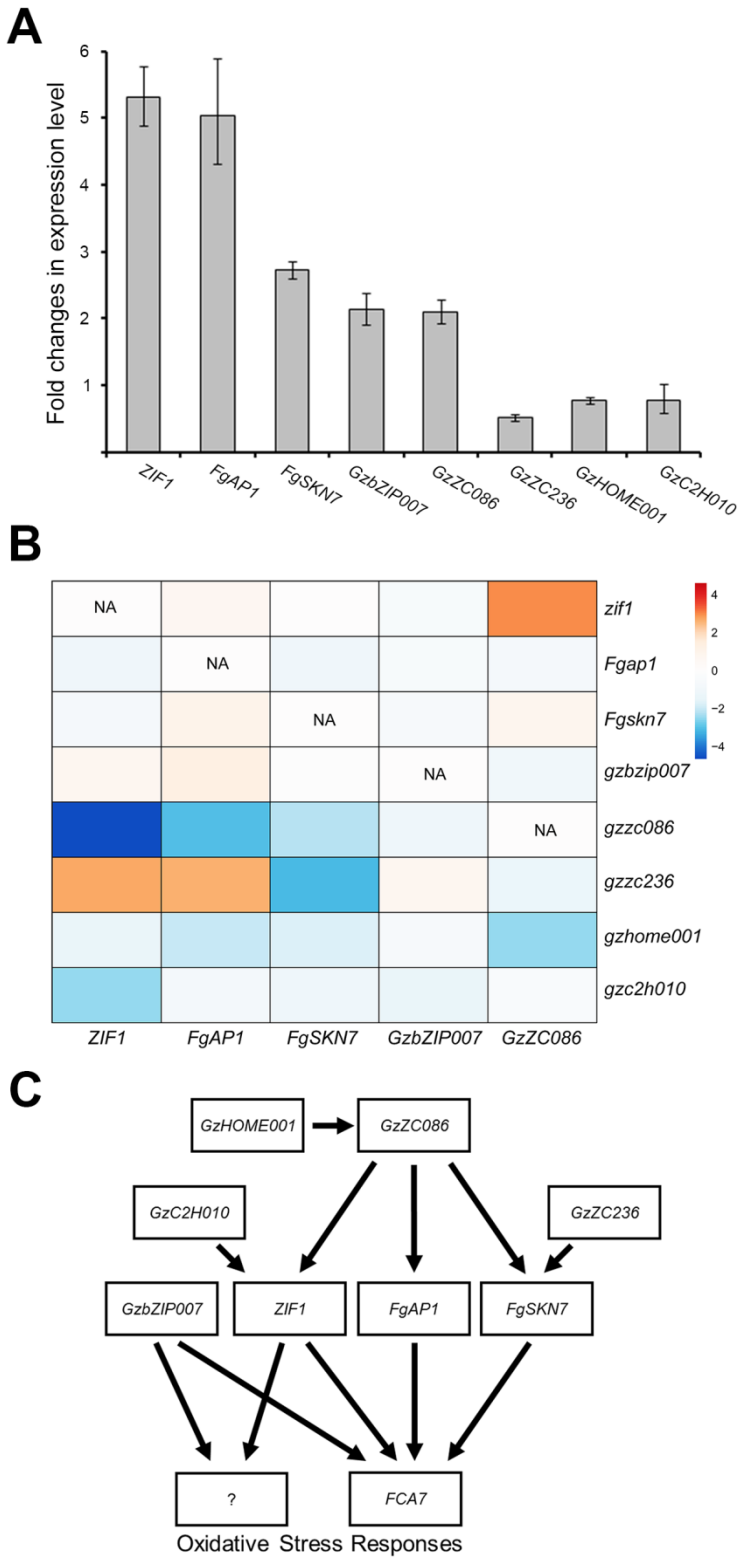
A
Fold changes in expression level
6
5
4
3
2
1
ZIF1
FgAP1
FgSKN7
GzbZIP007
GzZC086
GzZC236
GzHOME001
GzC2H010
B
NA
zif1
Fgap1
Fgskn7
gzbzip007
gzzc086
gzzc236
gzhome001
gzc2h010
4
2
0
−2
−4
ZIF1
FgAP1
FgSKN7
GzbZIP007
GzZC086
C
GzHOME001
GzZC086
GzC2H010
GzZC236
GzbZIP007
ZIF1
FgAP1
FgSKN7
?
FCA7
Oxidative Stress Responses

Fig. 10 Genetic network of TF genes involved in the oxidative stress response in *F. graminearum*. (A) Fold change values in the expression of TF genes after H_2O_2 treatment in the wild-type strain. The transcript levels of the TF genes were analyzed by qRT-PCR. Total RNA was isolated from the wild-type strain grown for 30 min in CM only or in CM supplemented with 5 mM H_2O_2. (B) Heatmap of selected TF genes that were upregulated in the wild-type strain in response to H_2O_2. The log base ratio of the fold change in gene expression in each deletion mutant compared with that in the wild-type strain was converted to a heatmap using ClustVis (Metsalu & Vilo, 2015). (C) Proposed genetic network of TFs and *FCA7* in the oxidative stress response. “?” indicates unknown antioxidant components.

under our experimental conditions. To investigate the genetic regulatory network with which TF genes are associated, we examined the expression of the five TF genes that showed increased expression under oxidative stress conditions in eight TF deletion mutants. We compared the fold change values in the expression of those five TF genes after H_2O_2 treatment in the eight TF deletion mutants to the fold change values in the wild-type strain (Fig. 10B). H_2O_2-mediated induction of *ZIF1*, *FgAP1*, and *FgSKN7* was nearly abolished in the *gzzc086* mutants, and *GzZC086* was not induced in *gzhome001*. We also found that the expression of *ZIF1* and *FgSKN7* did not increase in response to H_2O_2 in the *gzc2h010* and *gzzc236* mutants, respectively. The expression of *GzbZIP007* was not reduced in any of the TF deletion mutants, indicating that *GzbZIP007* is involved in a completely independent regulatory system for oxidative stress responses. Furthermore, it appeared that feedback regulatory mechanisms among the TFs *ZIF1-GzZC086*, *ZIF1-Gz236*, and *FgAP1-GzZC236* modulate the genetic regulatory networks. Based on our data, we proposed a simplified genetic regulatory network that illustrates how TF genes are involved in the oxidative stress response in *F. graminearum* (Fig. 10C).

In conclusion, we found that although the expression of *FCA7* was not the only component of the oxidative stress response, Fca7 was the major antioxidant enzyme produced. We also concluded that at least six TFs (*FgAP1, FgSKN7, GzZC086, GzZC236, GzHOME001, and GzC2H010*) regulate the expression of *FCA7* under oxidative stress conditions, demonstrating the existence of a complex network of transcriptional activators of antioxidant genes.

DISCUSSION

Because plant pathogenic fungi encounter both internal and external oxidative stresses during development and during the process of plant infection, they have evolved effective ROS-detoxifying mechanisms (Heller & Tudzynski, 2011). In particular, the rapid generation of H_2O_2 is one of the earliest plant defense responses to occur following the perception by plants of signals associated with the presence of pathogens (Lamb & Dixon, 1997, Levine *et al*., 1994), and the roles of H_2O_2-scavenging enzymes such as catalases and catalase-peroxidases during plant invasion have been investigated in various phytopathogenic fungi (Garre *et al*., 1998, Robbertse *et al*., 2003, Schouten *et al*., 2002, Skamnioti *et al*., 2007, Tanabe *et al.*, 2011). H_2O_2 also plays an important role as a signaling molecule in various developmental processes of fungi such as cell differentiation and sexual development (Hansberg *et al.*, 1993, Lara-Ortíz *et al*., 2003, Gessler *et al*., 2007). Thus, cellular ROS levels should be extremely fine-tuned by peroxidases by fungal development. In this study, we investigated the roles of putative peroxidases in *F. graminearum*. I identified 31 genes encoding putative peroxidases in *F. graminearum* and characterized their functions not only in the oxidative stress response but also in various developmental processes.

The *F. graminearum* genome contains 23 peroxidases belonging to the 11 heme peroxidase families and 8 peroxidases belonging to the 6 non-heme peroxidase families. In yeast, only 2 heme peroxidase families and 5 non-heme peroxidase families have been found (Choi et al., 2014). A comparison of the predicted peroxidase genes in plant pathogenic fungi including *F. graminearum*, *M. oryzae*, *C. heterostrophus* and yeast revealed that the genomes of plant pathogenic

fungi generally contain numerous heme peroxidase genes (Choi et al., 2014). Several studies have reported that certain heme peroxidase genes such as haloperoxidase genes and catalase-peroxidase genes are mainly found in the genomes of phytopathogens (Zámocký & Obinger, 2010, Gasselhuber *et al.*, 2015, Zámocký *et al.*, 2012). These results imply a potential role of heme peroxidases in pathogenicity.

Phenome analysis of 31 peroxidase deletion mutants in *F. graminearum* revealed that only five peroxidase deletion mutants (*fca6*, *fca7*, *fpx1*, *fpx15*, and *noxA*) were involved in the various developmental processes examined. Other peroxidases may be able to functionally compensate for the loss of a single peroxidase, indicating overlapping and redundant functions of these peroxidases. The clustered peroxidase gene expression profiles observed during reproductive processes also support the overlapping functions of peroxidases in *F. graminearum* (Fig. 1C). Likewise, the deletion of multiple catalase genes in *Cryptococcus neoformans* did not cause visible phenotypic changes, due to the presence of a robust and redundant antioxidant defense system in this species (Giles *et al.*, 2006). Moreover, in other filamentous fungi such as *B. cinerea* and *M. oryzae*, deletion of the genes required for the oxidative stress response did not cause phenotypic changes in the fungal growth rate or in conidia production (Huang *et al.*, 2011, Temme & Tudzynski, 2009).

With respect to sexual development, only *noxA* deletion mutants showed defective perithecia production. Previous studies demonstrated that NADPH oxidase-dependent ROS signaling is important for cellular differentiation and development in fungi (Takemoto *et al.*, 2007, Heller & Tudzynski, 2011). In this

study, we identified three NADPH oxidase homologs in *F. graminearum*: NoxA, NoxB and NoxC. The function of NoxC has been very little studied in filamentous fungi, whereas the functions of NoxA and NoxB in various cellular differentiation processes, including sexual development and pathogenicity, have been well-characterized (Cano-Domínguez *et al.*, 2008, Segmüller *et al.*, 2008, Lara-Ortíz et al., 2003, Scott & Eaton, 2008, Takemoto et al., 2007, Wang et al., 2014, Giesbert *et al.*, 2008, Egan *et al.*, 2007, Zhang et al., 2016). A recent study reported that NoxC exists in only seven Ascomycota and that most of these seven species are phytopathogenic fungi, suggesting that NoxC may have a specialized function in pathogenicity (Takemoto *et al.*, 2007). Moreover, *NOXC* showed distinct and unique expression patterns during fungal reproduction compared with those of *NOXA* and *NOXB* (Fig. 1C). However, deletion of *NOXC* did not affect the pathogenicity of *F. graminearum*. Thus, the function of *NOXC* remains unclear.

Four peroxidase genes, *FCA6*, *FCA7*, *FPX1*, and *FPX15*, were closely involved in the oxidative stress response, but deletion of *FPX15* did not affect peroxidase activity in *F. graminearum* (Fig. 3B). *FPX15* is predicted to encode a non-heme peroxidase belonging to the typical 2-Cys peroxiredoxin family. Peroxiredoxins possess both peroxidase and molecular chaperone activities (Jang *et al.*, 2004), and the peroxidase-to-chaperone switch is triggered by oxidative stress (Jang et al., 2004, Kim *et al.*, 2009). Based on previous and current results, we concluded that the increased sensitivity of *fpx15* to oxidative stress was not directly related to its peroxidase activity but to its chaperone activity.

Although the total peroxidase enzyme activity of *fca6* was decreased to a level similar to that of *fca7*, the concentration of accumulated H_2O_2 in the mycelia

of *fca7* was much higher than that of *fca6*. *FCA7* homologs were predicted to encode an extracellular catalase-peroxidase (Zámocký *et al.*, 2009), and Fca7 contains a potential signal sequence for secretion predicted by SignalP 4.0 (Petersen *et al.*, 2011). These results suggest that Fca7 may play a predominant role in the detoxification of external H_2O_2 in *F. graminearum*. Consistent with the fact that plant-derived ROS scavenging by extracellular peroxidases is critical for successful infection, only *fca7* mutants were reduced in virulence compared with that of the wild-type strain.

Proteomic analysis of wheat spikelets during infection by *F. graminearum* revealed that proteins related to the oxidative burst pathway are induced at the early infection stage (Zhou *et al.*, 2006, Zhou *et al.*, 2005). In this study, we discovered that although deletion mutants of *FCA6*, *FCA7*, *FPX1*, and *FPX15* showed increased sensitivity to oxidative stress mediated by H_2O_2, only *fca7* deletion mutants exhibited reduced virulence compared with that of the wild-type strain. In a number of phytopathogenic fungi, deletion of a gene that is essential for survival in the presence of high concentrations of H_2O_2 does not lessen virulence; this may be due to the presence of alternative antioxidant systems (Robbertse *et al*., 2003, Temme & Tudzynski, 2009). Taken together, we conclude that Fca7 may function as a major H_2O_2-scavenging enzyme and that it may play an irreplaceable role during the infection process in *F. graminearum*.

Recent studies have reported that oxidative stress and secondary metabolism are tightly linked in filamentous fungi and have suggested that secondary metabolites play a protective role in the adaptation of plants to stress conditions (Montibus et al., 2015, Hong et al., 2013a). In *F. graminearum*, trichothecenes have

been reported to be virulence factors for fungal infection of wheat heads (Maier *et al.*, 2006, Desjardins *et al.*, 1996), and trichothecene biosynthesis has been shown to be triggered by exogenous H_2O_2 treatment associated with the increased expression of *TRI* genes (Ponts *et al*., 2006, Ponts *et al*., 2007). In this study, we found that an *fca7* deletion mutant produced more trichothecene than the wild-type strain and that Fca7 is the major H_2O_2-scavenging enzyme expressed in *F. graminearum* under oxidative stress conditions (Fig. 3C and E). Based on these findings, we concluded that Fca7-mediated modulation of H_2O_2 might be one the major determinants of trichothecene production in *F. graminearum.*

Eight TFs involved in the oxidative stress response were identified in *F. graminearum*. Previously, homologs of Yap1 and Skn7 were identified and functionally characterized in *F. graminearum* (Jiang *et al*., 2015, Montibus *et al*., 2013). Yap1 and Skn7 are central TFs that regulate the expression of oxidative stress-related genes in *S. cerevisiae* (Lee *et al*., 1999). A novel bZIP TF, Zif1, has also been reported in *F. graminearum* (Wang *et al*., 2011). In this study, we identified five new TFs (*GzbZIP007*, *GzZC086*, *GzZC236*, *GzHOME001*, and *GzC2H010*) that are involved in the oxidative stress response in this fungus. We proposed a hypothetical simplified genetic network of TF genes in the oxidative stress response (Fig. 6C). Because studies of genetic networks governing the oxidative stress response have been limited due to the lack of TF mutants, further studies of these TFs in filamentous fungi, including *F. graminearum*, will expand our understanding of the molecular mechanisms underlying the oxidative stress response in this type of fungus.

We found that multiple TFs (*FgAP1*, *FgSKN7*, *GzZC086*, *GzZC236*,

GzHOME001, and *GzC2H010*) co-regulated the expression of *FCA7* in response to oxidative stress, reflecting a complex network of transcriptional activators of antioxidant genes. A cooperative role of these TFs has been reported in previous studies (Shalaby *et al*., 2014, Mulford & Fassler, 2011, Calvo *et al.*, 2012). In *S. cerevisiae* and *C. heterostrophus*, Yap1 and Skn7 cooperate to activate the expression of antioxidant genes in response to oxidative stress (Mulford & Fassler, 2011, Shalaby *et al*., 2014). In *F. graminearum*, the genetic relationship between orthologs of Skn7 and Atf1 has been investigated (Jiang *et al.*, 2015). We further identified the putative TF binding sites in the upstream regions (-500 to -1 bp) of *FCA7* using MatchTM software (Kel *et al.*, 2003). The promoter of *FCA7* was found to contain two C2H2 zinc finger protein-binding regions (GCCCC and TTGGC) and several binding motifs (ACCTG, GCTGT, CCTGT, etc.) for homeobox proteins, suggesting that *FCA7* might be under the direct regulation of GzC2H010 (C2H2 zinc finger) and/or GzHOME001 (homeobox).We also found that three TFs (*ZIF1*, *GzZC086*, and *GzbZIP007*) may be involved in alternative antioxidant systems such as the non-enzymatic antioxidant response (Apel & Hirt, 2004). Non-enzymatic antioxidants include low-molecular-weight compounds such as glutathione, ascorbate and cysteine. Homologs of *CYS-3* have been reported to regulate sulfur metabolism, which is involved in the biosynthesis of amino acids such as cysteine and methionine (Kong *et al.*, 2015, Marzluf, 1997). The roles of cysteine and methionine residues in proteins in antioxidant functions have been reported in several studies (Fauchon *et al.*, 2002, Pócsi *et al.*, 2004, Levine *et al.*, 2000). Thus, the increased H_2O_2 sensitivity of the *gzbzip007* deletion mutant may be due to defects in sulfur metabolism. In *M. oryzae*, deletion mutants of Mo*METR*,

an ortholog of *CYS-3*, showed methionine auxotrophy and hypersensitivity to H_2O_2 (Kong *et al*., 2015).

In conclusion, our work reveals that *F. graminearum* possesses a robust antioxidant system that is involved in maintaining cellular ROS balance during cell differentiation and proliferation and that major peroxidases are involved in the oxidative stress response in this species. We suggest that Fca7 is particularly important for pathogen-host interactions and that multiple TFs co-regulate the expression of *FCA7* under oxidative stress conditions.

LITERATURE CITED

Apel, K. and Hirt, H. (2004) Reactive oxygen species: metabolism, oxidative stress, and signal transduction. *Annu. Rev. Plant Biol.,* **55,** 373-399.

Arunachalam, C. and Doohan, F. M. (2013) Trichothecene toxicity in eukaryotes: Cellular and molecular mechanisms in plants and animals. *Toxicol. Lett.,* **217,** 149-158.

Bowden, R. L. and Leslie, J. F. (1999) Sexual recombination in *Gibberella zeae*. *Phytopathology,* **89,** 182-188.

Calvo, I. A., García, P., Ayté, J. and Hidalgo, E. (2012) The transcription factors Pap1 and Prr1 collaborate to activate antioxidant, but not drug tolerance, genes in response to H_2O_2. *Nucleic Acids Res.,* **40,** 4816-4824.

Camhi, S. L., Lee, P. and Choi, A. M. (1995) The oxidative stress response. *New Horizons,* **3,** 170-182.

Cano-Domínguez, N., Álvarez-Delfín, K., Hansberg, W. and Aguirre, J. (2008) NADPH oxidases NOX-1 and NOX-2 require the regulatory subunit NOR-1 to control cell differentiation and growth in *Neurospora crassa*. *Eukaryot. Cell,* **7,** 1352-1361.

Cappellini, R. A. and Peterson, J. L. (1965) Macroconidium formation in submerged cultures by a non-sporulating strain of *Gibberella zeae*. *Mycologia,* **57,** 962-966.

Chen, L.-H., Lin, C.-H. and Chung, K.-R. (2012) Roles for SKN7 response regulator in stress resistance, conidiation and virulence in the citrus pathogen *Alternaria alternata*. *Fungal Genet. Biol.,* **49,** 802-813.

Choi, J., Détry, N., Kim, K.-T., Asiegbu, F. O., Valkonen, J. P. and Lee, Y.-H. (2014)

fPoxDB: fungal peroxidase database for comparative genomics. *BMC Microbiol.,* **14,** 117.

Desjardins, A. E. and Proctor, R. H. (2007) Molecular biology of *Fusarium* mycotoxins. *Int. J. Food Microbiol.,* **119,** 47-50.

Desjardins, A. E., Proctor, R. H., Bai, G., McCormick, S. P., Shaner, G., Buechley, G., *et al.* (1996) Reduced virulence of trichothecene-nonproducing mutants of *Gibberella zeae* in wheat field tests. *Mol. Plant-Microbe Interact.,* **9,** 775-781.

Egan, M. J., Wang, Z.-Y., Jones, M. A., Smirnoff, N. and Talbot, N. J. (2007) Generation of reactive oxygen species by fungal NADPH oxidases is required for rice blast disease. *Proc. Natl. Acad. Sci. U. S. A.,* **104,** 11772-11777.

Fauchon, M., Lagniel, G., Aude, J.-C., Lombardia, L., Soularue, P., Petat, C., *et al.* (2002) Sulfur sparing in the yeast proteome in response to sulfur demand. *Mol. Cell,* **9,** 713-723.

Fourquet, S., Huang, M.-E., D'Autreaux, B. and Toledano, M. B. (2008) The dual functions of thiol-based peroxidases in H_2O_2 scavenging and signaling. *Antioxid. Redox Signal.,* **10,** 1565-1576.

Fu, Y.-H., Paietta, J. V., Mannix, D. G. and Marzluf, G. A. (1989) *cys-3*, the positive-acting sulfur regulatory gene of *Neurospora crassa*, encodes a protein with a putative leucine zipper DNA-binding element. *Mol. Cell. Biol.,* **9,** 1120-1127.

Furukawa-Hibi, Y., Kobayashi, Y., Chen, C. and Motoyama, N. (2005) FOXO transcription factors in cell-cycle regulation and the response to oxidative

stress. *Antioxid. Redox Signal.,* **7,** 752-760.

Gardiner, D. M., Kazan, K. and Manners, J. M. (2009) Novel genes of *Fusarium graminearum* that negatively regulate deoxynivalenol production and virulence. *Mol. Plant-Microbe Interact.,* **22,** 1588-1600.

Garre, V., Tenberge, K. B. and Eising, R. (1998) Secretion of a fungal extracellular catalase by *Claviceps purpurea* during infection of rye: putative role in pathogenicity and suppression of host defense. *Phytopathology,* **88,** 744-753.

Gasselhuber, B., Jakopitsch, C., Zámocký, M., Furtmüller, P. G. and Obinger, C. (2015) Mechanistic aspects of catalase-peroxidase. In: *Heme Peroxidases.* Royal Society of Chemistry, pp. 156-180.

Gessler, N. N., Aver'Yanov, A. A. and Belozerskaya, T. A. (2007) Reactive oxygen species in regulation of fungal development. *Biochemistry,* **72,** 1091-1109.

Giesbert, S., Schuerg, T., Scheele, S. and Tudzynski, P. (2008) The NADPH oxidase Cpnox1 is required for full pathogenicity of the ergot fungus *Claviceps purpurea*. *Mol. Plant Pathol.,* **9,** 317-327.

Giles, S. S., Stajich, J. E., Nichols, C., Gerrald, Q. D., Alspaugh, J. A., Dietrich, F., *et al.* (2006) The *Cryptococcus neoformans* catalase gene family and its role in antioxidant defense. *Eukaryot. Cell,* **5,** 1447-1459.

Goswami, R. S. and Kistler, H. C. (2004) Heading for disaster: *Fusarium graminearum* on cereal crops. *Mol. Plant Pathol.,* **5,** 515-525.

Guo, M., Chen, Y., Du, Y., Dong, Y., Guo, W., Zhai, S., *et al.* (2011) The bZIP transcription factor MoAP1 mediates the oxidative stress response and is critical for pathogenicity of the rice blast fungus *Magnaporthe oryzae*.

PLoS Pathog., **7,** e1001302.

Hansberg, W., De Groot, H. and Sies, H. (1993) Reactive oxygen species associated with cell differentiation in *Neurospora crassa*. *Free Radic. Biol. Med.,* **14,** 287-293.

Harris, L. J., Balcerzak, M., Johnston, A., Schneiderman, D. and Ouellet, T. (2016) Host-preferential *Fusarium graminearum* gene expression during infection of wheat, barley, and maize. *Fungal Biol.,* **120,** 111-123.

Harris, S. D. (2005) Morphogenesis in germinating *Fusarium graminearum* macroconidia. *Mycologia,* **97,** 880-887.

Heller, J. and Tudzynski, P. (2011) Reactive oxygen species in phytopathogenic fungi: signaling, development, and disease. *Annu. Rev. Phytopathol.,* **49,** 369-390.

Hong, S.-Y., Roze, L. V. and Linz, J. E. (2013a) Oxidative stress-related transcription factors in the regulation of secondary metabolism. *Toxins,* **5,** 683-702.

Hong, S. Y., Roze, L. V., Wee, J. and Linz, J. E. (2013b) Evidence that a transcription factor regulatory network coordinates oxidative stress response and secondary metabolism in aspergilli. *Microbiologyopen,* **2,** 144-160.

Huang, K., Czymmek, K. J., Caplan, J. L., Sweigard, J. A. and Donofrio, N. M. (2011) *HYR1*-mediated detoxification of reactive oxygen species is required for full virulence in the rice blast fungus. *PLoS Pathog.,* **7,** e1001335.

Jang, H. H., Lee, K. O., Chi, Y. H., Jung, B. G., Park, S. K., Park, J. H., *et al.* (2004)

Two enzymes in one: two yeast peroxiredoxins display oxidative stress-dependent switching from a peroxidase to a molecular chaperone function. *Cell,* **117,** 625-635.

Jiang, C., Zhang, S., Zhang, Q., Tao, Y., Wang, C. and Xu, J. R. (2015) *FgSKN7* and *FgATF1* have overlapping functions in ascosporogenesis, pathogenesis and stress responses in *Fusarium graminearum*. *Environ. Microbiol.,* **17,** 1245-1260.

Kel, A. E., Gößling, E., Reuter, I., Cheremushkin, E., Kel-Margoulis, O. V. and Wingender, E. (2003) MATCHTM: a tool for searching transcription factor binding sites in DNA sequences. *Nucleic acids research,* **31,** 3576-3579.

Kim, S. Y., Jang, H. H., Lee, J. R., Sung, N. R., Lee, H. B., Lee, D. H., *et al.* (2009) Oligomerization and chaperone activity of a plant 2-Cys peroxiredoxin in response to oxidative stress. *Plant Science,* **177,** 227-232.

Kong, S., Park, S. Y. and Lee, Y. H. (2015) Systematic characterization of the bZIP transcription factor gene family in the rice blast fungus, *Magnaporthe oryzae*. *Environ. Microbiol.,* **17,** 1425-1443.

König, J., Muthuramalingam, M. and Dietz, K.-J. (2012) Mechanisms and dynamics in the thiol/disulfide redox regulatory network: transmitters, sensors and targets. *Curr. Opin. Plant Biol.,* **15,** 261-268.

Lamb, C. and Dixon, R. A. (1997) The oxidative burst in plant disease resistance. *Annu. Rev. Plant Biol.,* **48,** 251-275.

Lara-Ortíz, T., Riveros-Rosas, H. and Aguirre, J. (2003) Reactive oxygen species generated by microbial NADPH oxidase NoxA regulate sexual development in *Aspergillus nidulans*. *Mol. Microbiol.,* **50,** 1241-1255.

Lee, J., Godon, C., Lagniel, G., Spector, D., Garin, J., Labarre, J., *et al.* (1999) Yap1 and Skn7 control two specialized oxidative stress response regulons in yeast. *J. Biol. Chem.,* **274,** 16040-16046.

Lee, Y., Min, K., Son, H., Park, A. R., Kim, J.-C., Choi, G. J., *et al.* (2014) ELP3 is involved in sexual and asexual development, virulence, and the oxidative stress response in *Fusarium graminearum*. *Mol. Plant-Microbe Interact.,* **27,** 1344-1355.

Leslie, J. F. and Summerell, B. A. (2006) *The Fusarium laboratory manual*. Ames, IA, U.S.A.: Blackwell Publishing.

Lev, S., Hadar, R., Amedeo, P., Baker, S. E., Yoder, O. and Horwitz, B. A. (2005) Activation of an AP1-like transcription factor of the maize pathogen *Cochliobolus heterostrophus* in response to oxidative stress and plant signals. *Eukaryot. Cell,* **4,** 443-454.

Levine, A., Tenhaken, R., Dixon, R. and Lamb, C. (1994) H_2O_2 from the oxidative burst orchestrates the plant hypersensitive disease resistance response. *Cell,* **79,** 583-593.

Levine, R. L., Moskovitz, J. and Stadtman, E. R. (2000) Oxidation of methionine in proteins: roles in antioxidant defense and cellular regulation. *IUBMB Life,* **50,** 301-307.

Lin, C.-H., Yang, S. L. and Chung, K.-R. (2009) The YAP1 homolog-mediated oxidative stress tolerance is crucial for pathogenicity of the necrotrophic fungus *Alternaria alternata* in citrus. *Mol. Plant-Microbe Interact.,* **22,** 942-952.

Livak, K. J. and Schmittgen, T. D. (2001) Analysis of relative gene expression data

using real-time quantitative PCR and the $2^{-\Delta\Delta CT}$ method. *Methods,* **25,** 402-408.

Lysøe, E., Pasquali, M., Breakspear, A. and Kistler, H. C. (2011) The transcription factor FgStuAp influences spore development, pathogenicity, and secondary metabolism in *Fusarium graminearum*. *Mol. Plant-Microbe Interact.,* **24,** 54-67.

Maier, F. J., Miedaner, T., Hadeler, B., Felk, A., Salomon, S., Lemmens, M., *et al.* (2006) Involvement of trichothecenes in fusarioses of wheat, barley and maize evaluated by gene disruption of the trichodiene synthase (Tri5) gene in three field isolates of different chemotype and virulence. *Mol. Plant Pathol.,* **7,** 449-461.

Marzluf, G. A. (1997) Molecular genetics of sulfur assimilation in filamentous fungi and yeast. *Annu. Rev. Microbiol.,* **51,** 73-96.

Mehdy, M. C. (1994) Active oxygen species in plant defense against pathogens. *Plant Physiol.,* **105,** 467.

Metsalu, T. and Vilo, J. (2015) ClustVis: a web tool for visualizing clustering of multivariate data using Principal Component Analysis and heatmap. *Nucleic Acids Res.,* **43,** W566-W570.

Mir, A. A., Park, S.-Y., Sadat, M. A., Kim, S., Choi, J., Jeon, J., *et al.* (2015) Systematic characterization of the peroxidase gene family provides new insights into fungal pathogenicity in *Magnaporthe oryzae*. *Sci. Rep.,* **5,** 11831.

Molina, L. and Kahmann, R. (2007) An *Ustilago maydis* gene involved in H_2O_2 detoxification is required for virulence. *Plant Cell,* **19,** 2293-2309.

Montibus, M., Ducos, C., Bonnin-Verdal, M.-N., Bormann, J., Ponts, N., Richard-Forget, F., *et al.* (2013) The bZIP transcription factor Fgap1 mediates oxidative stress response and trichothecene biosynthesis but not virulence in *Fusarium graminearum*. *PLoS One,* **8,** e83377.

Montibus, M., Pinson-Gadais, L., Richard-Forget, F., Barreau, C. and Ponts, N. (2015) Coupling of transcriptional response to oxidative stress and secondary metabolism regulation in filamentous fungi. *Crit. Rev. Microbiol.,* **41,** 295-308.

Mulford, K. E. and Fassler, J. S. (2011) Association of the Skn7 and Yap1 transcription factors in the *Saccharomyces cerevisiae* oxidative stress response. *Eukaryot. Cell,* **10,** 761-769.

Natorff, R., Sieńko, M., Brzywczy, J. and Paszewski, A. (2003) The *Aspergillus nidulans metR* gene encodes a bZIP protein which activates transcription of sulphur metabolism genes. *Mol. Microbiol.,* **49,** 1081-1094.

Petersen, T. N., Brunak, S., von Heijne, G. and Nielsen, H. (2011) SignalP 4.0: discriminating signal peptides from transmembrane regions. *Nature methods,* **8,** 785-786.

Pócsi, I., Prade, R. A. and Penninckx, M. J. (2004) Glutathione, altruistic metabolite in fungi. *Adv. Microb. Physiol.,* **49,** 1-76.

Ponts, N., Pinson-Gadais, L., Barreau, C., Richard-Forget, F. and Ouellet, T. (2007) Exogenous H_2O_2 and catalase treatments interfere with *Tri* genes expression in liquid cultures of *Fusarium graminearum*. *FEBS Lett.,* **581,** 443-447.

Ponts, N., Pinson-Gadais, L., Verdal-Bonnin, M.-N., Barreau, C. and Richard-

Forget, F. (2006) Accumulation of deoxynivalenol and its 15-acetylated form is significantly modulated by oxidative stress in liquid cultures of *Fusarium graminearum*. *FEMS Microbiol. Lett.,* **258,** 102-107.

Proctor, R. H., Hohn, T. M. and McCormick, S. P. (1995) Reduced virulence of *Gibberella zeae* caused by disruption of a trichthecene toxin biosynthetic gene. *Mol. Plant-Microbe Interact.,* **8,** 593-601.

Reverberi, M., Gazzetti, K., Punelli, F., Scarpari, M., Zjalic, S., Ricelli, A., *et al.* (2012) Ao*yap1* regulates OTA synthesis by controlling cell redox balance in *Aspergillus ochraceus*. *Appl. Microbiol. Biotechnol.,* **95,** 1293-1304.

Robbertse, B., Yoder, O. C., Nguyen, A., Schoch, C. L. and Turgeon, B. G. (2003) Deletion of all *Cochliobolus heterostrophus* monofunctional catalase-encoding genes reveals a role for one in sensitivity to oxidative stress but none with a role in virulence. *Mol. Plant-Microbe Interact.,* **16,** 1013-1021.

Sambrook, J. and Russell, D. W. (2001) *Molecular cloning : a laboratory manual*. Cold Spring Harbor, NY, U.S.A.: Cold Spring Harbor Laboratory Press.

Schouten, A., Tenberge, K. B., Vermeer, J., Stewart, J., Wagemakers, L., Williamson, B., *et al.* (2002) Functional analysis of an extracellular catalase of *Botrytis cinerea*. *Mol. Plant Pathol.,* **3,** 227-238.

Scott, B. and Eaton, C. J. (2008) Role of reactive oxygen species in fungal cellular differentiations. *Curr. Opin. Microbiol.,* **11,** 488-493.

Segmüller, N., Kokkelink, L., Giesbert, S., Odinius, D., van Kan, J. and Tudzynski, P. (2008) NADPH oxidases are involved in differentiation and pathogenicity in *Botrytis cinerea*. *Mol. Plant-Microbe Interact.,* **21,** 808-819.

Shalaby, S., Larkov, O., Lamdan, N. L. and Horwitz, B. A. (2014) Genetic interaction of the stress response factors ChAP1 and Skn7 in the maize pathogen *Cochliobolus heterostrophus*. *FEMS Microbiol. Lett.,* **350,** 83-89.

Sikhakolli, U. R., López-Giráldez, F., Li, N., Common, R., Townsend, J. P. and Trail, F. (2012) Transcriptome analyses during fruiting body formation in *Fusarium graminearum* and *Fusarium verticillioides* reflect species life history and ecology. *Fungal Genet. Biol.,* **49,** 663-673.

Skamnioti, P., Henderson, C., Zhang, Z., Robinson, Z. and Gurr, S. J. (2007) A novel role for catalase B in the maintenance of fungal cell-wall integrity during host invasion in the rice blast fungus *Magnaporthe grisea*. *Mol. Plant-Microbe Interact.,* **20,** 568-580.

Son, H., Kim, M.-G., Min, K., Seo, Y.-S., Lim, J. Y., Choi, G. J., *et al.* (2013) AbaA regulates conidiogenesis in the ascomycete fungus *Fusarium graminearum*. *PLoS One,* **8,** e72915.

Son, H., Lee, J., Park, A. R. and Lee, Y.-W. (2011a) ATP citrate lyase is required for normal sexual and asexual development in *Gibberella zeae*. *Fungal Genet. Biol.,* **48,** 408-417.

Son, H., Lim, J. Y., Lee, Y. and Lee, Y.-W. (2016) Utilization of a conidia-deficient mutant to study sexual development in *Fusarium graminearum*. *PLoS One,* **11,** e0155671.

Son, H., Seo, Y.-S., Min, K., Park, A. R., Lee, J., Jin, J.-M., *et al.* (2011b) A phenome-based functional analysis of transcription factors in the cereal head blight fungus, *Fusarium graminearum*. *PLoS Pathog.*, **7,** e1002310.

Takemoto, D., Tanaka, A. and Scott, B. (2007) NADPH oxidases in fungi: diverse

roles of reactive oxygen species in fungal cellular differentiation. *Fungal Genet. Biol.,* **44,** 1065-1076.

Tamura, K., Stecher, G., Peterson, D., Filipski, A. and Kumar, S. (2013) MEGA6: molecular evolutionary genetics analysis version 6.0. *Mol. Biol. Evol.,* **30,** 2725-2729.

Tanabe, S., Ishii-Minami, N., Saitoh, K.-I., Otake, Y., Kaku, H., Shibuya, N., *et al.* (2011) The role of catalase-peroxidase secreted by *Magnaporthe oryzae* during early infection of rice cells. *Mol. Plant-Microbe Interact.,* **24,** 163-171.

Temme, N. and Tudzynski, P. (2009) Does *Botrytis cinerea* ignore H_2O_2-induced oxidative stress during infection? Characterization of *Botrytis* activator protein 1. *Mol. Plant-Microbe Interact.,* **22,** 987-998.

Torres, M. A., Jones, J. D. G. and Dangl, J. L. (2006) Reactive oxygen species signaling in response to pathogens. *Plant Physiol.,* **141,** 373-378.

Wang, L., Mogg, C., Walkowiak, S., Joshi, M. and Subramaniam, R. (2014) Characterization of NADPH oxidase genes *NoxA* and *NoxB* in *Fusarium graminearum*. *Can. J. Plant Pathol.,* **36,** 12-21.

Wang, Y., Liu, W., Hou, Z., Wang, C., Zhou, X., Jonkers, W., *et al.* (2011) A novel transcriptional factor important for pathogenesis and ascosporogenesis in *Fusarium graminearum*. *Mol. Plant-Microbe Interact.,* **24,** 118-128.

Windels, C. E. (2000) Economic and social impacts of Fusarium head blight: changing farms and rural communities in the Northern Great Plains. *Phytopathology,* **90,** 17-21.

Wojtaszek, P. (1997) Oxidative burst: an early plant response to pathogen infection.

Biochem. J., **322,** 681-692.

Wong, P., Walter, M., Lee, W., Mannhaupt, G., Münsterkötter, M., Mewes, H.-W., *et al.* (2011) FGDB: revisiting the genome annotation of the plant pathogen *Fusarium graminearum*. *Nucleic Acids Res.*, **39,** D637-D639.

Yu, J.-H., Hamari, Z., Han, K.-H., Seo, J.-A., Reyes-Dominguez, Y. and Scazzocchio, C. (2004) Double-joint PCR: a PCR-based molecular tool for gene manipulations in filamentous fungi. *Fungal Genet. Biol.*, **41,** 973-981.

Zámocký, M., Furtmüller, P. G. and Obinger, C. (2009) Two distinct groups of fungal catalase/peroxidases. *Biochem. Soc. Trans.*, **37**, 772-777.

Zámocký, M., Gasselhuber, B., Furtmüller, P. G. and Obinger, C. (2012) Molecular evolution of hydrogen peroxide degrading enzymes. *Archives of biochemistry and biophysics*, **525,** 131-144.

Zámocký, M. and Obinger, C. (2010) Molecular phylogeny of heme peroxidases. In: *Biocatalysis based on heme peroxidases*. Springer, pp. 7-35.

Zhang, C., Lin, Y., Wang, J., Wang, Y., Chen, M., Norvienyeku, J., *et al.* (2016) FgNoxR, a regulatory subunit of NADPH oxidases, is required for female fertility and pathogenicity in Fusarium graminearum. *FEMS microbiology letters*, **363,** fnv223.

Zhou, W., Eudes, F. and Laroche, A. (2006) Identification of differentially regulated proteins in response to a compatible interaction between the pathogen *Fusarium graminearum* and its host, *Triticum aestivum*. *Proteomics*, **6,** 4599-4609.

Zhou, W., Kolb, F. L. and Riechers, D. E. (2005) Identification of proteins induced or upregulated by Fusarium head blight infection in the spikes of hexaploid

wheat (*Triticum aestivum*). *Genome*, **48,** 770-780.

요약 (국문초록)

*Fusarium graminearum*의 산화스트레스반응에 관련된 유전자들의 기능 분석

이 윤 지

붉은곰팡이(*Fusarium graminearum*)는 밀, 보리, 옥수수, 벼 등에 큰 피해를 주는 중요한 식물병원균으로, 붉은곰팡이가 일으키는 붉은곰팡이병은 전 세계적으로 대발생하여 경제적으로 큰 손실을 가져온다. 붉은곰팡이병은 생산량 감소를 초래할 뿐만 아니라 감염된 곡류에 인축에 유해한 trichothecenes 및 zearalenone 과 같은 곰팡이독소를 잔류시킴으로써 곡류의 질을 저하시킨다. 산화스트레스환경은 병원체가 식물에 침입하는 과정에서 식물의 방어메커니즘의 일환인 활성산소종(reactive oxygen species, ROS)의 급격한 증가에 의해 노출 될 수 있는 스트레스 환경이다. 식물체로부터 발생하는 ROS는 병원균을 직접적으로 죽이는데 관여할 뿐만 아니라 식물의 다른 방어메커니즘을 유도한다. ROS는 병원체의 정상적인 발달과정에도 중요한 역할을 한다. 세포 내에서 산화적 대사과정에 의해서 발생하는 ROS는 과도하게 생성될 경우 산화스트레스를 유발하기도 하지만

발달과정에서 중요한 신호전달자로서의 역할을 수행한다. 따라서 식물병원균에서 산화스트레스환경에서 ROS 분해에 관련된 유전자에 대한 연구는 곰팡이의 병원성뿐만 아니라 전 발달과정을 이해하는데 있어 매우 중요하다. 본 연구에서는 붉은곰팡이에서 전방향유전학적 연구기법을 통해 yeast의 *ELP3* 유전자의 ortholog를 찾아 그 기능을 연구하였다. Elp3는 histone acetyltransferase (HAT)로 다양한 진핵생물에서 외부 스트레스에 의해 유도되는 유전자들의 발현 조절에 중요한 기능을 한다고 알려져 있다. 붉은곰팡이에서 *ELP3* 유전자를 삭제하였을 때 곰팡이의 무성생식, 유성생식, 병원성 등 다양한 발달과정에서 장애가 발생하였다. 특히 *elp3* 삭제균주는 여러 스트레스 중에서 산화스트레스(H_2O_2)에 대하여 야생형보다 취약하였다. *elp3* 삭제균주에서 붉은곰팡이에서 H_2O_2를 분해한다고 알려진 catalase, catalase-peroxidase 추정 유전자들의 발현을 관찰한 결과, 산화스트레스 환경에서 이들의 발현량이 야생형보다 감소하는 것을 알 수 있었다. 실제 이 유전자들이 붉은곰팡이의 산화스트레스 반응에 중요한 역할을 하는지는 알아보기 위하여 총 31개의 peroxidase 추정 유전자들을 찾아 이들의 기능을 연구한 결과, 이들 중 오직 4개의 peroxidase 추정 유전자(*FCA6*, *FCA7*, *FPX1*, *FPX15*)만이 붉은곰팡이의 산화스트레스반응에 관련이 되어 있음을 알 수 있었다. 특히 Fca7은 산화스트레스반응 외에도 곰팡이독소생성과 병원성에도 관련되어 있었다. 이를 통하여 Fca7이 붉은곰팡이에서 기주식물과의 상호작용에 있어 가장 중요한 역할을 한다는 것을 알 수 있었

다. 산화스트레스 반응에 관련된 전사조절인자(transcription factor, TF)를 찾아 이 TF 삭제균주들에서 *FCA6*, *FCA7*, *FPX1*, *FPX15*의 발현량을 야생형과 비교하여 관찰한 결과, 여러 TF들이 함께 *FCA7*의 발현을 조절하여 산화스트레스반응에 관여한다는 것을 알 수 있었다. 해당 TF들간 상호 조절 관계를 구명하기 위하여 각 TF 삭제균주들에서 다른 TF 유전자의 발현을 관찰하였고 그 결과를 바탕으로 산화스트레스 반응에 관련된 TF 간 유전자네트워크를 제시할 수 있었다. 이 연구 결과는 식물병원균에서 산화스트레스반응에 관련된 유전자들의 기능을 이해하는 것에 있어 초석이 될 것이다

주요어: 붉은곰팡이, 산화스트레스반응, Elp3, Peroxidase, 병원성, 전사조절인자

학번: 2011-21306